Peter Huybers
Harvard University
August 1st, talk 2

Peking University - Harvard University
2017 Graduate Summer School

Sponsored by PKU and the Harvard Global Institute

Outline

Part 1.
Mean temperatures are increasing, but high-temperature excursions above the mean are generally stable.
(*M. Tingley* and *A. Rhines*)

Part 2.
The hottest temperatures have been cooling in regions with rapid agricultural intensification
(*N. Mueller, E. Butler*, A. Rhines, and *N. Holbrook*)

Part 3.
Implications for yield trends
(*N. Mueller, E. Butler*, and *N. Holbrook*)

Temperature has shifted higher, but have the tails also changed?

Northern Hemisphere Summer

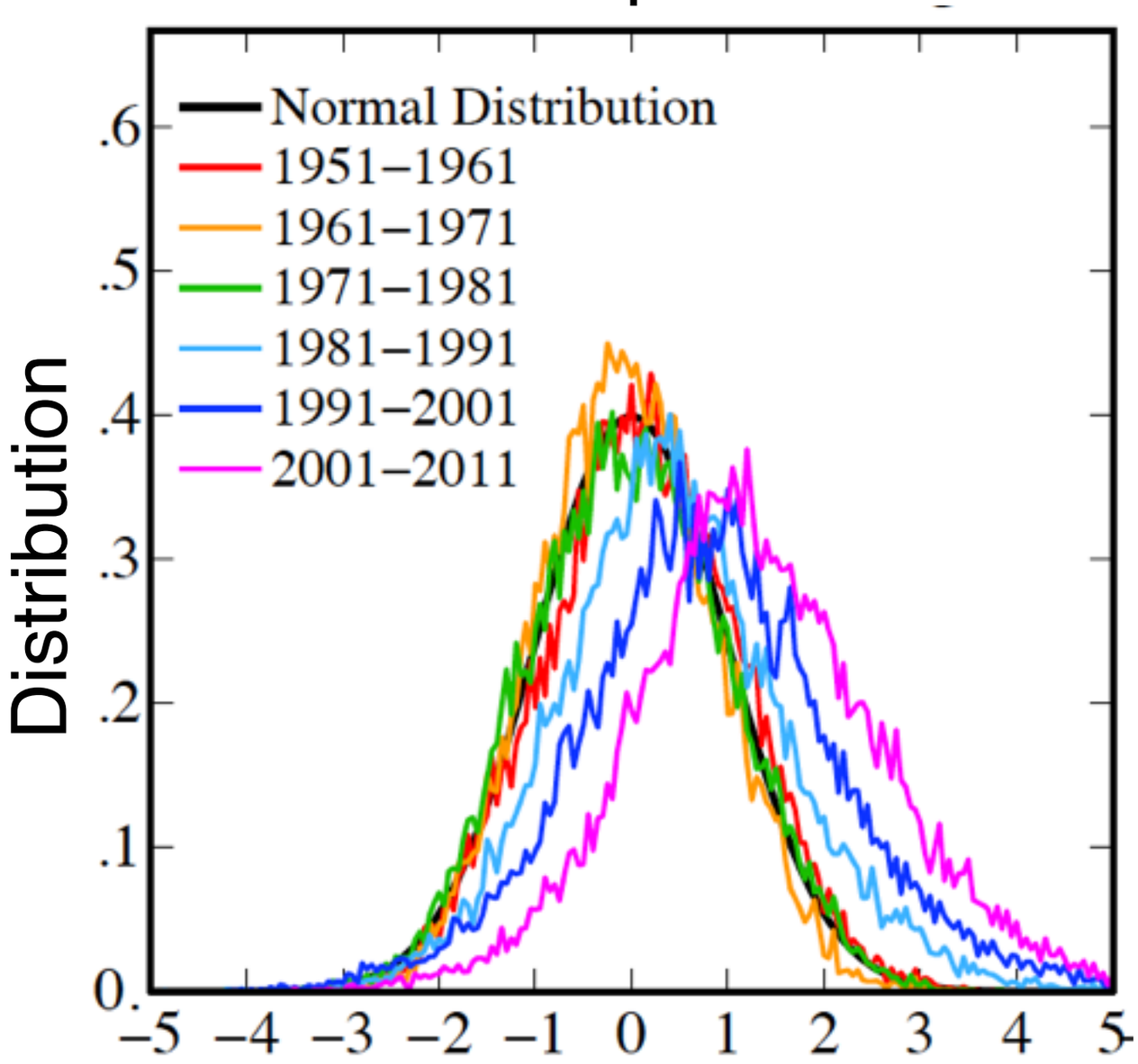

(Hansen et al., 2012)

- Sample temperature variance in 1981-2010 is **1.9** times that in 1951-1980.
- But removing the sample mean from both periods decreases the variance ratio to **1.5**.
- Detrending each time series during each period reduces the variance ratio to **1.2**.
- Accounting for the 35% decrease in temperature observations from the first to second period makes the variance ratio indistinguishable from **1**.

(Rhines and Huybers, 2013)

Are individual heat waves anomalous?

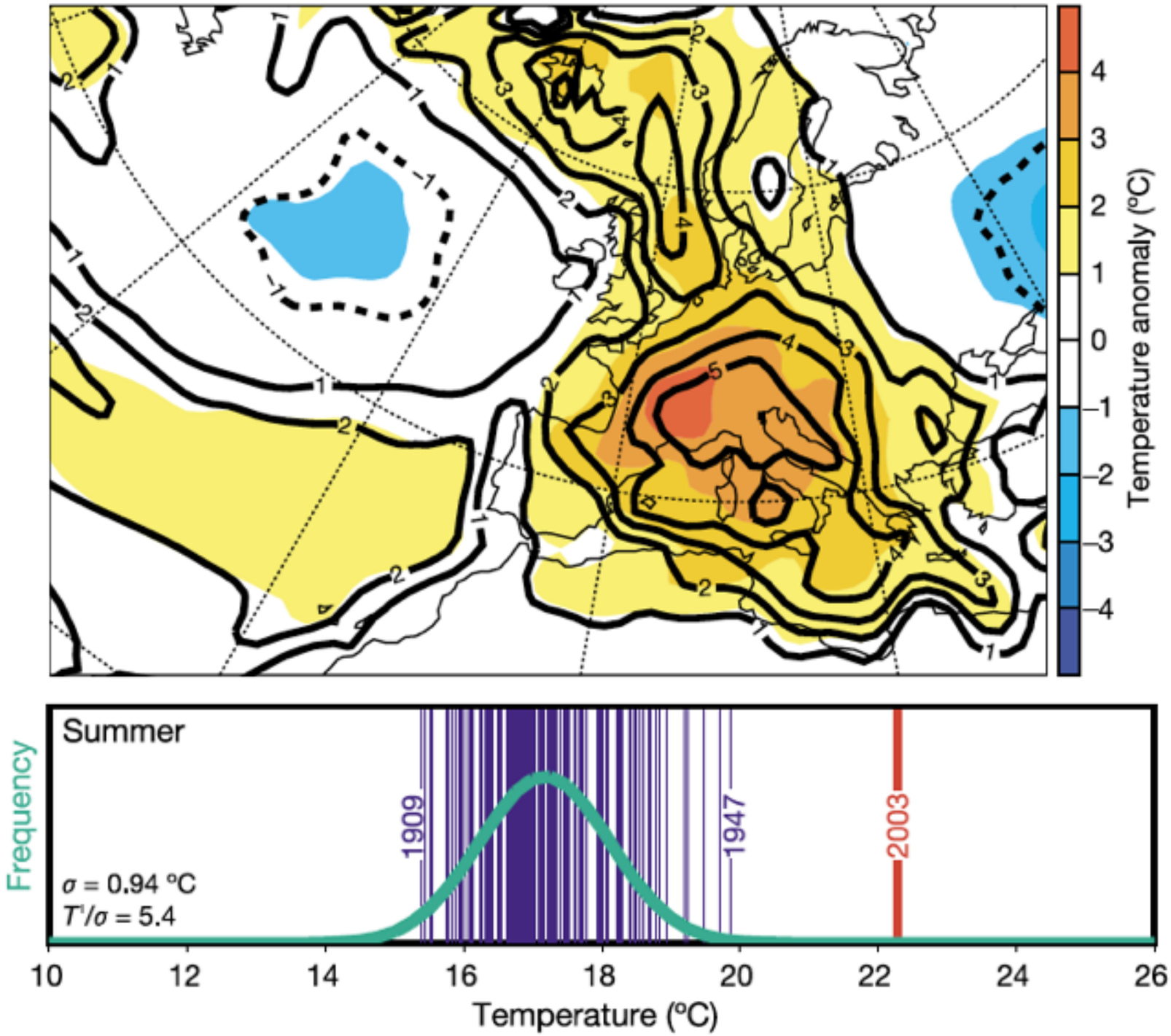

(Schär et al., 2004)

Are individual heat waves anomalous?

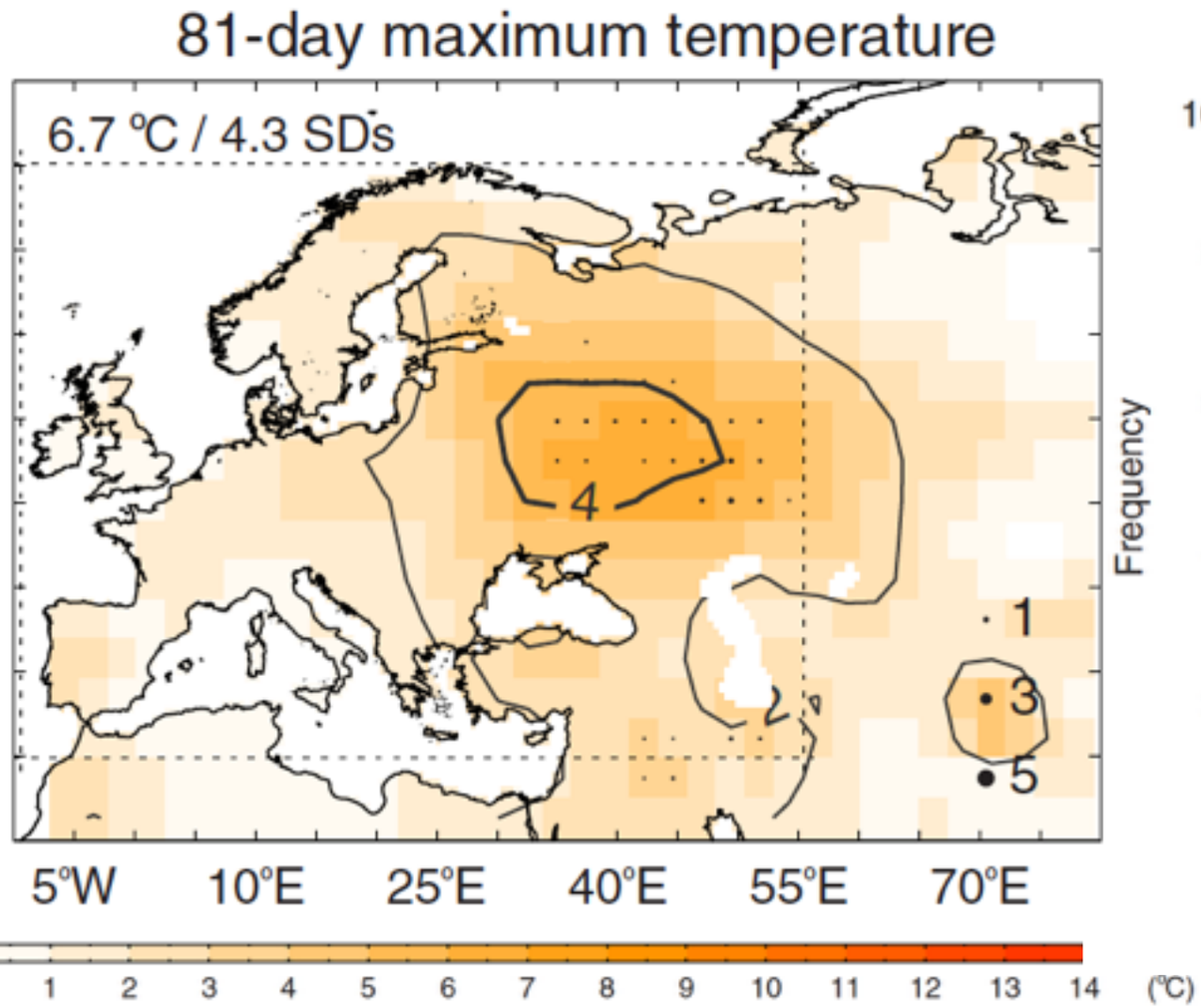

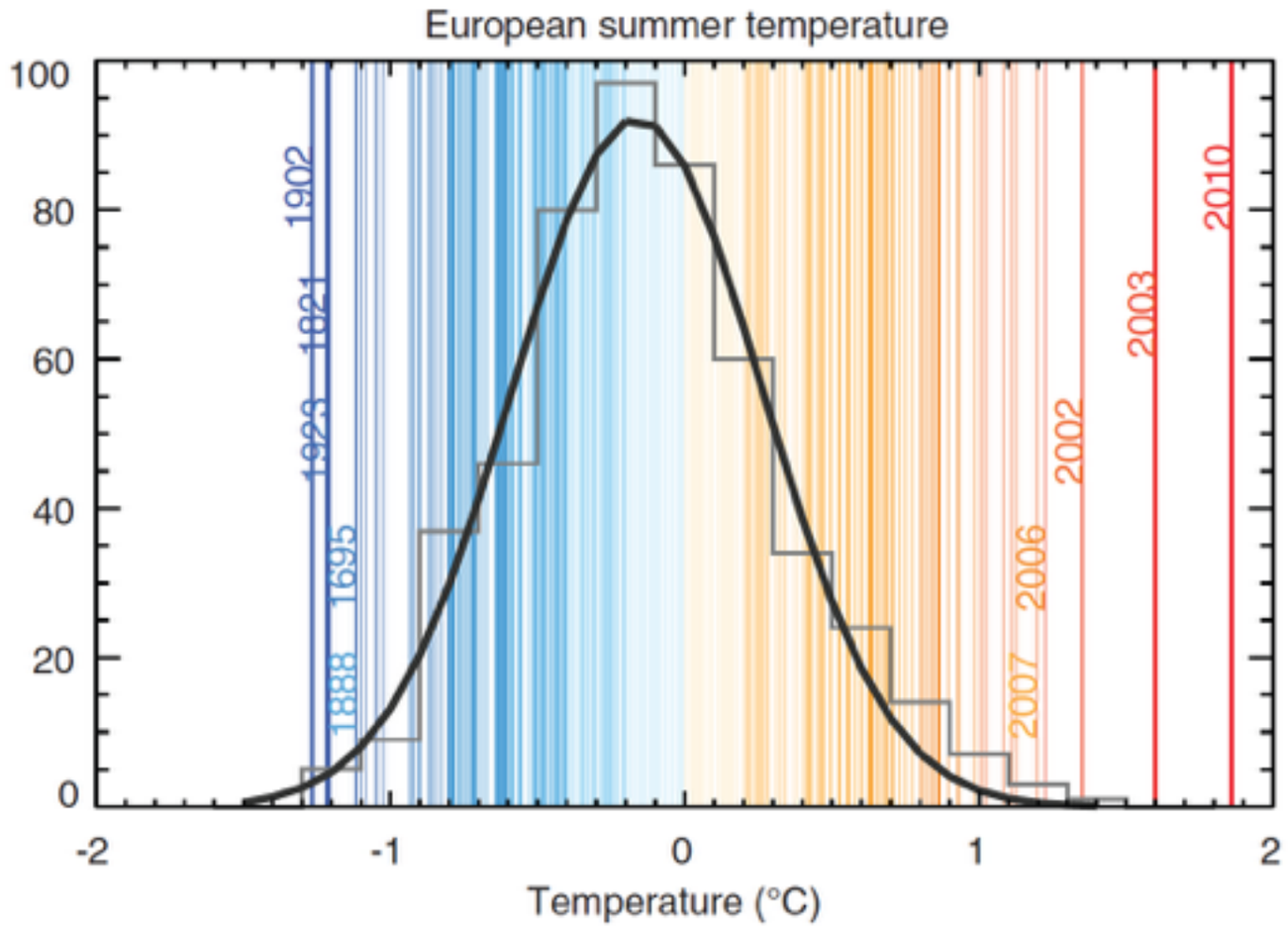

(Barriopedro et al., 2011)

A Bayesian Algorithm for Reconstructing Climate Anomalies in Space and Time (BARCAST)

Temperatures evolve as an auto-regressive order one process in time,

$$\mathbf{T}_t - \mu\mathbf{1} = \alpha\left(\mathbf{T}_{t-1} - \mu\mathbf{1}\right) + \epsilon_t \qquad (1)$$

Where the innovations are multivariate normal and have a spatial covariance that decays exponentially,

$$\Sigma_{ij} = \sigma^2 \exp\left(-\phi|\mathbf{x}_i - \mathbf{x}_j|\right) \qquad (2)$$

Instruments are represented as true temperature plus noise,

$$\mathbf{W}_{I,t} = \mathbf{T}_{I,t} + \mathbf{e}_{I,t} \qquad (3)$$

And proxies as having a linear relationship with true temperature and being noisy,

$$\mathbf{W}_{P,t} = \beta_1\mathbf{T}_{P,t} + \beta_o\mathbf{1} + \mathbf{e}_{P,t} \qquad (4)$$

(Tingley and Huybers, 2010a,b)

BARCAST differs from typical reconstruction techniques through estimating true temperature from both proxies and instruments

Typical formulation

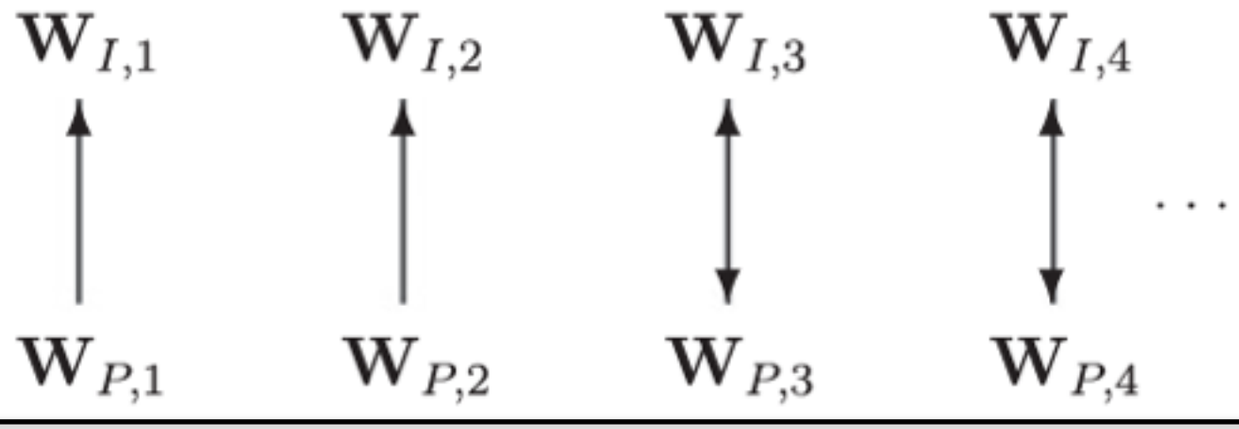

BARCAST

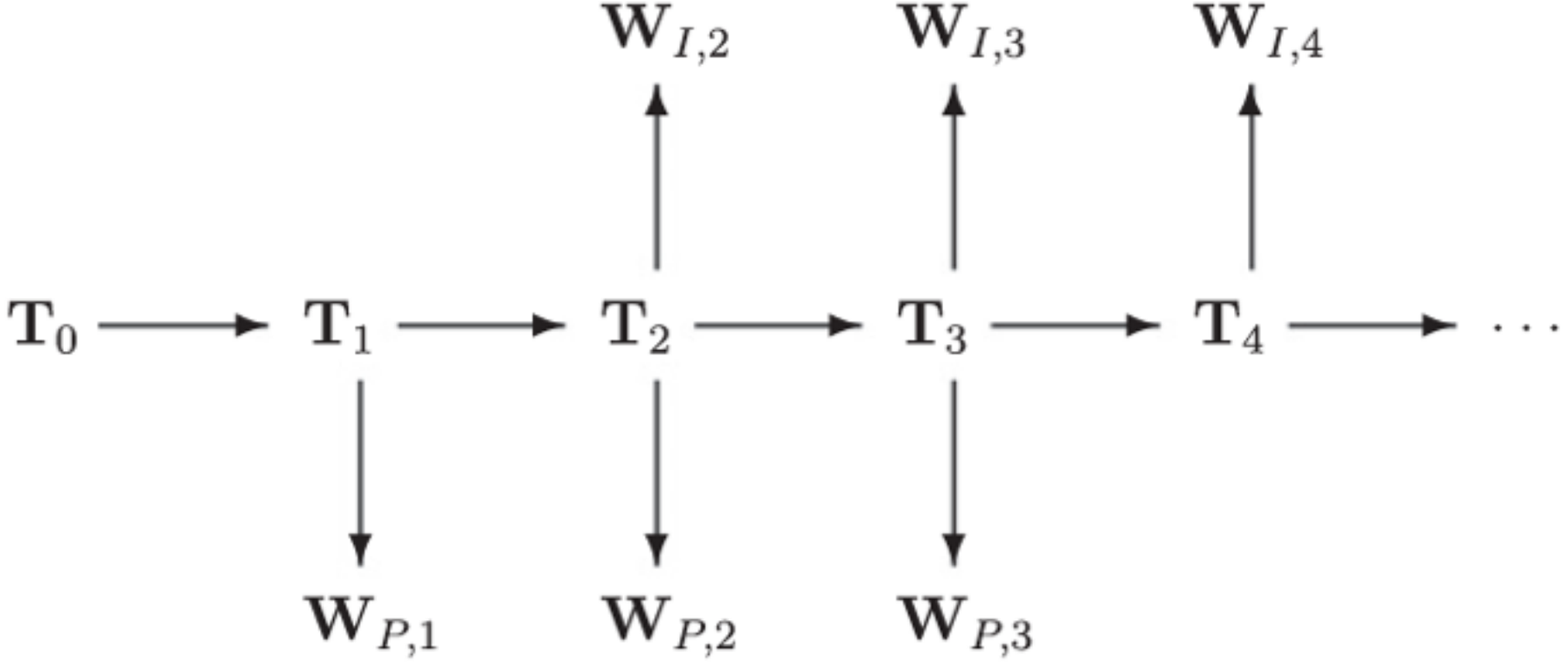

Applying BARCAST to a multi-proxy dataset

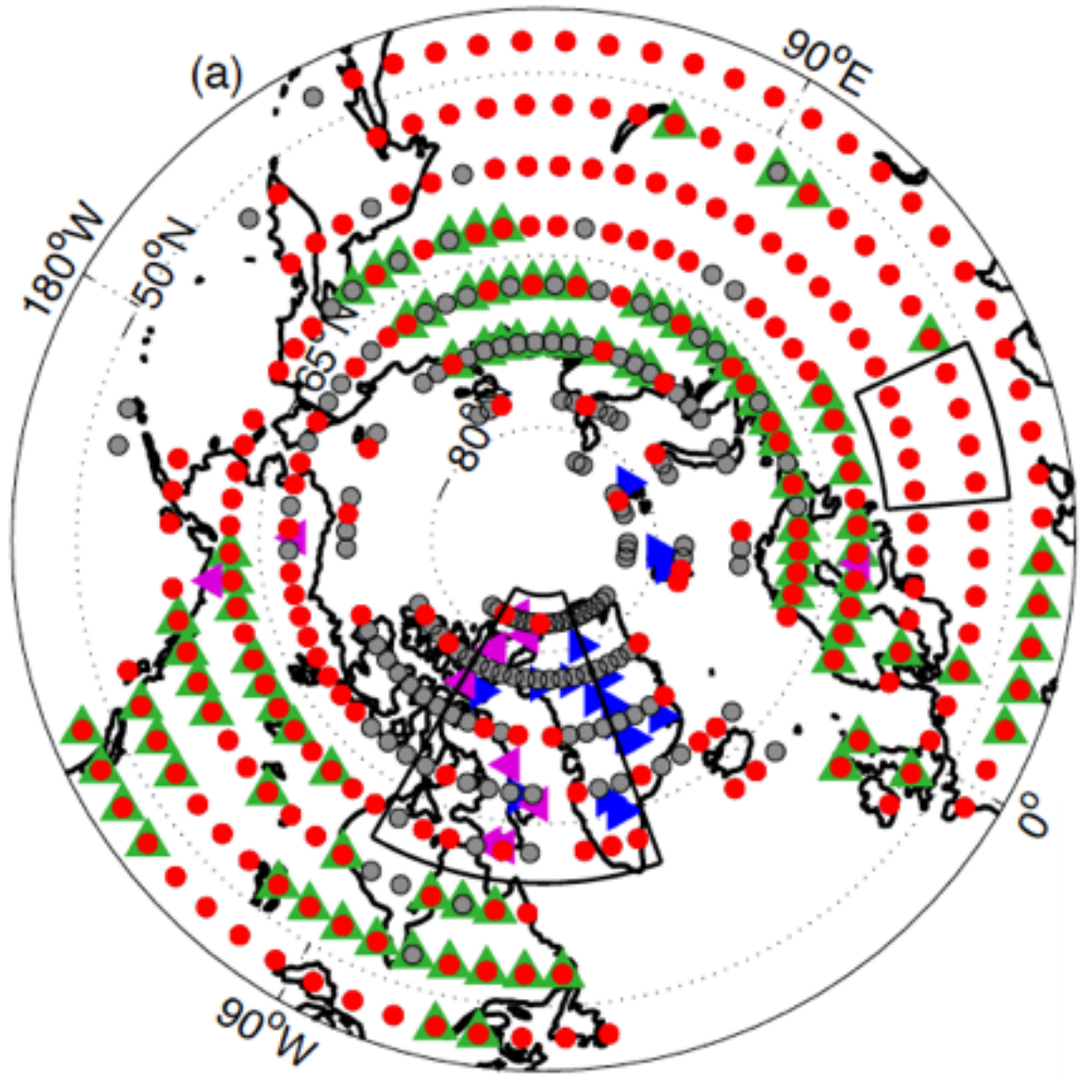

- 96 maximum tree ring density
- 18 ice core $\delta^{18}O$
- 11 varve sediment thickness
- 251 Instrumental (Apr-Sep)
- $5^{o}x5^{o}$ target location grid

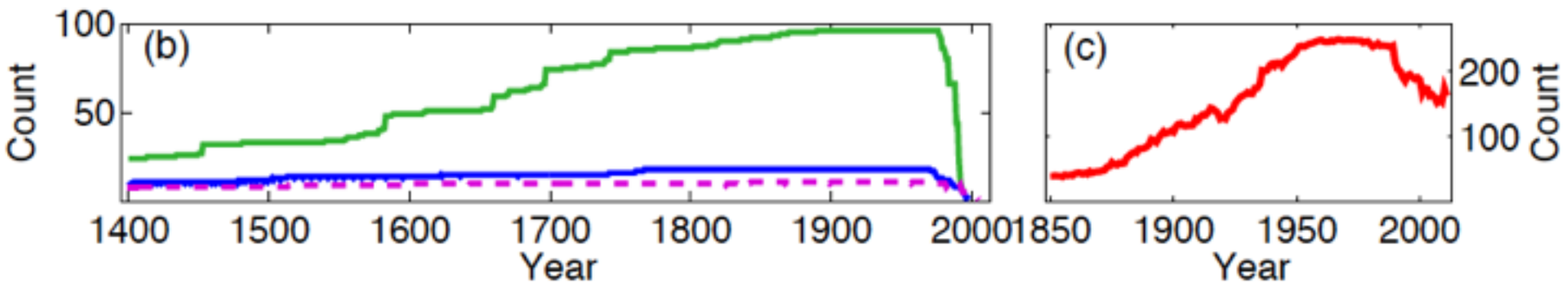

(Tingley and Huybers, 2013)

Statistical assessment of whether an event is uniquely extreme requires pathwise uncertainties, not pointwise ones.

600 independent draws from a normal distribution with zero mean and unit variance

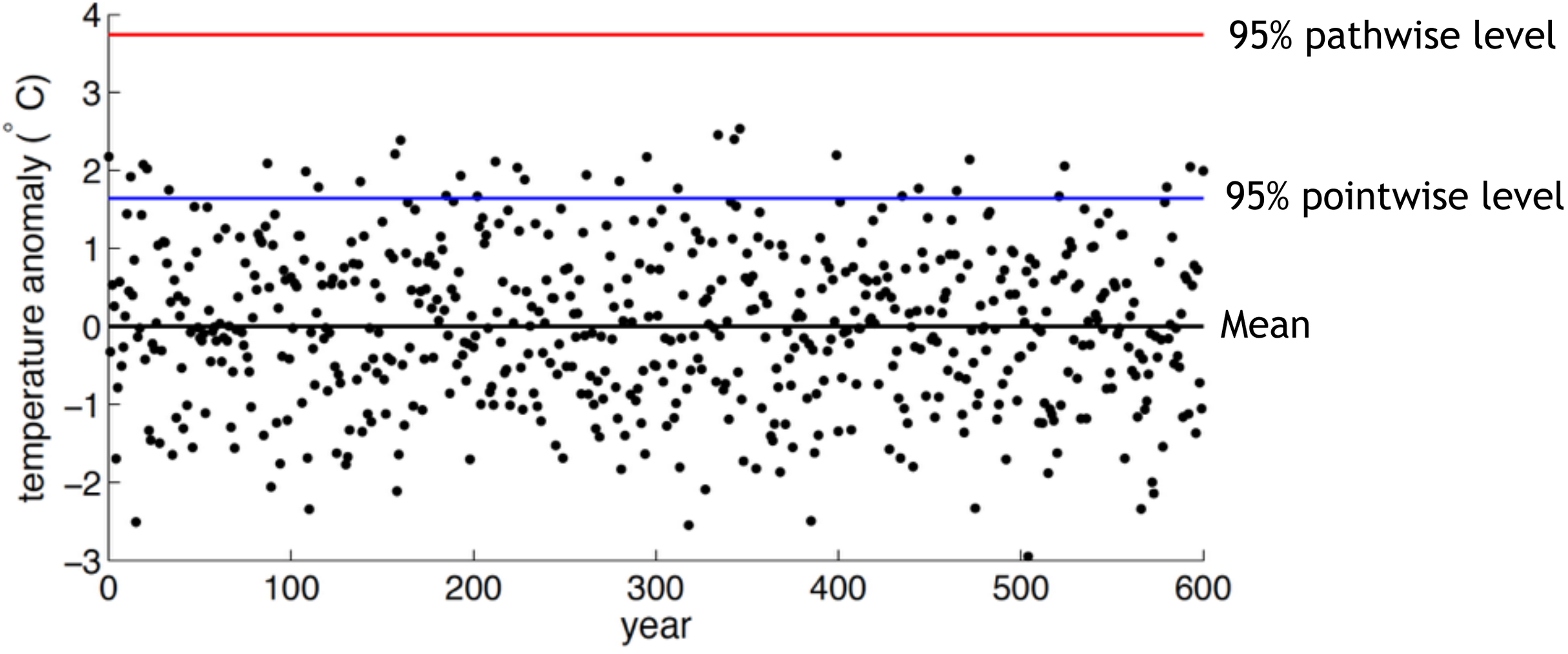

Reconstructed Arctic temperature over the last 600 years: 2005, 2007, 2011, and 2012 were the warmest on record

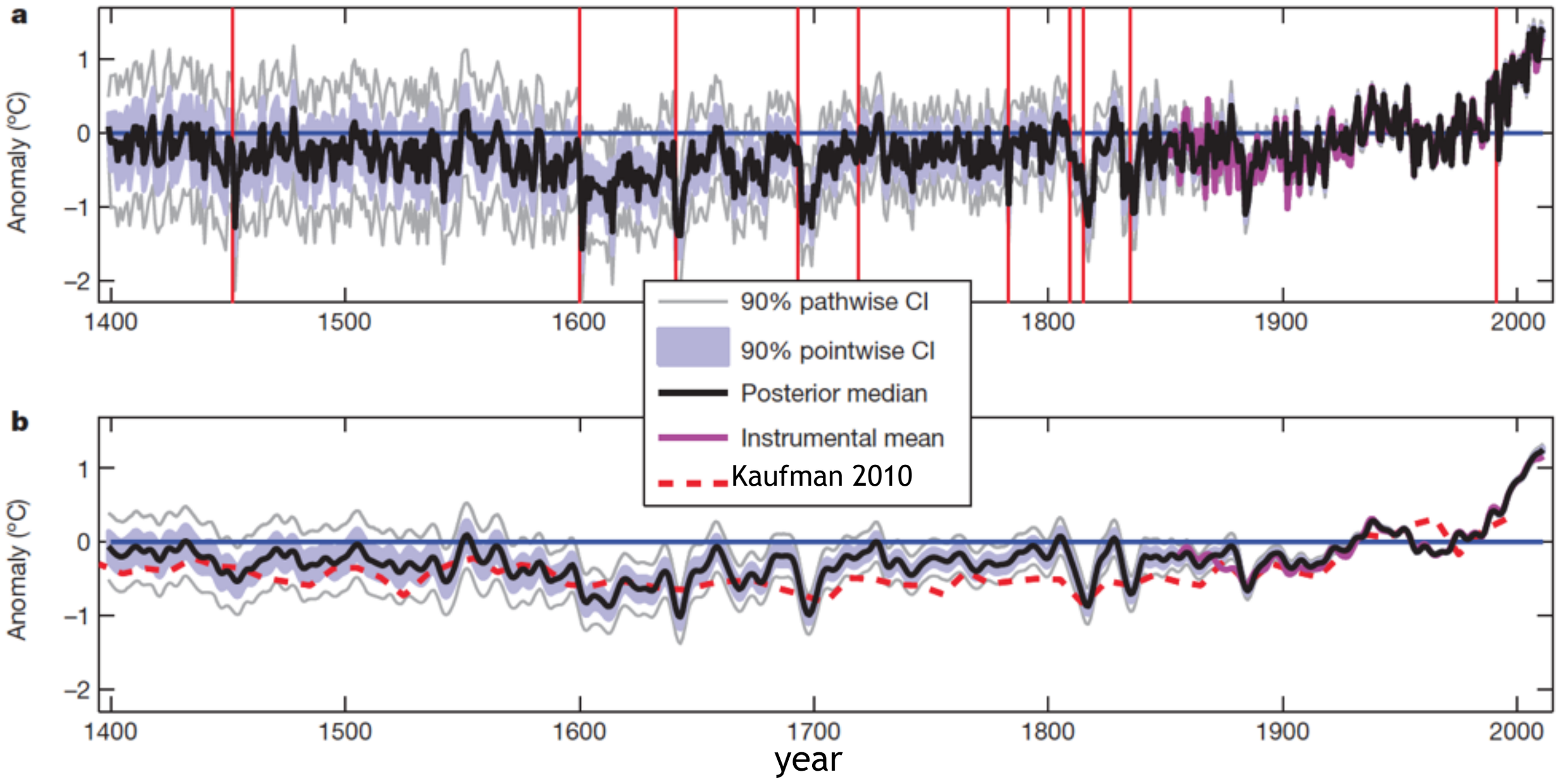

The hottest temperatures in the last 600 years are clustered in the last two decades.

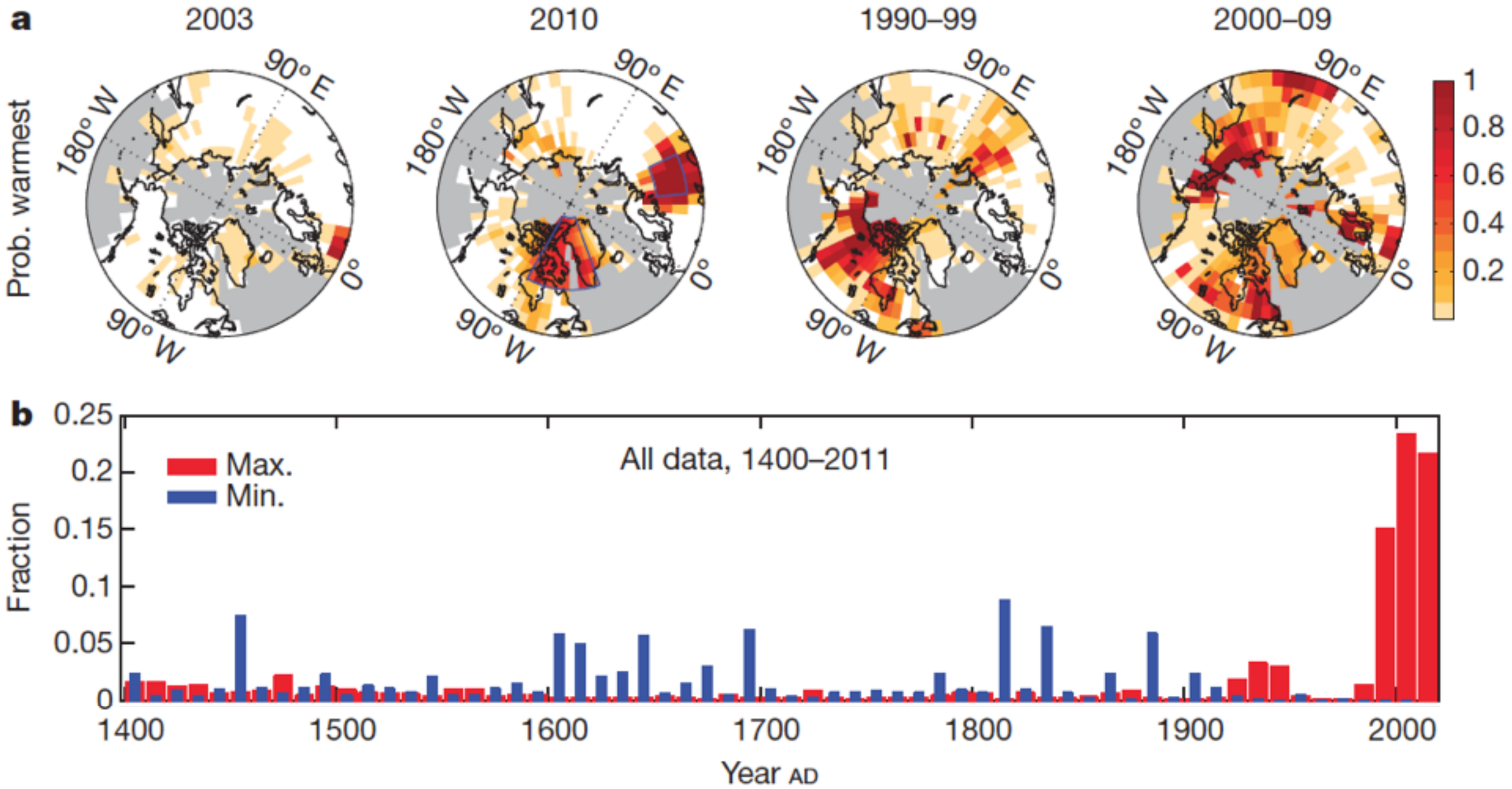

A similar distribution of extremes is obtained from ice and varve data alone, excepting that they do not cover the most recent decade.

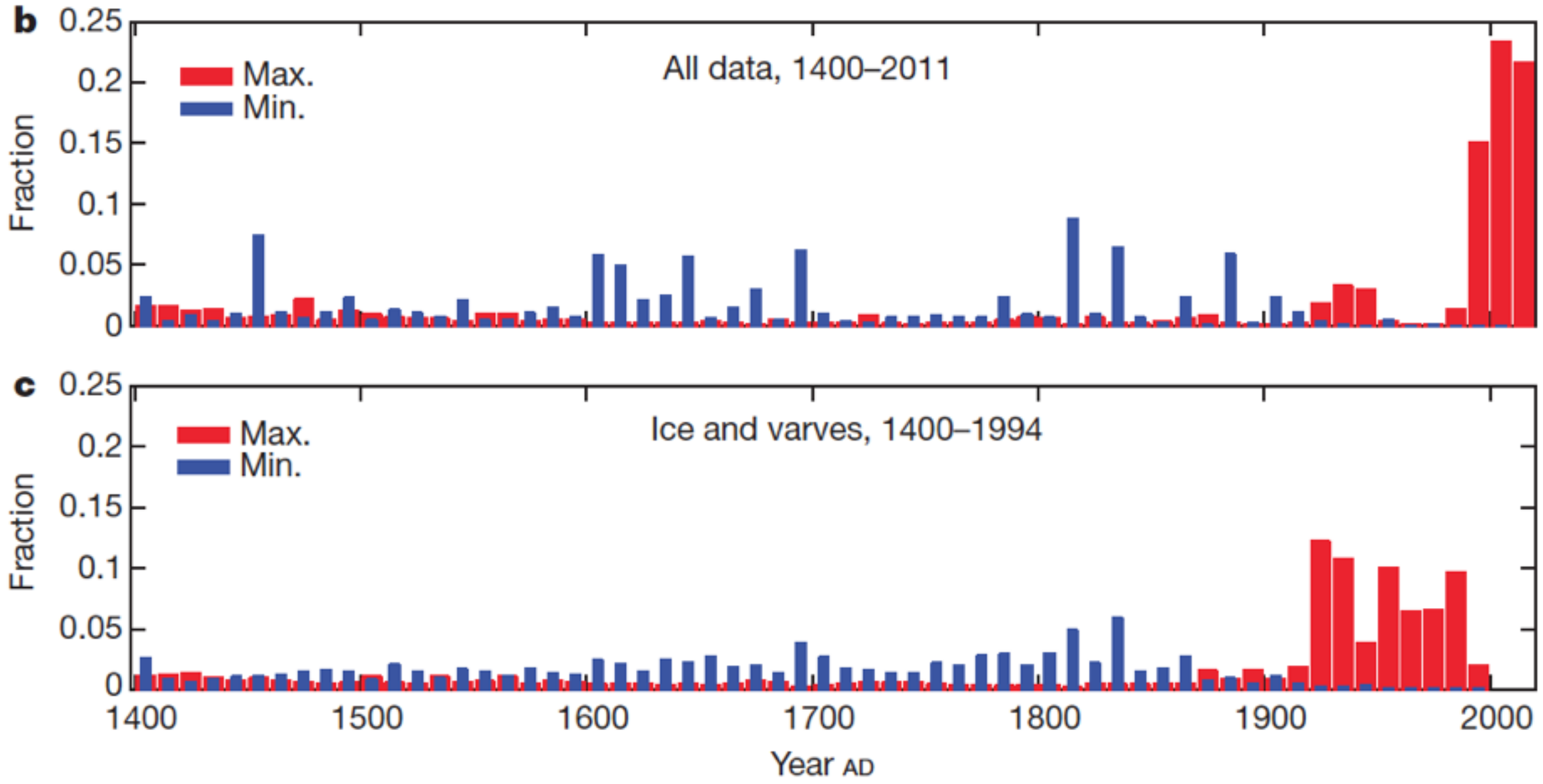

The five hottest anomalies in the last 20 years are far in the tail of inferred summer temperature variability, even after shifting the mean.

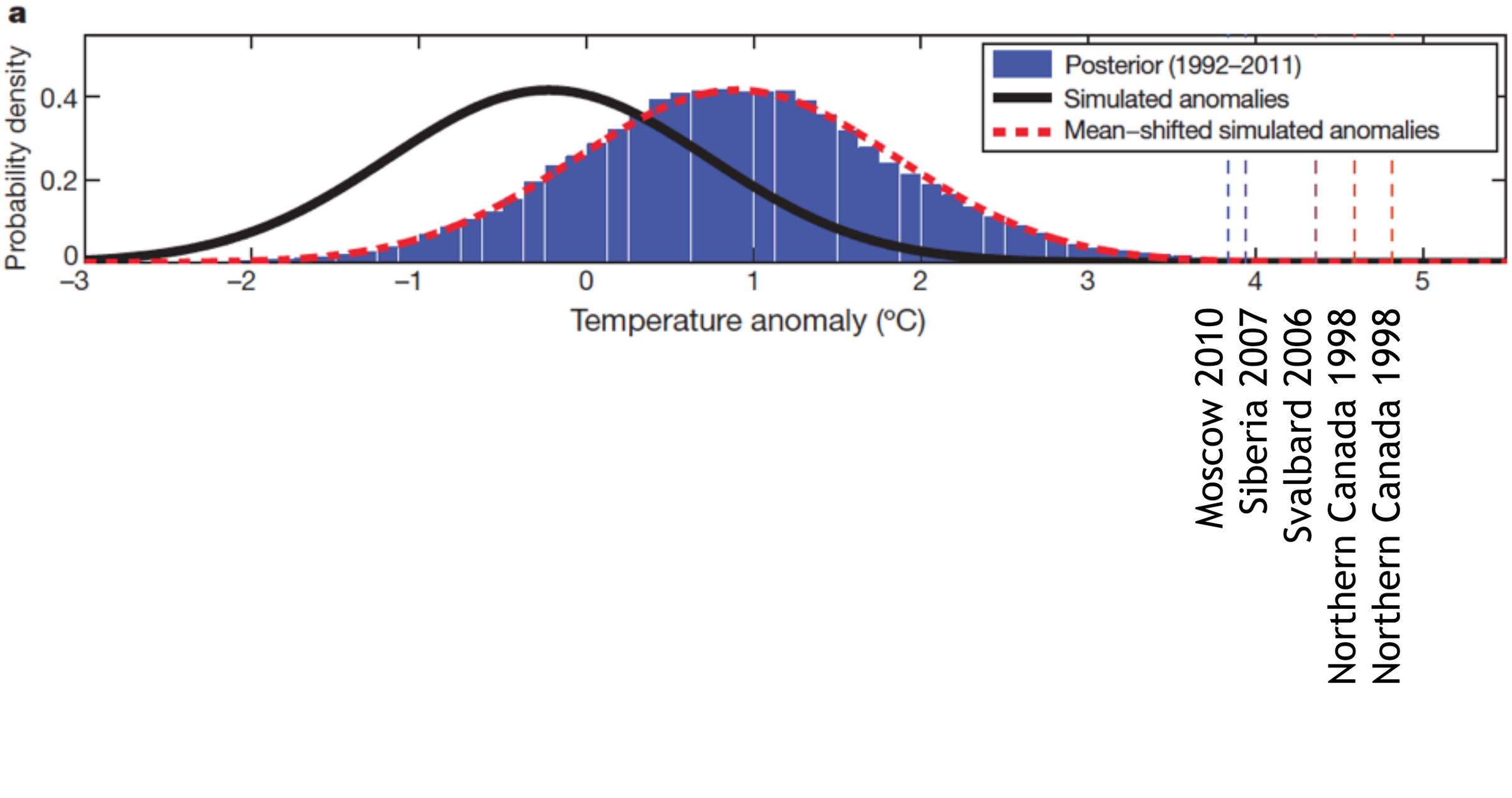

They are still far in the tail after selecting just the warmest years in the last twenty within each grid box.

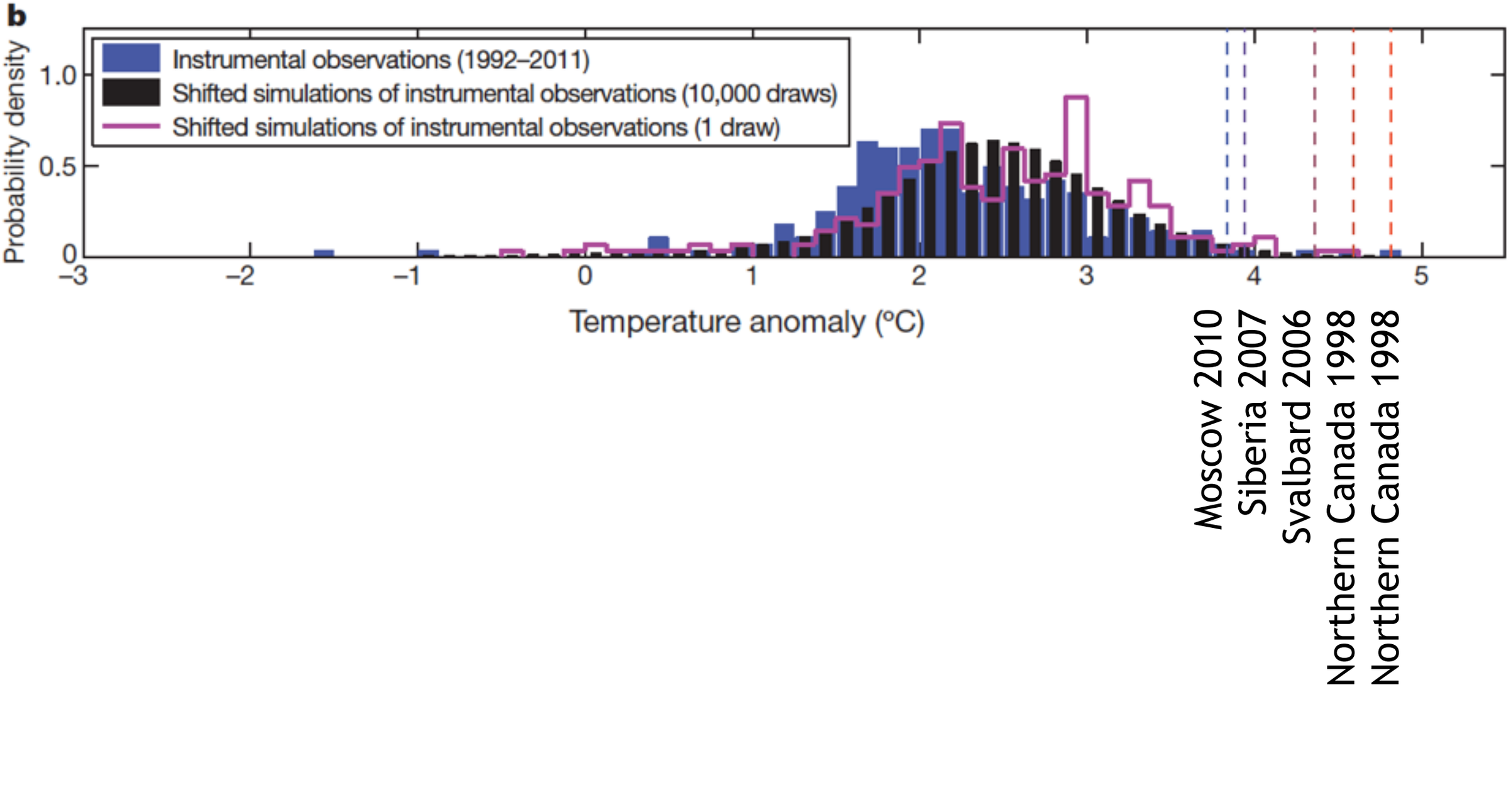

But these extreme events are consistent with expectation after shifting the mean and choosing the five hottest events from amongst all grid boxes during the last twenty years.

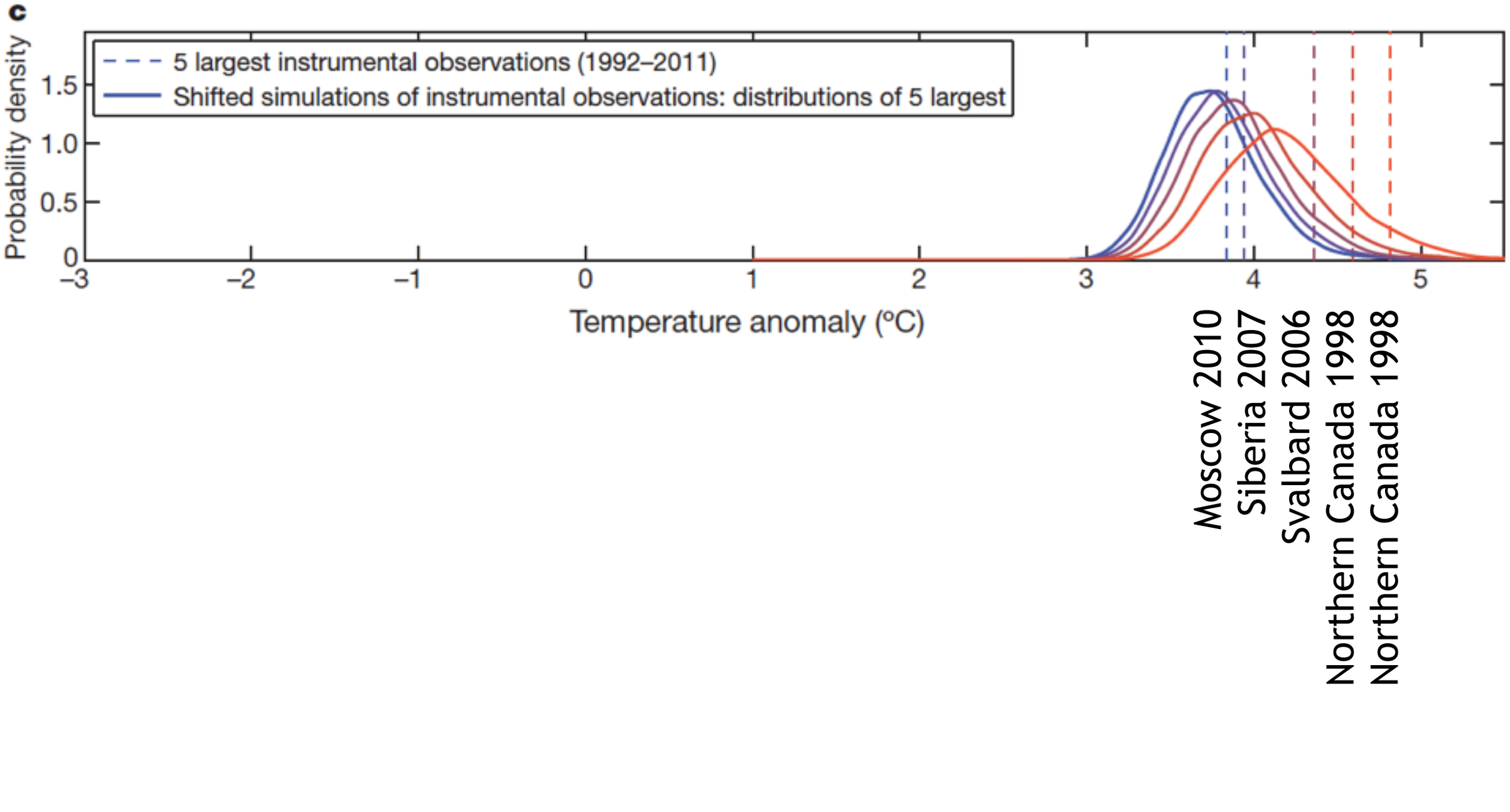

Outline

Part 1.
Mean temperatures are increasing, but high-temperature excursions above the mean are generally stable.
(*M. Tingley* and *A. Rhines*)

Part 2.
The hottest temperatures have been cooling in regions with rapid agricultural intensification
(*N. Mueller, E. Butler*, A. Rhines, and *N. Holbrook*)

Part 3.
Implications for yield trends
(*N. Mueller, E. Butler*, and *N. Holbrook*)

Changes in temperature extremes for Redwood County, MN.

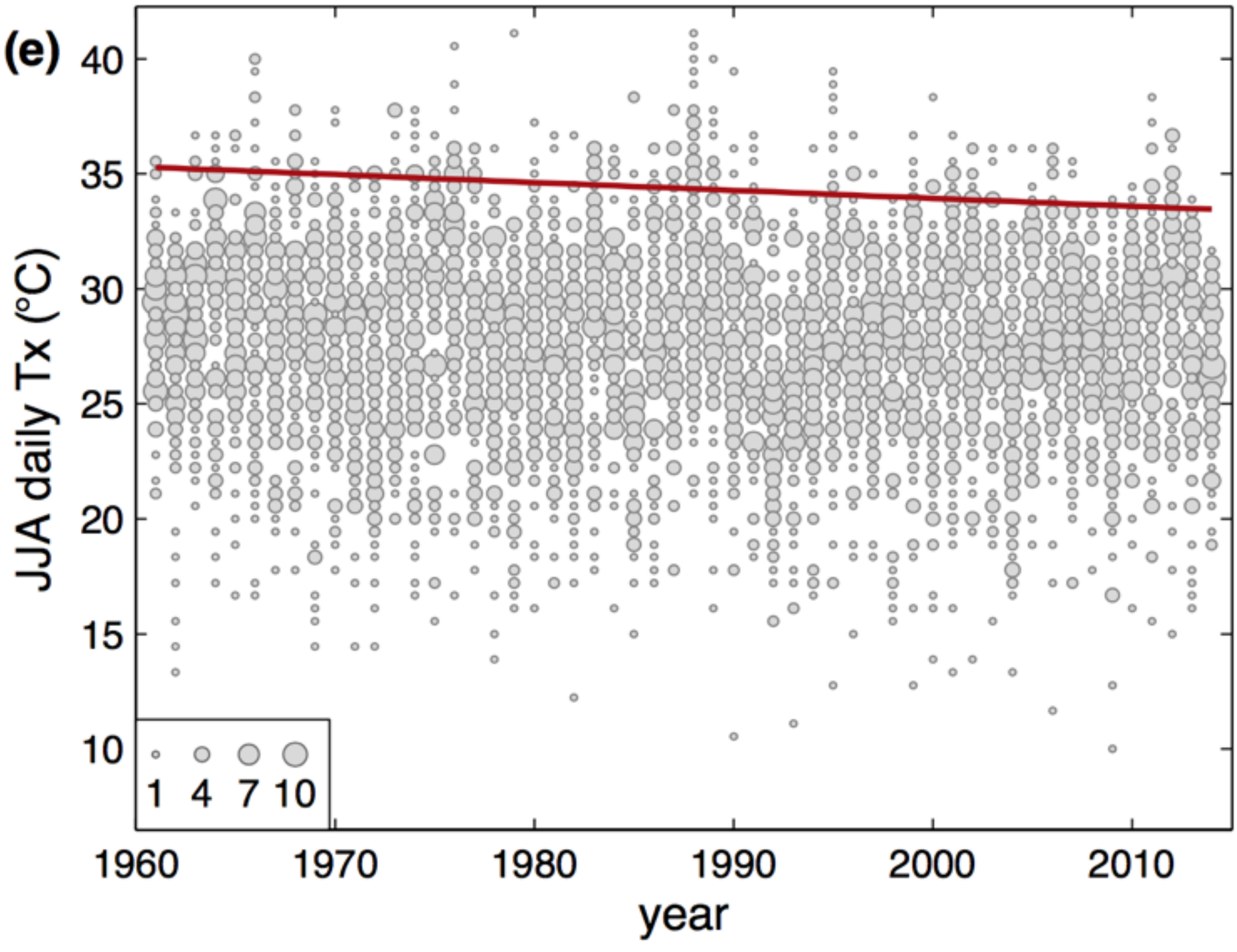

Trend in the 95th percentile of temperature determined using quantile regression

Trends in 95th percentile of summer growing-season temperature: curious cooling in agricultural regions

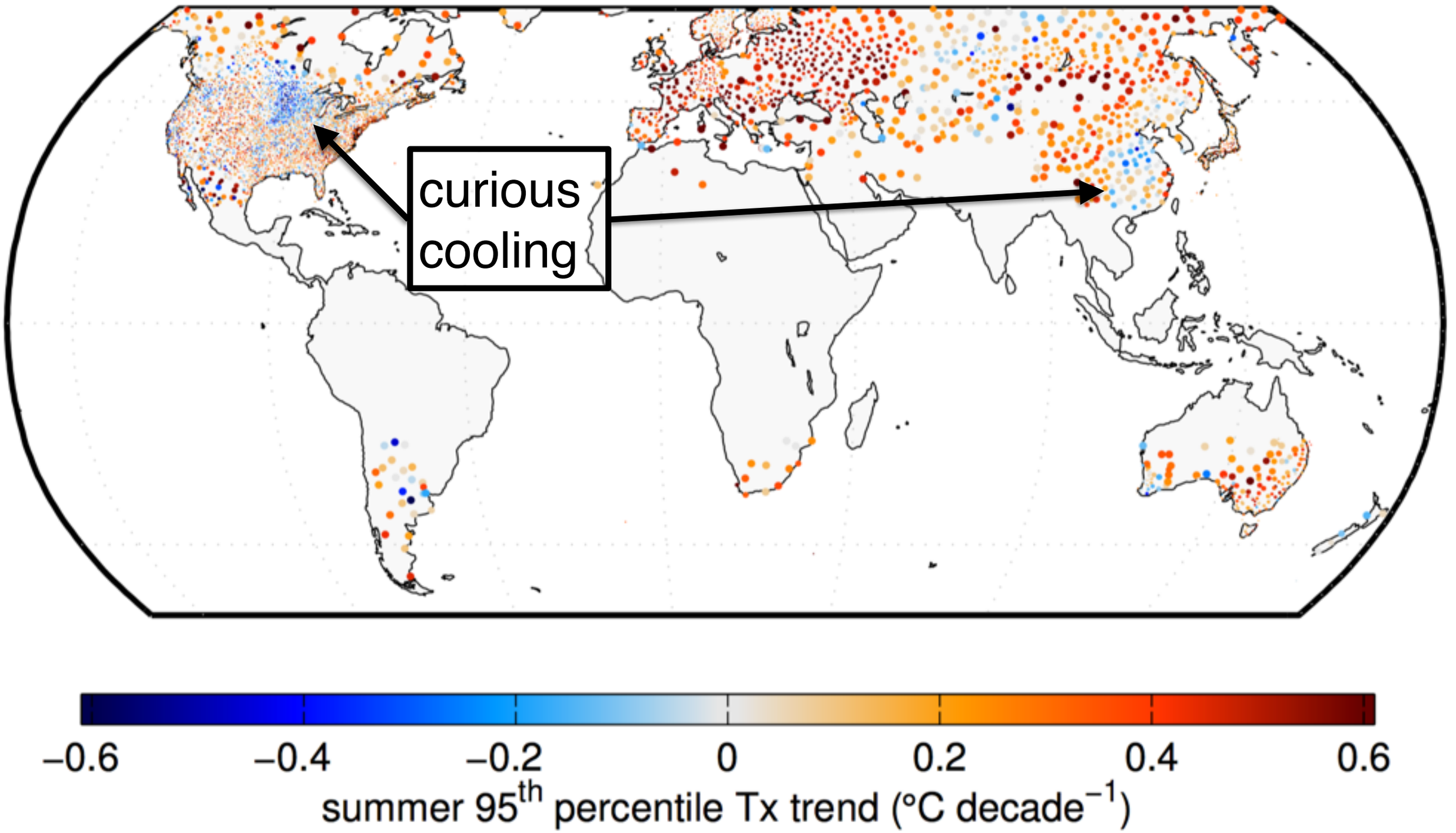

Zoom-in on the U.S. midwest

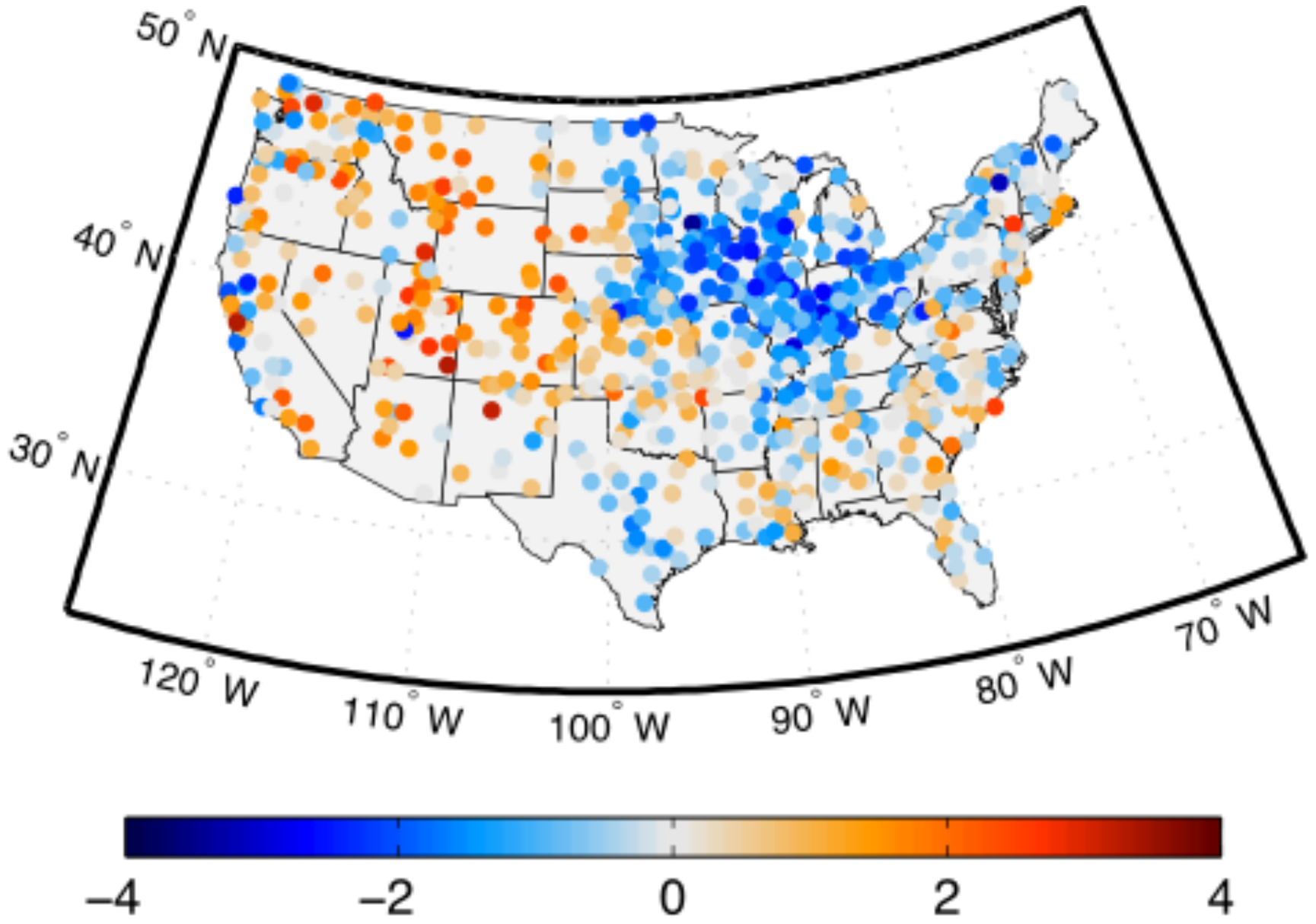

(Mueller et al., 2016)

Hypothesis i: conversion of land to crop use

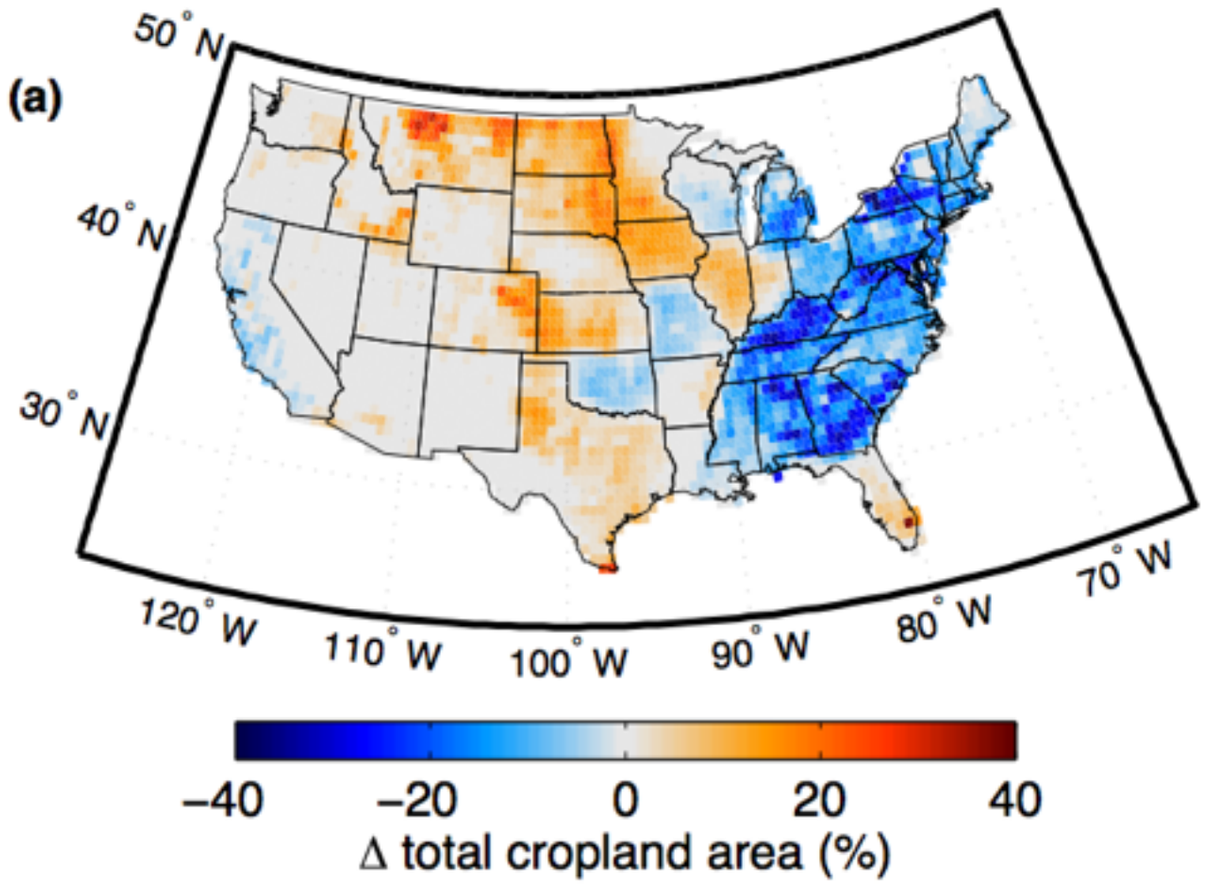

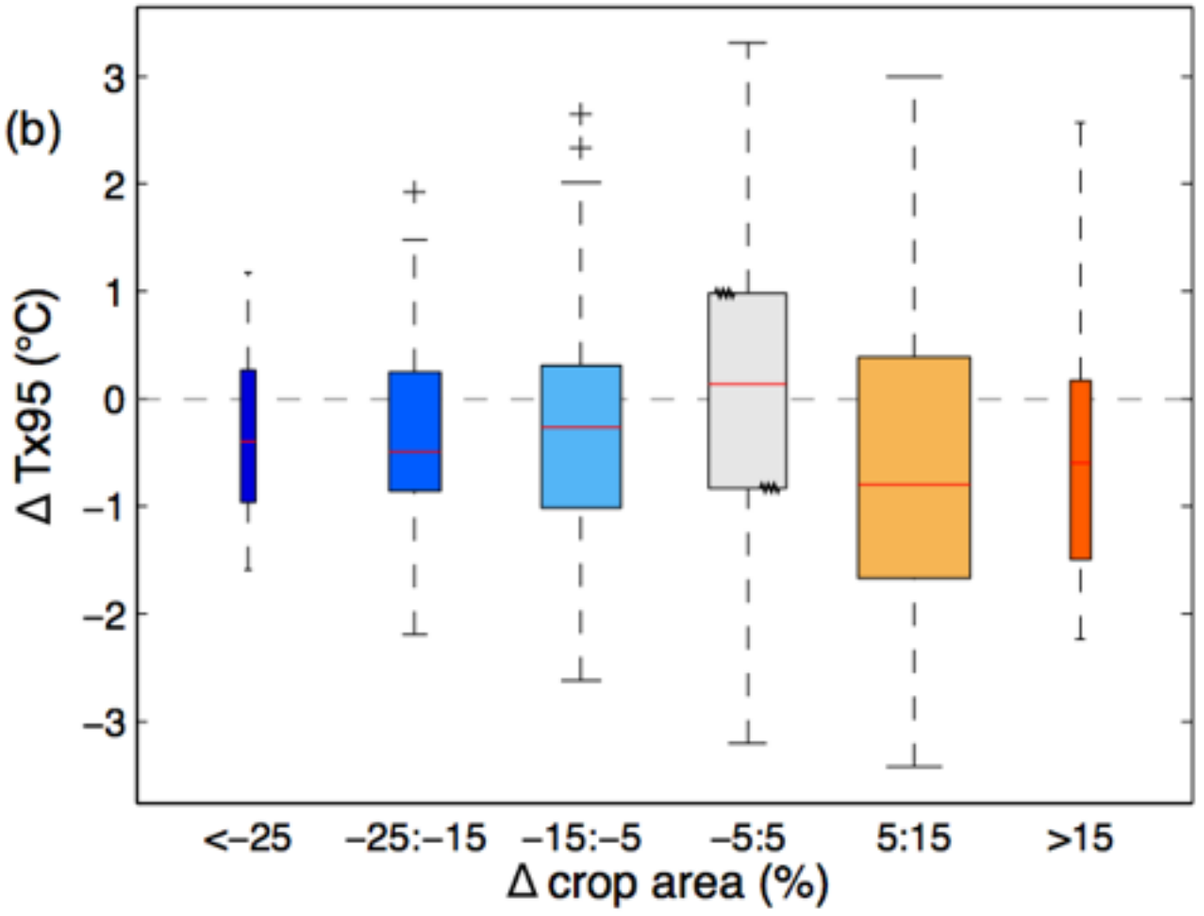

The pattern of crop conversion over the last century does not correspond to observed regions of cooling in extreme temperatures.

(Mueller et al., 2016)

Hypothesis ii: increased irrigation

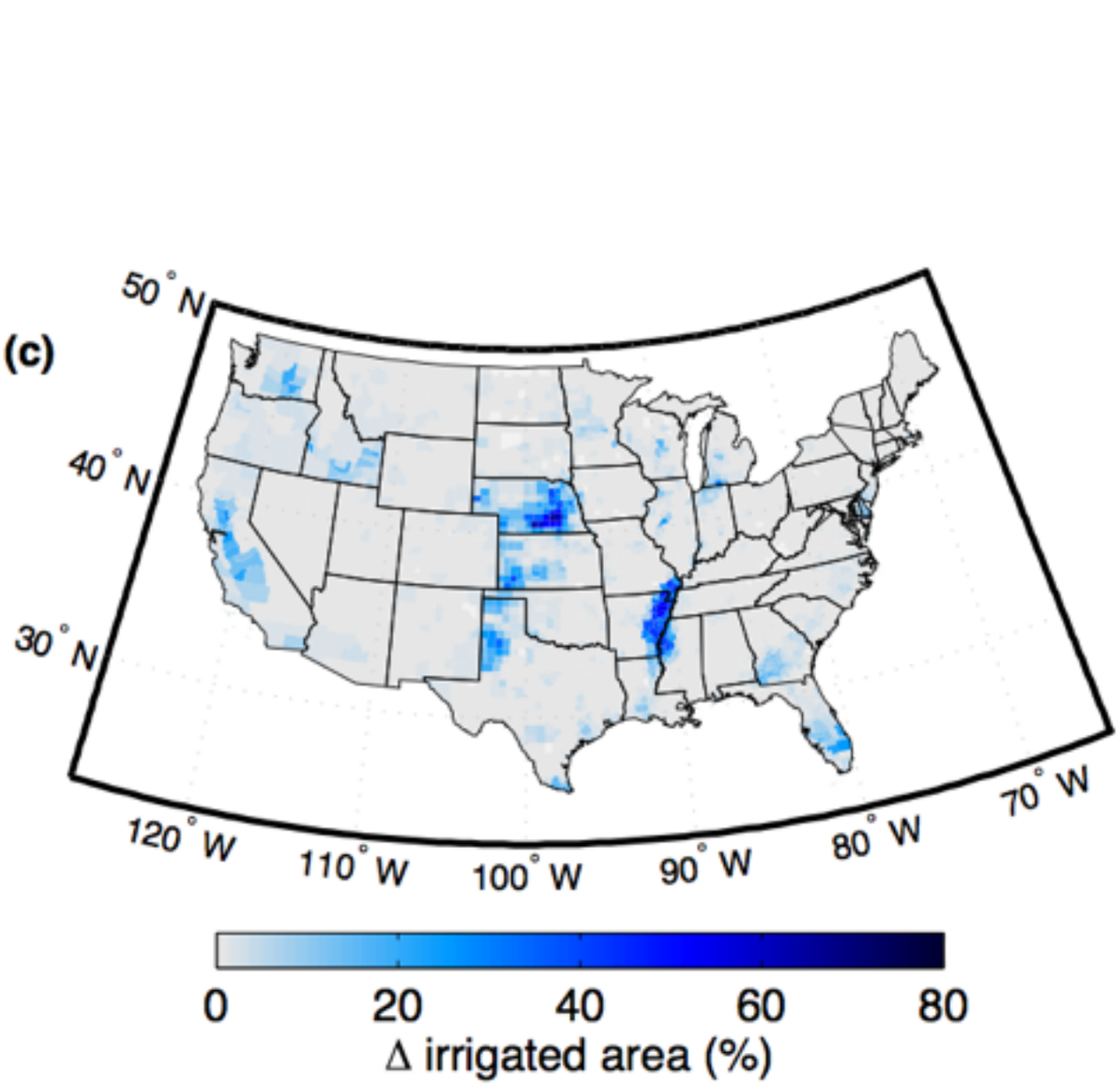

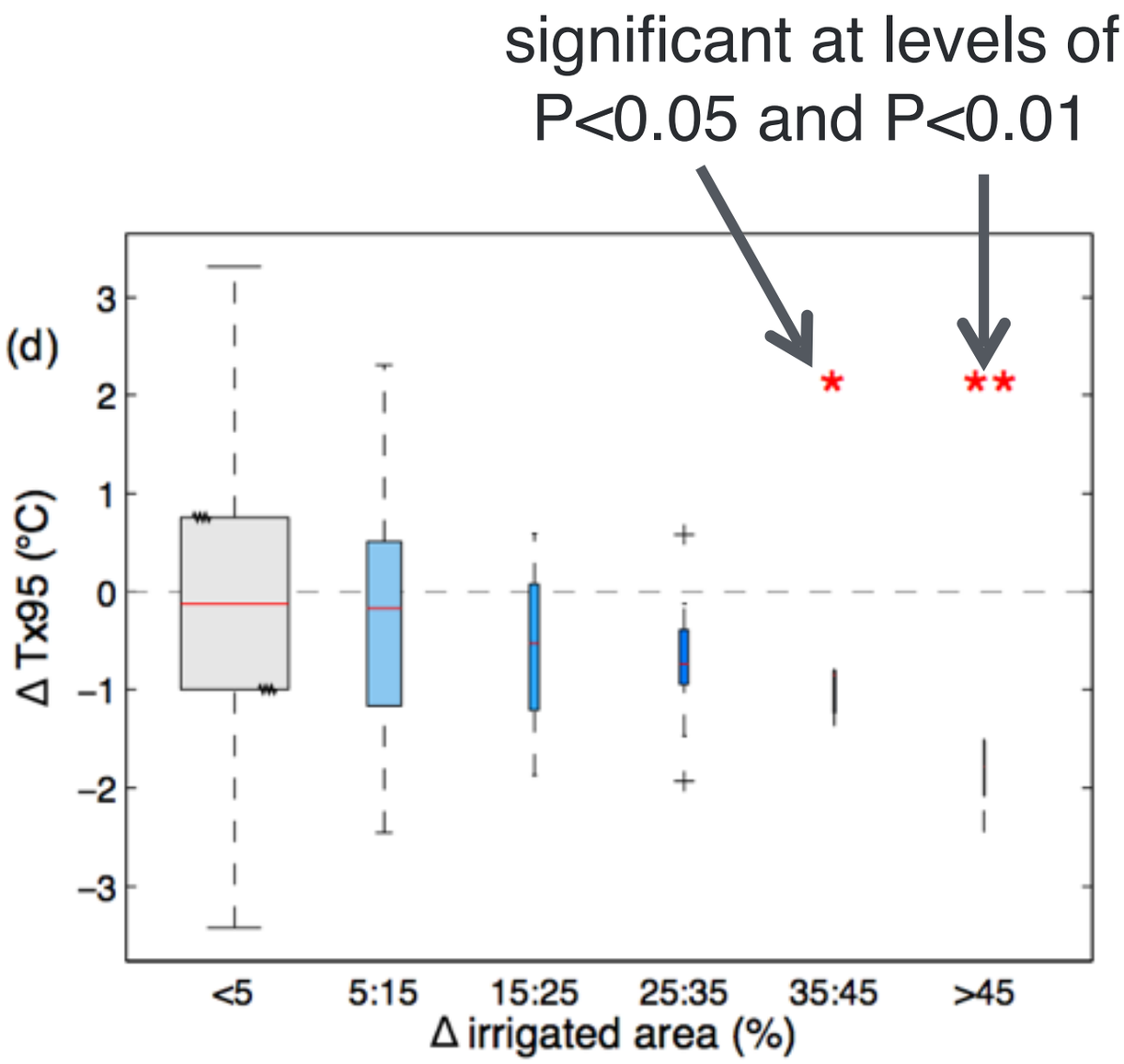

Regions with increased irrigation show marked cooling in extreme temperatures, but these do not account for much of the spatial pattern

✓ Hypothesis iii: increased agricultural intensity

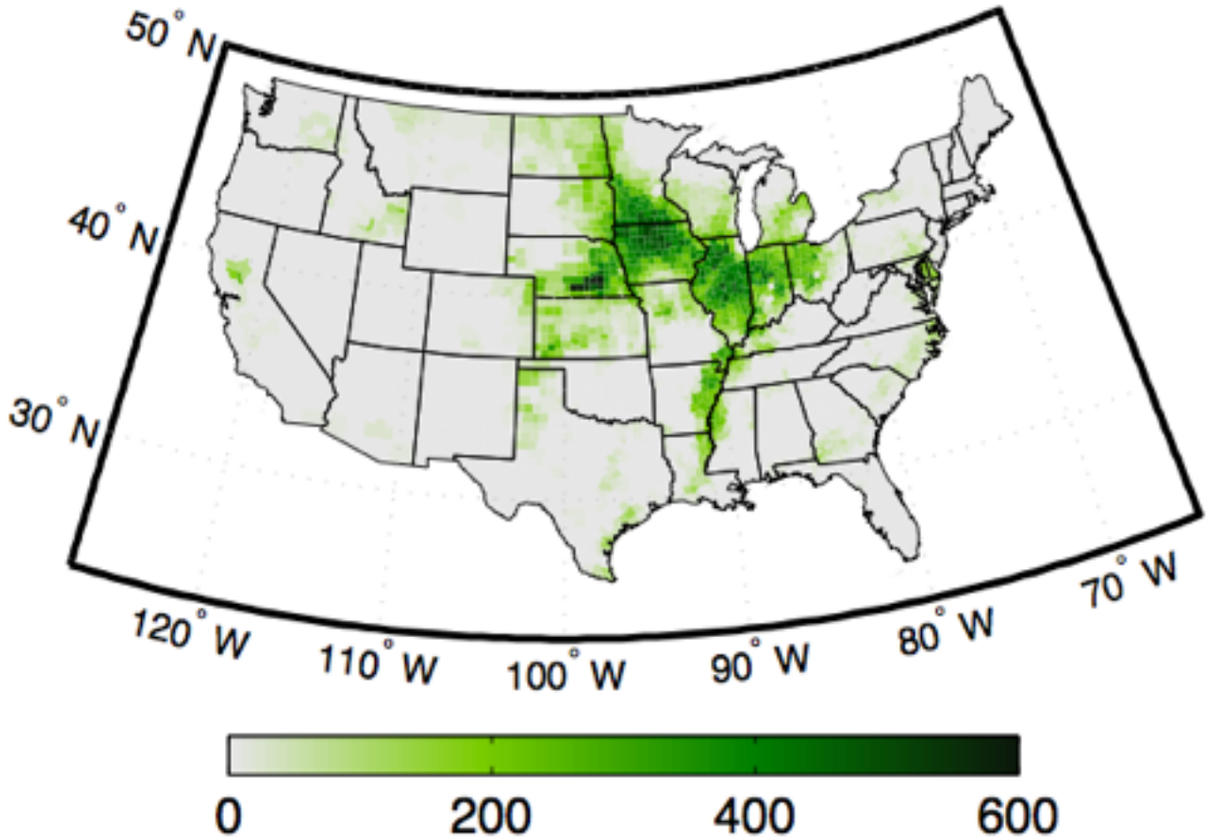

Change in Net Primary Production gC/(m²yr)

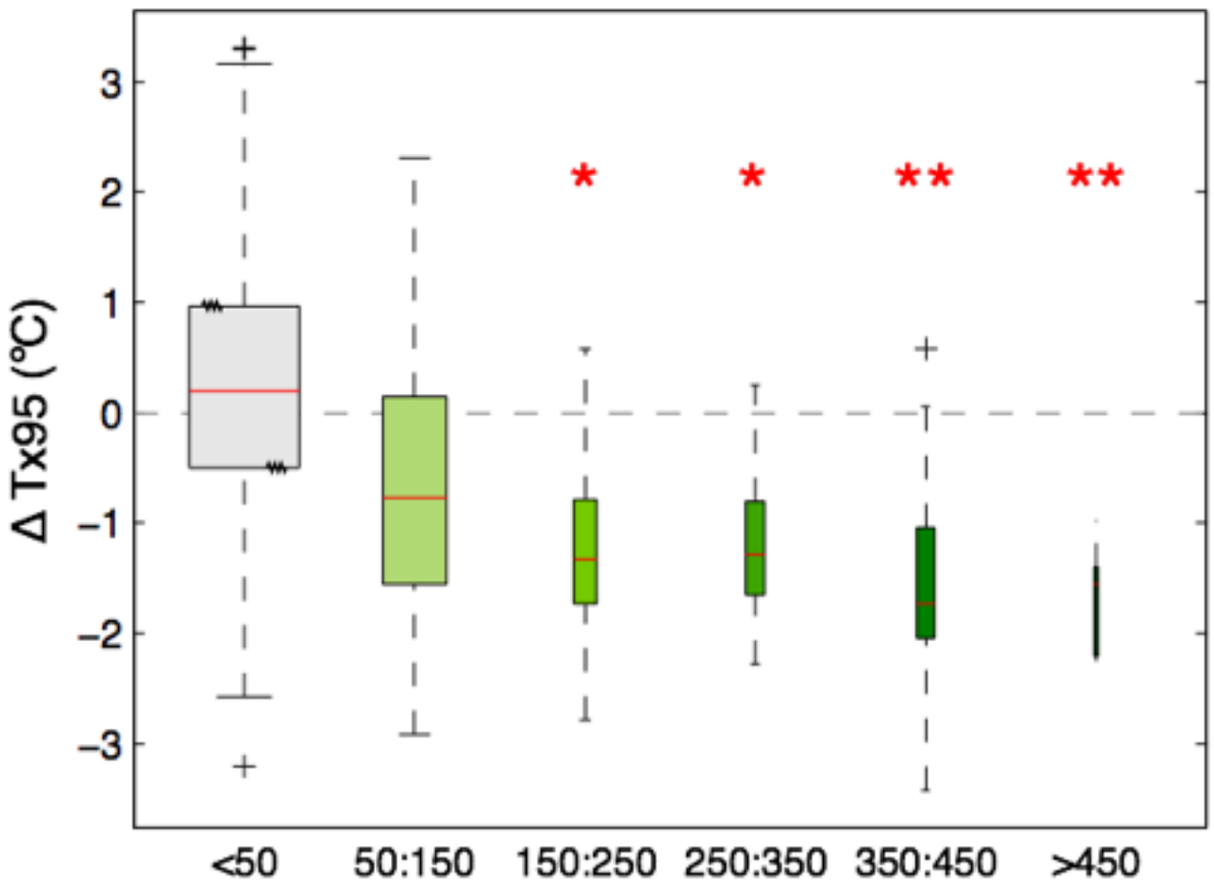

Change in Net Primary Production gC/(m²yr)

Field studies demonstrate that more recent cultivars of wheat, soy, and maize each show lower canopy temperatures. Wheat and soy cooling is associated with greater stomatal conductance. Maize cooling may be associated with delayed leaf senescence and rooting that gives greater access to water.

Loss of evaporative cooling leads to higher temperatures and greater plant stress.

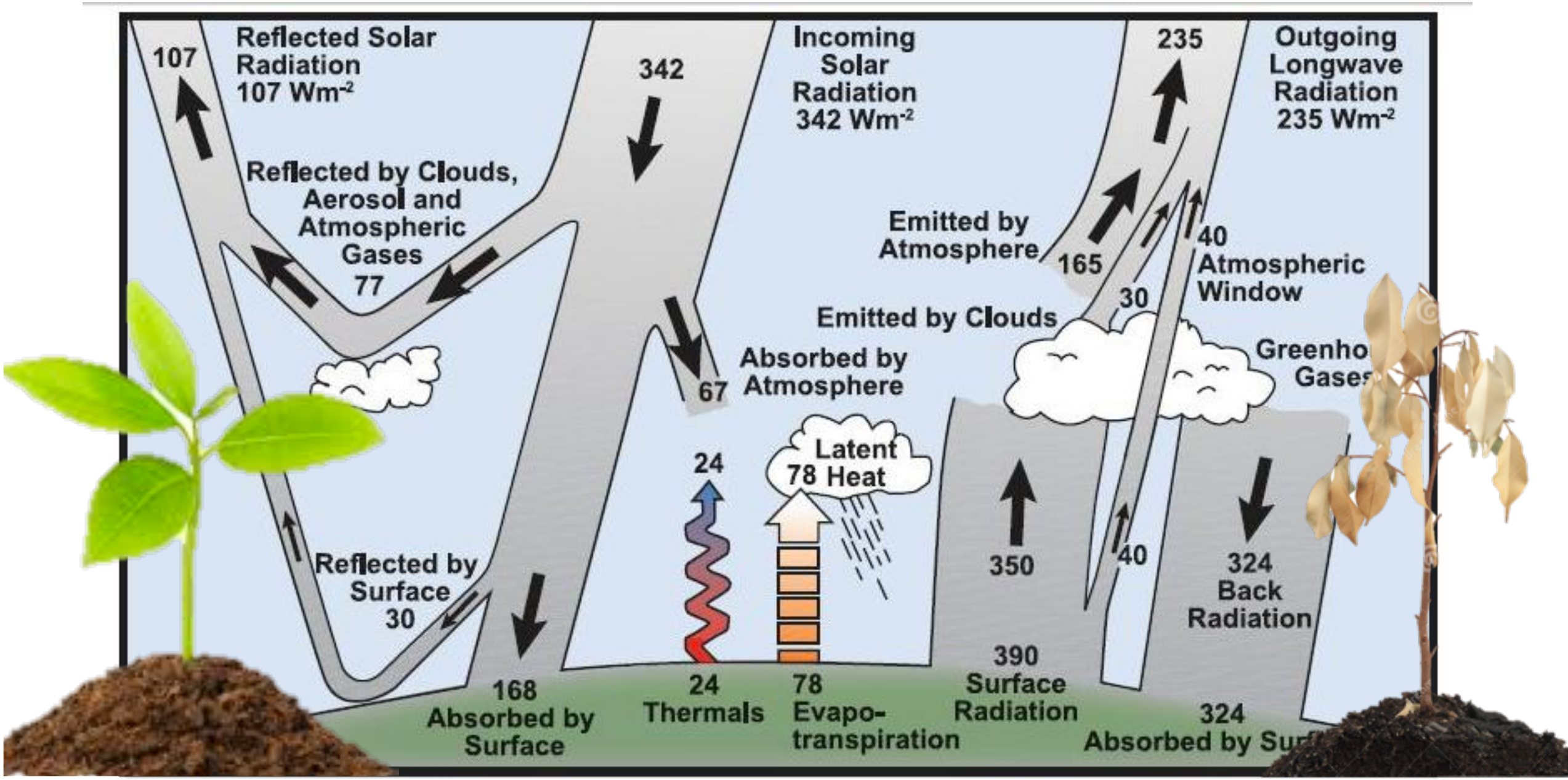

During drought, however, rainfed agricultural regions return to historically high temperatures

Irrigated

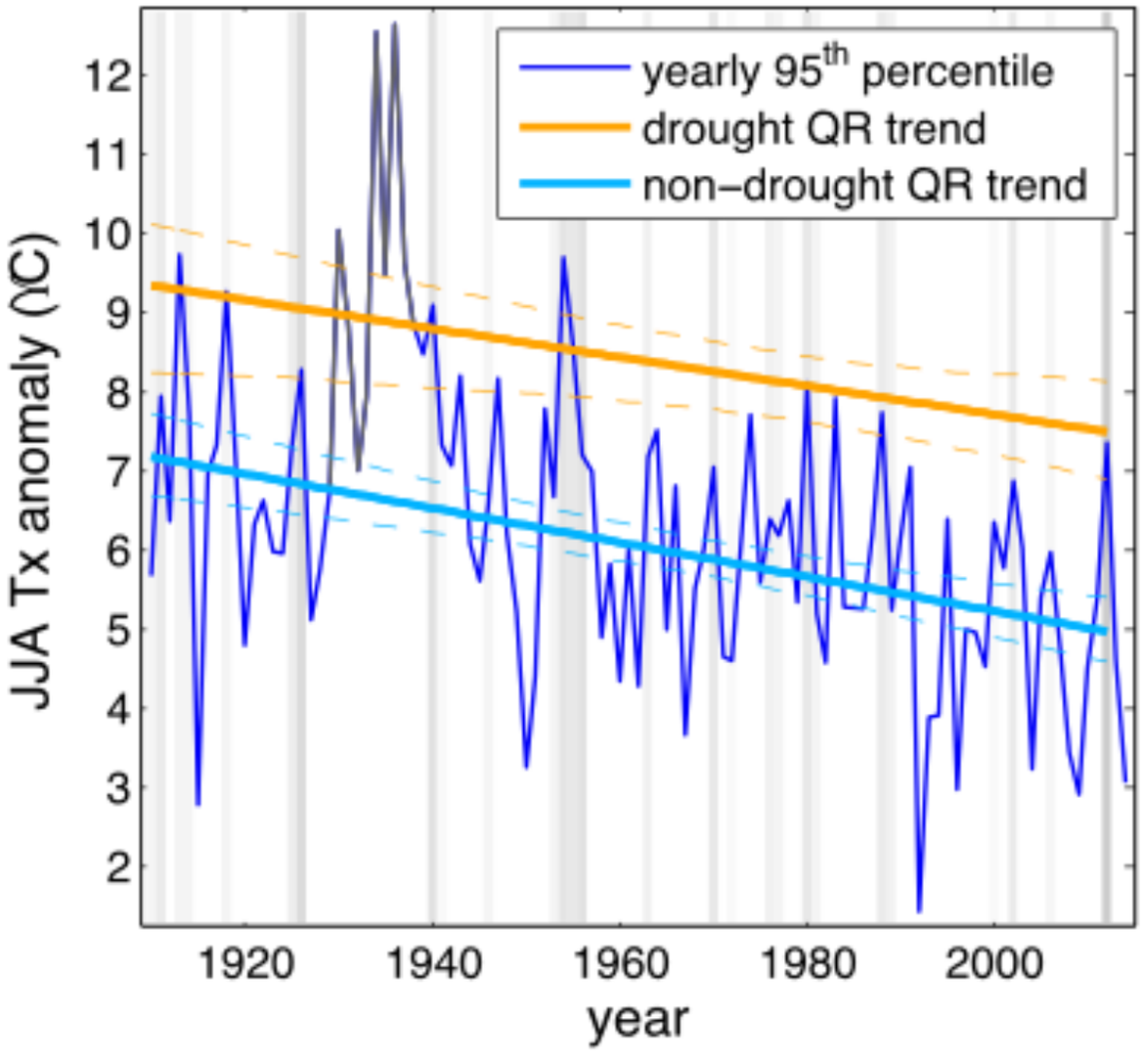

Rainfed

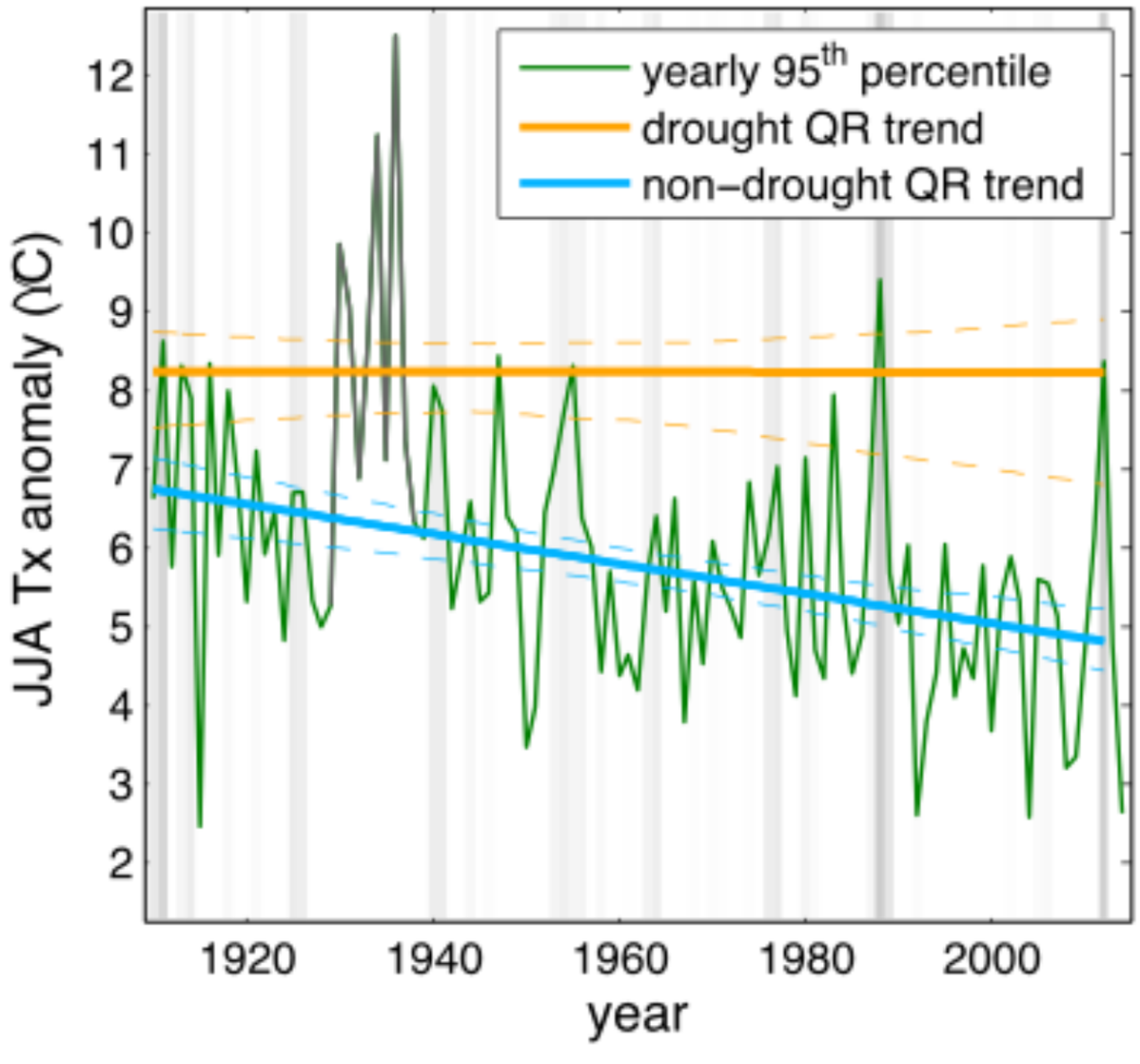

(Mueller et al., 2016)

Agricultural is a major driver of change. It involves 45% of Earth's land surface, 65% of global water withdrawal, and 25% of human greenhouse gas emissions.

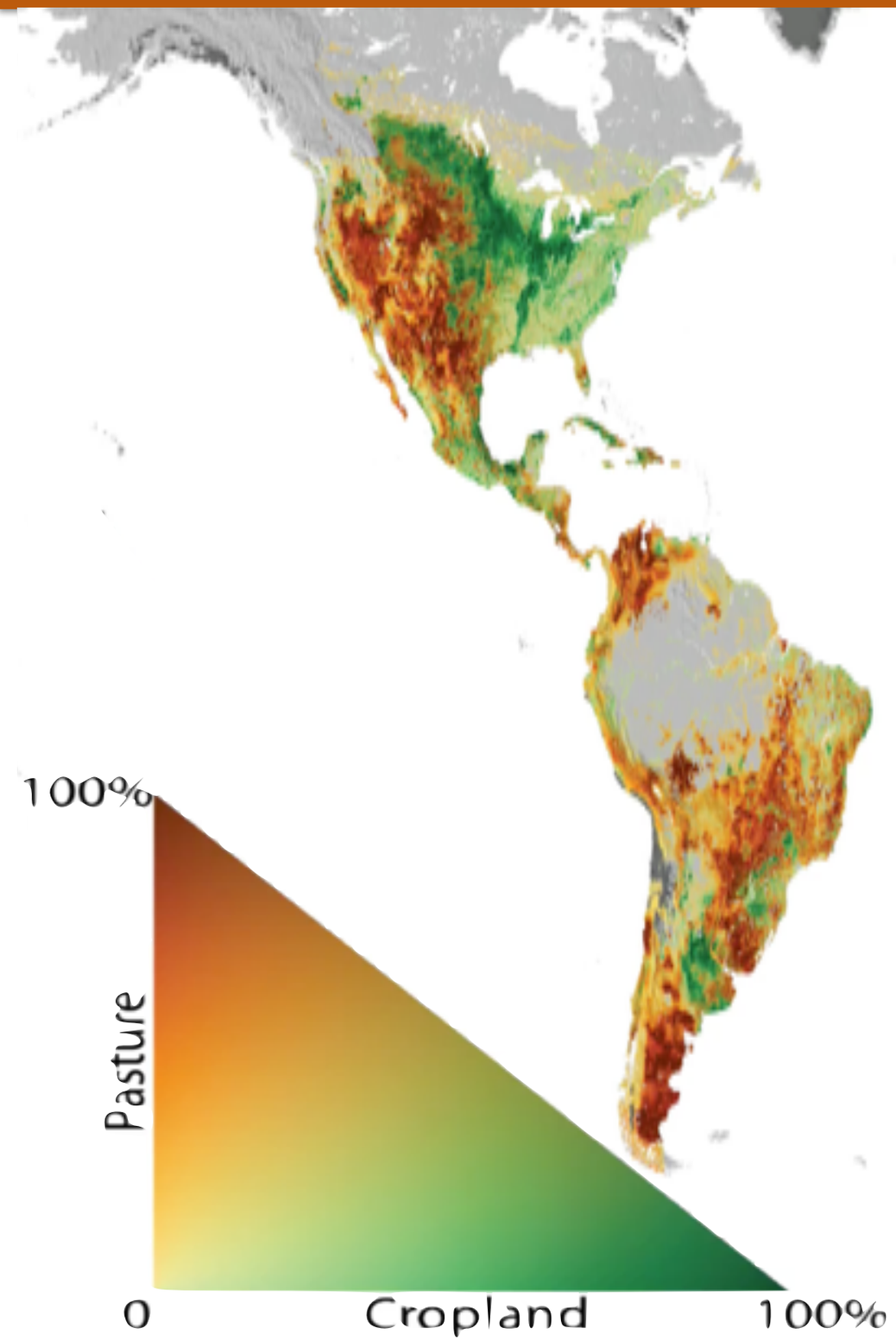

(*Ramankuty* et al., 2008)

Peak monthly chlorophyll fluorescence is greater in mid-latitude agricultural regions than in tropical rainforests

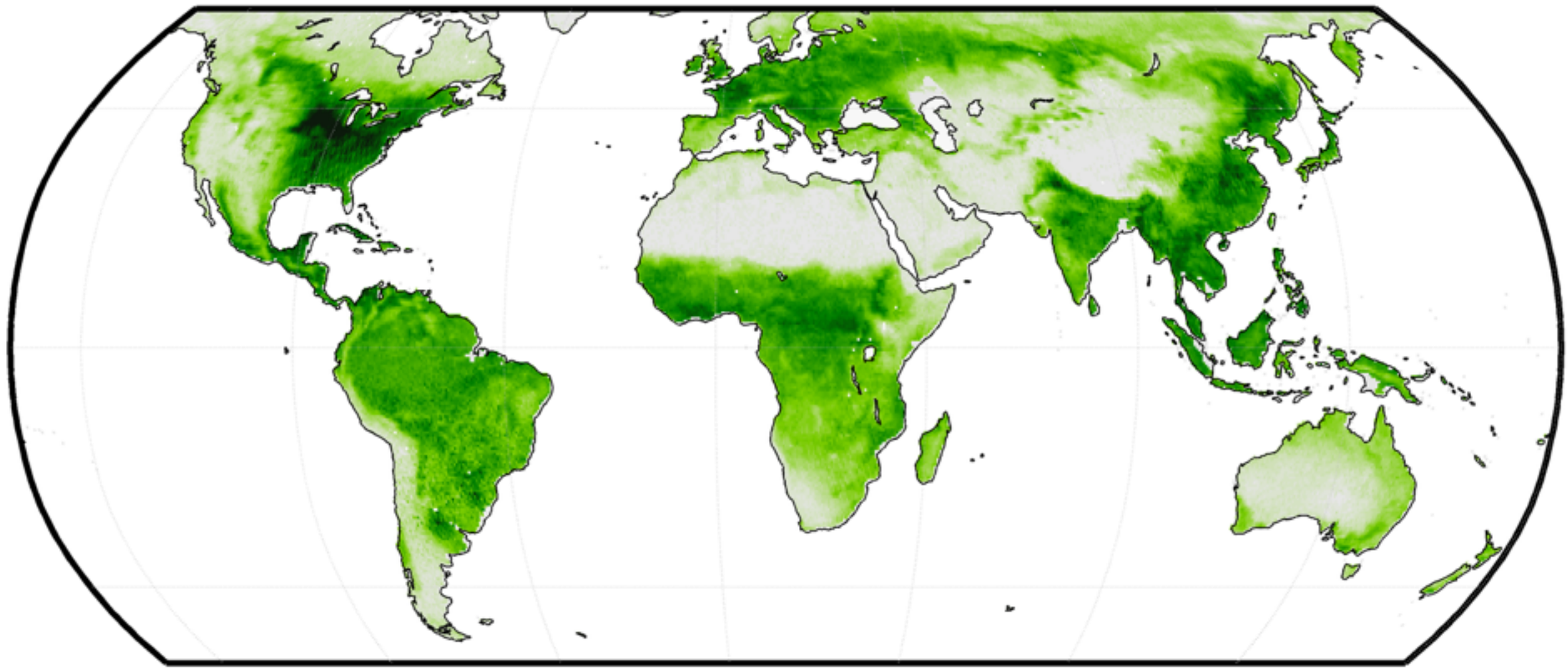

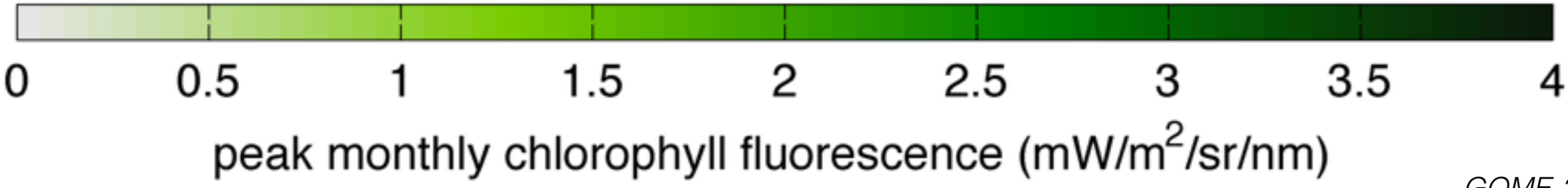

GOME-2 data from Joiner et al. 2013

Seven agricultural regions where summer primary production has increased since 1960.

North China Plain: Sun-induced chlorophyll fluorescence (SIF) peaks during summer cropping.

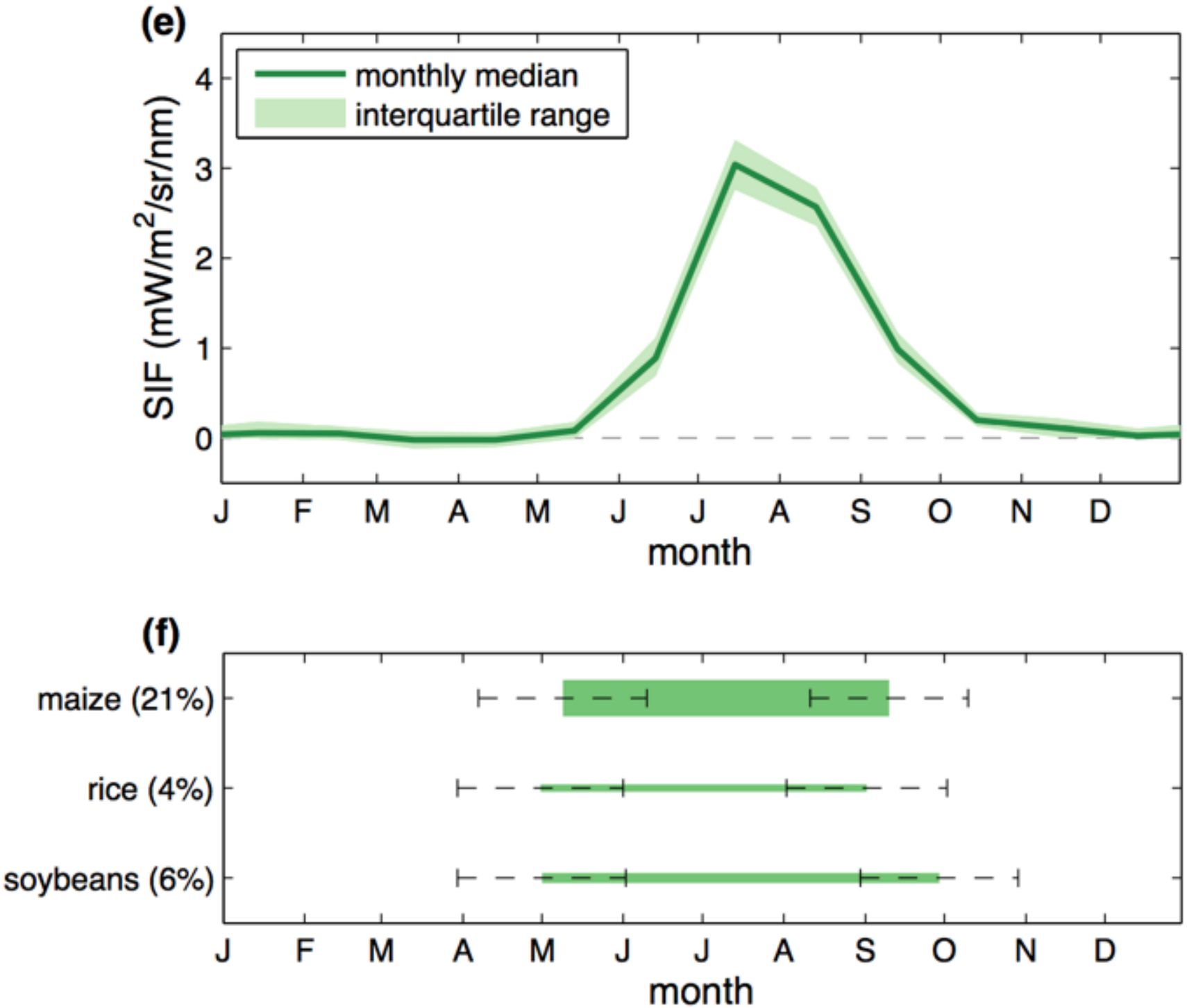

(*Mueller* et al. 2017)

North China Plain: The spatial pattern in cropland area trends do not correspond with cooling of 95th percentile temperatures, but trends in irrigation show some relationship

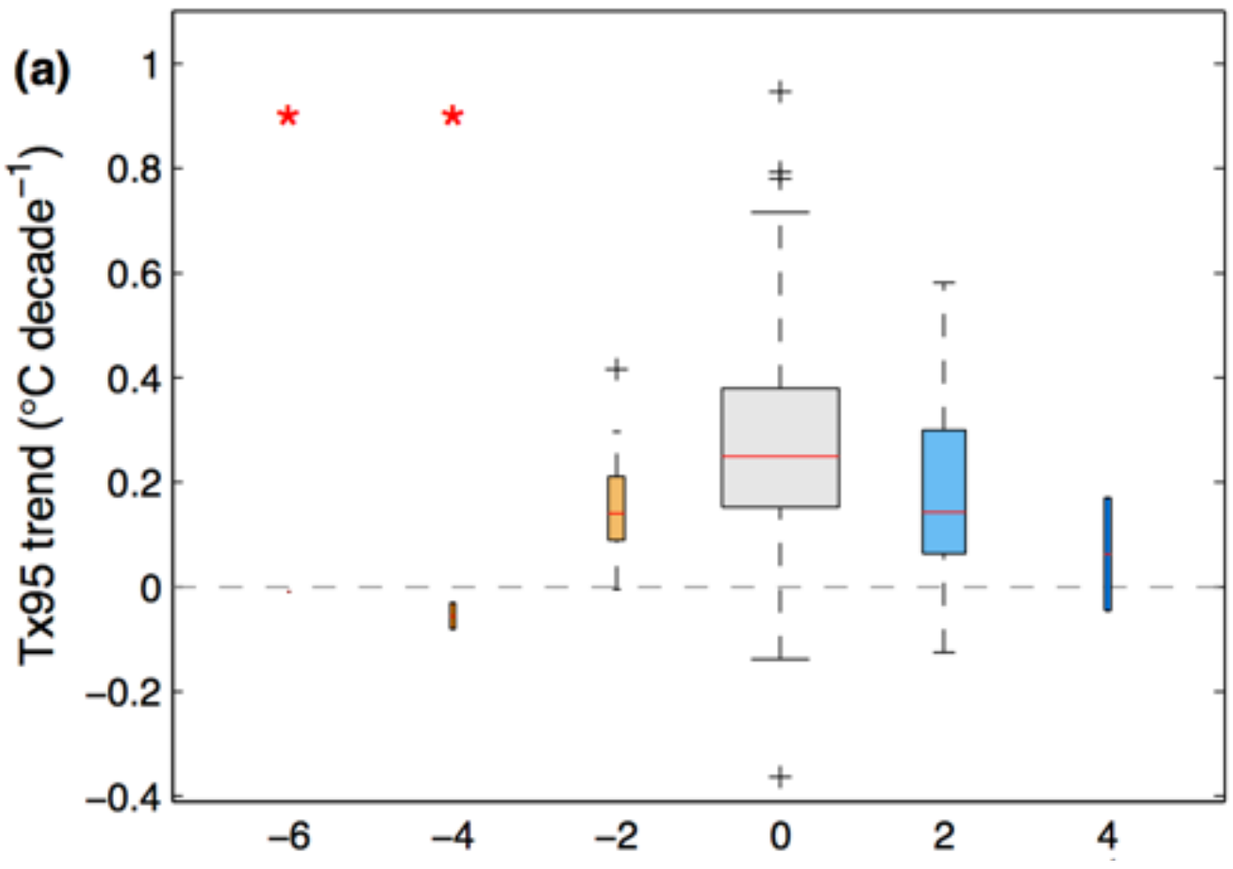

Cropland Area Trend
(% grid cell per decade)

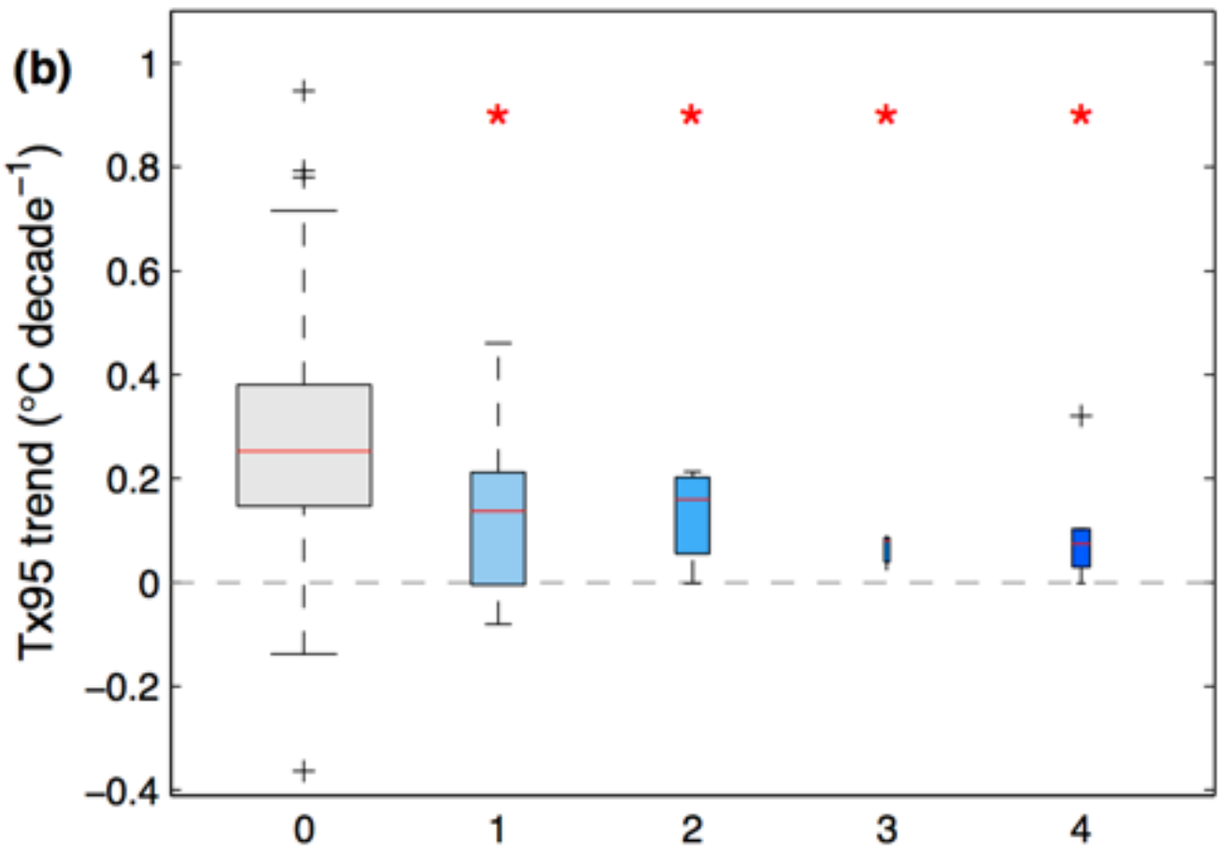

Area Equipped for Irrigation
(% grid cell per decade)

North China Plain: Precipitation variations are weak, but trends in summer cropping intensity are clearly associated.

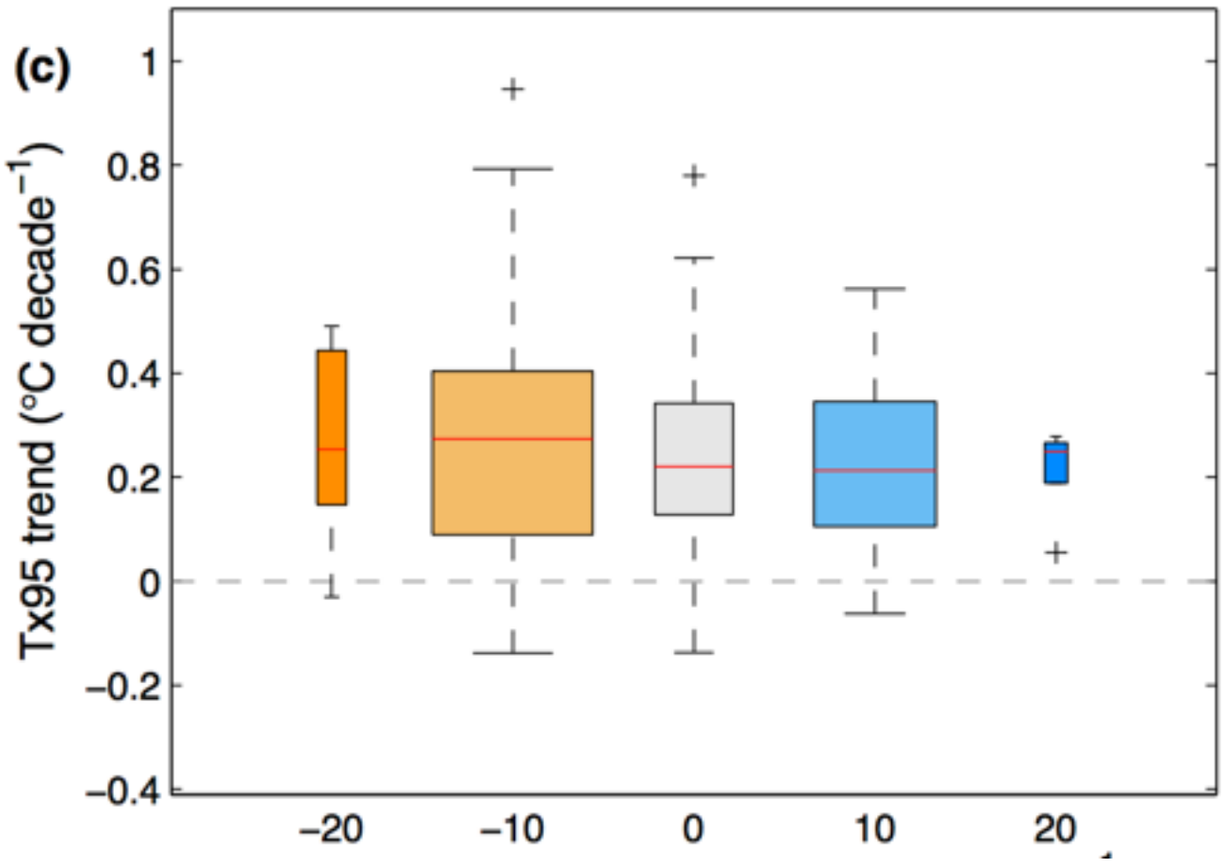

Summer Precipitation trend
(mm per decade)

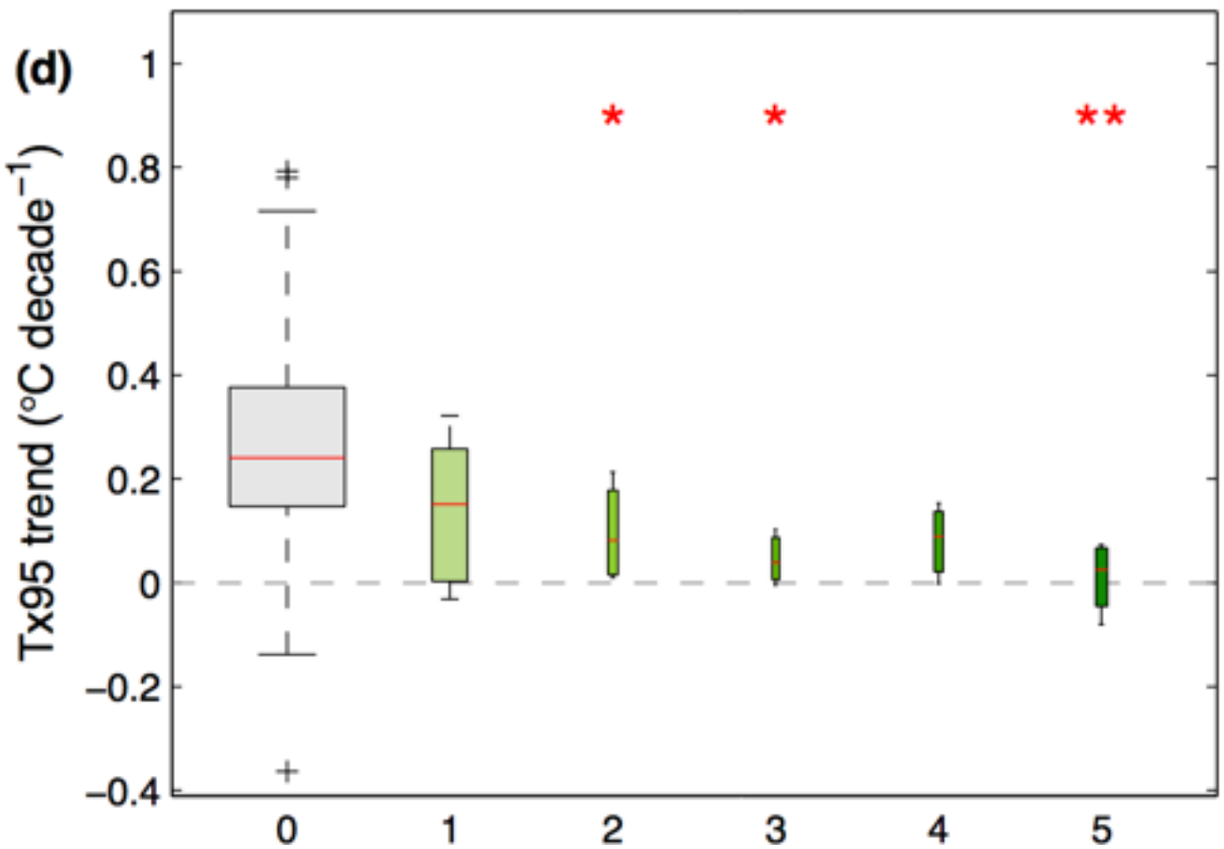

Trend in Summer Primary Production
(g C m^{-2} year^{-1})

East China: Sun-induced chlorophyll fluorescence (SIF) shows two peaks associated with double cropping an winter wheat

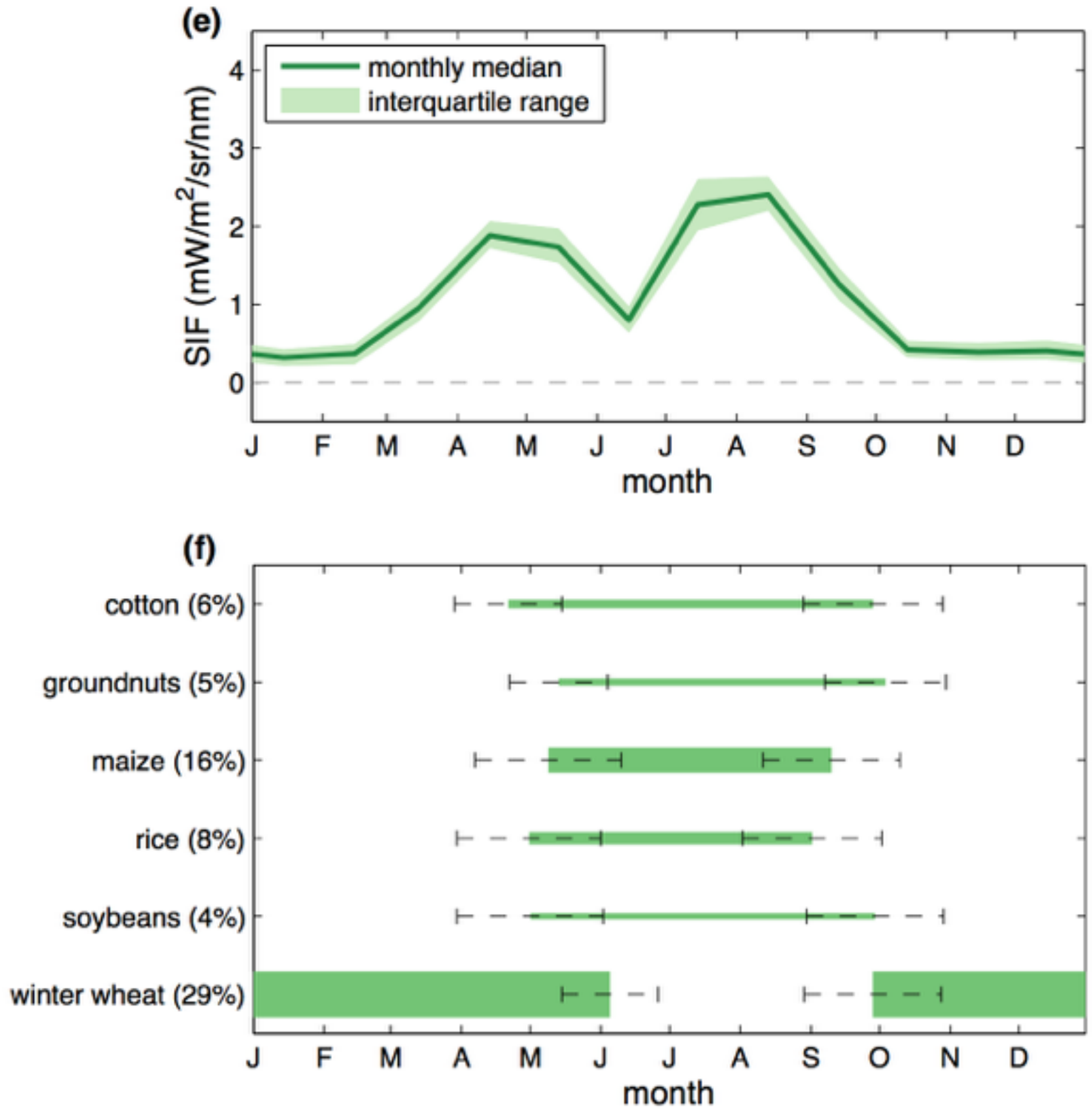

East China: Not cropland area, but irrigation corresponds with regional cooling

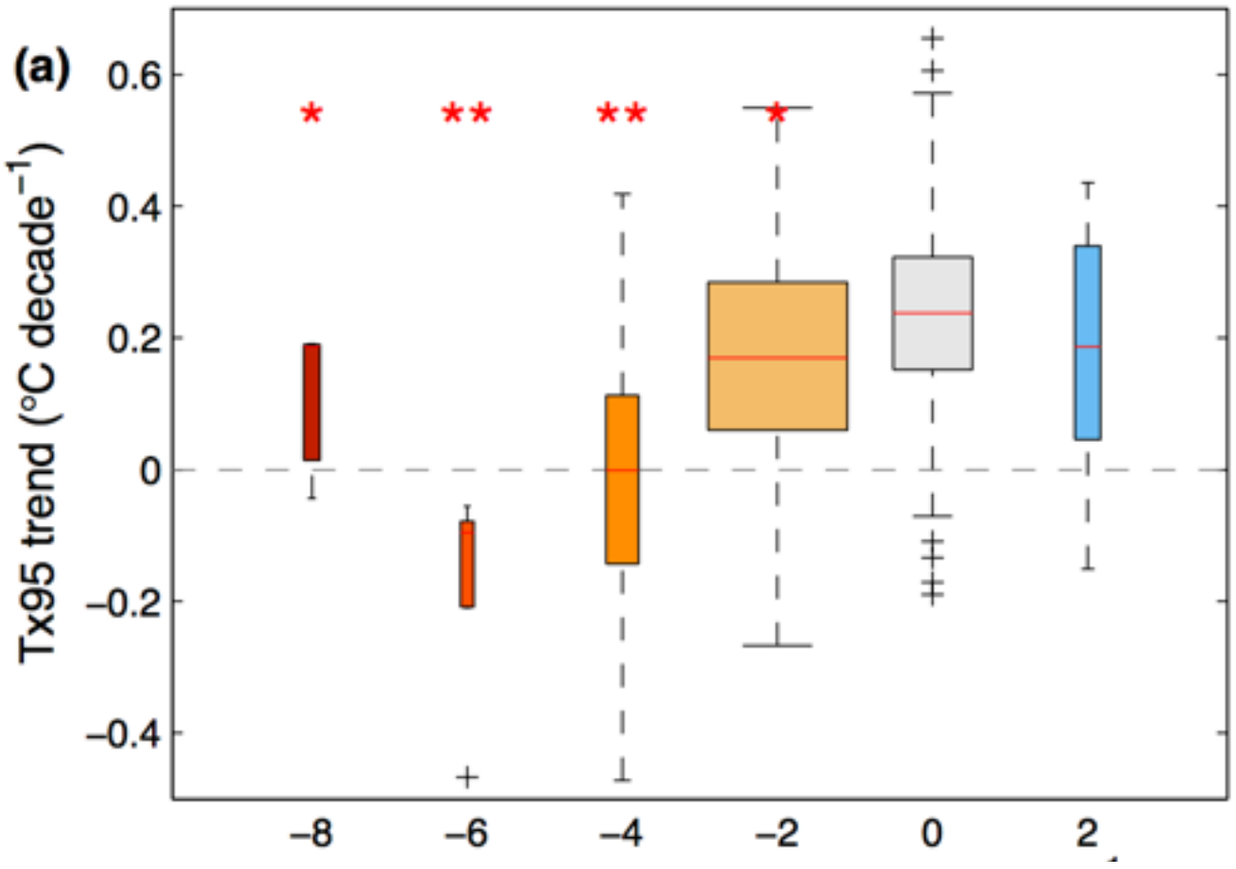

Cropland Area Trend
(% grid cell per decade)

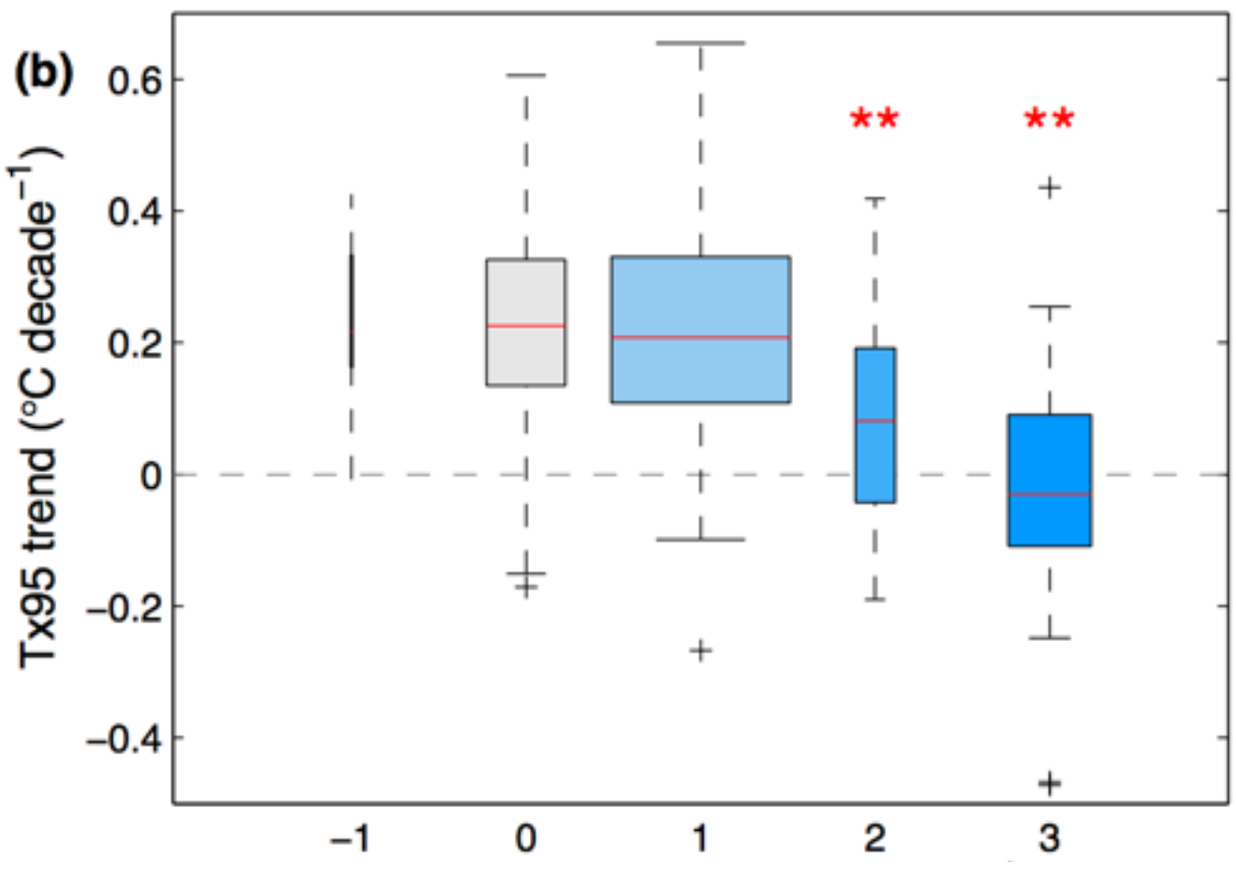

Area Equipped for Irrigation
(% grid cell per decade)

East China: Precipitation has a weak relationship, whereas trends in summer primary production are clearly associated.

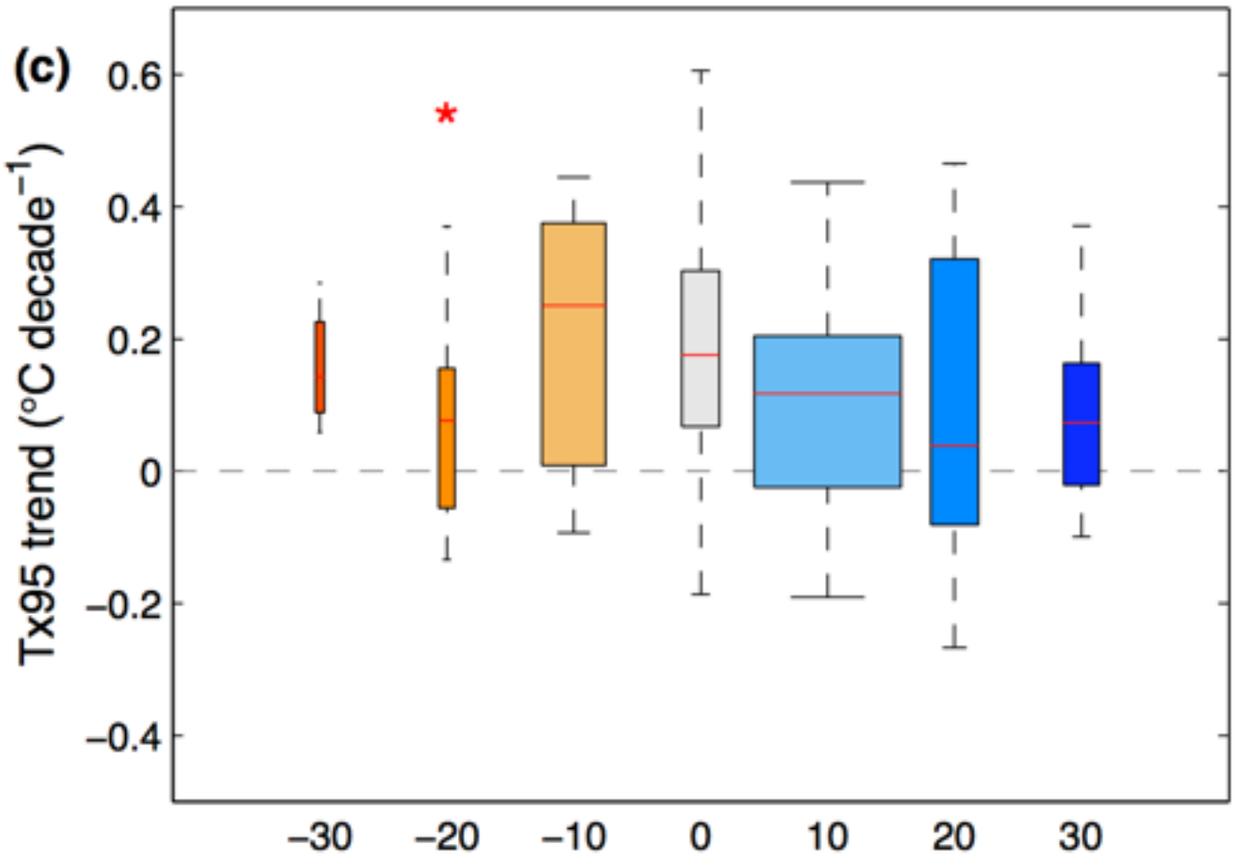

Summer Precipitation trend
(mm per decade)

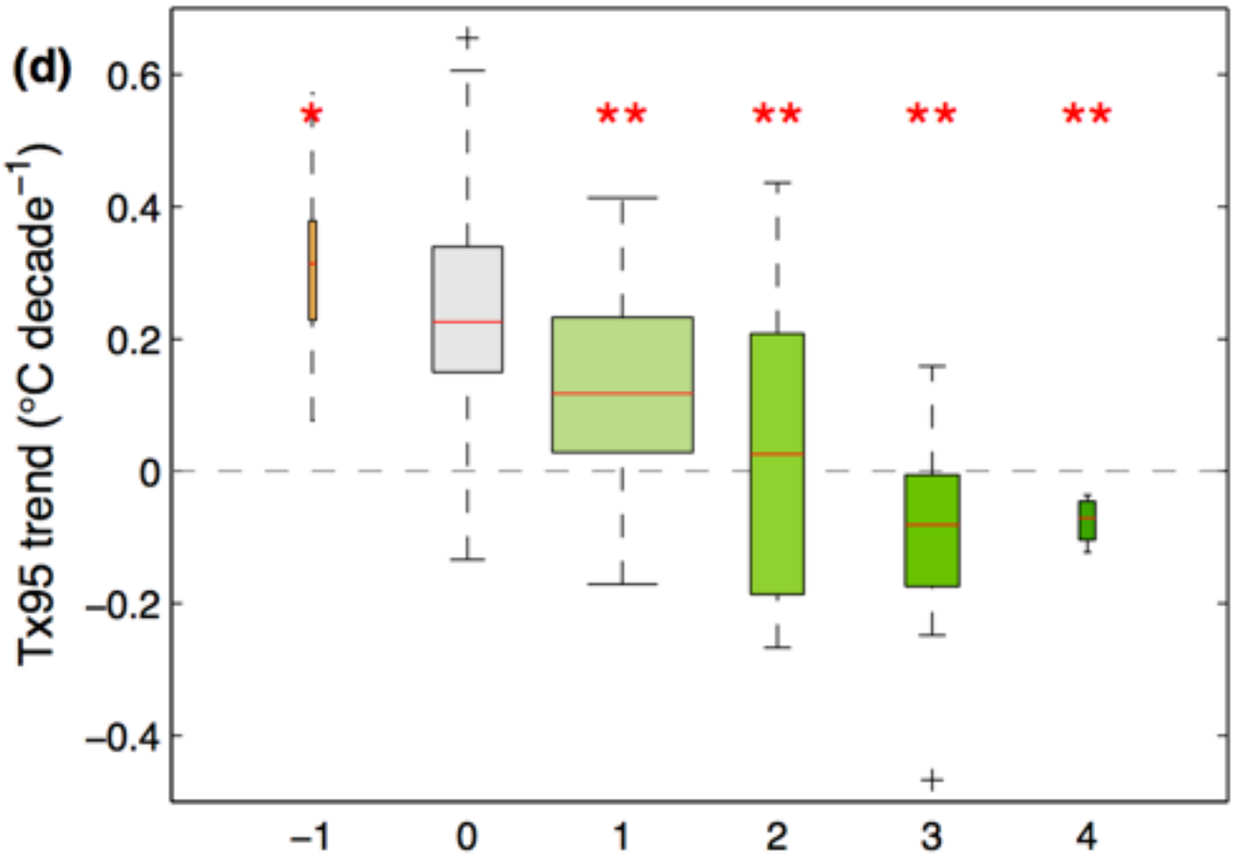

Trend in Summer Primary Production
(g C m^{-2} year^{-1})

These results are broadly consistent with those of *Hu et al*. (2010), *Cao et al.* (2015), and *Zhao et al.* (2016).

Outline

Part 1.
Mean temperatures are increasing, but high-temperature excursions above the mean are generally stable.
(*M. Tingley* and *A. Rhines*)

Part 2.
The hottest temperatures have been cooling in regions with rapid agricultural intensification
(*N. Mueller, E. Butler*, A. Rhines, and *N. Holbrook*)

Part 3.
Implications for yield trends
(*N. Mueller, E. Butler*, and *N. Holbrook*)

Food requirements are anticipated to rise at only slightly less than a linear rate based upon UN population predictions.

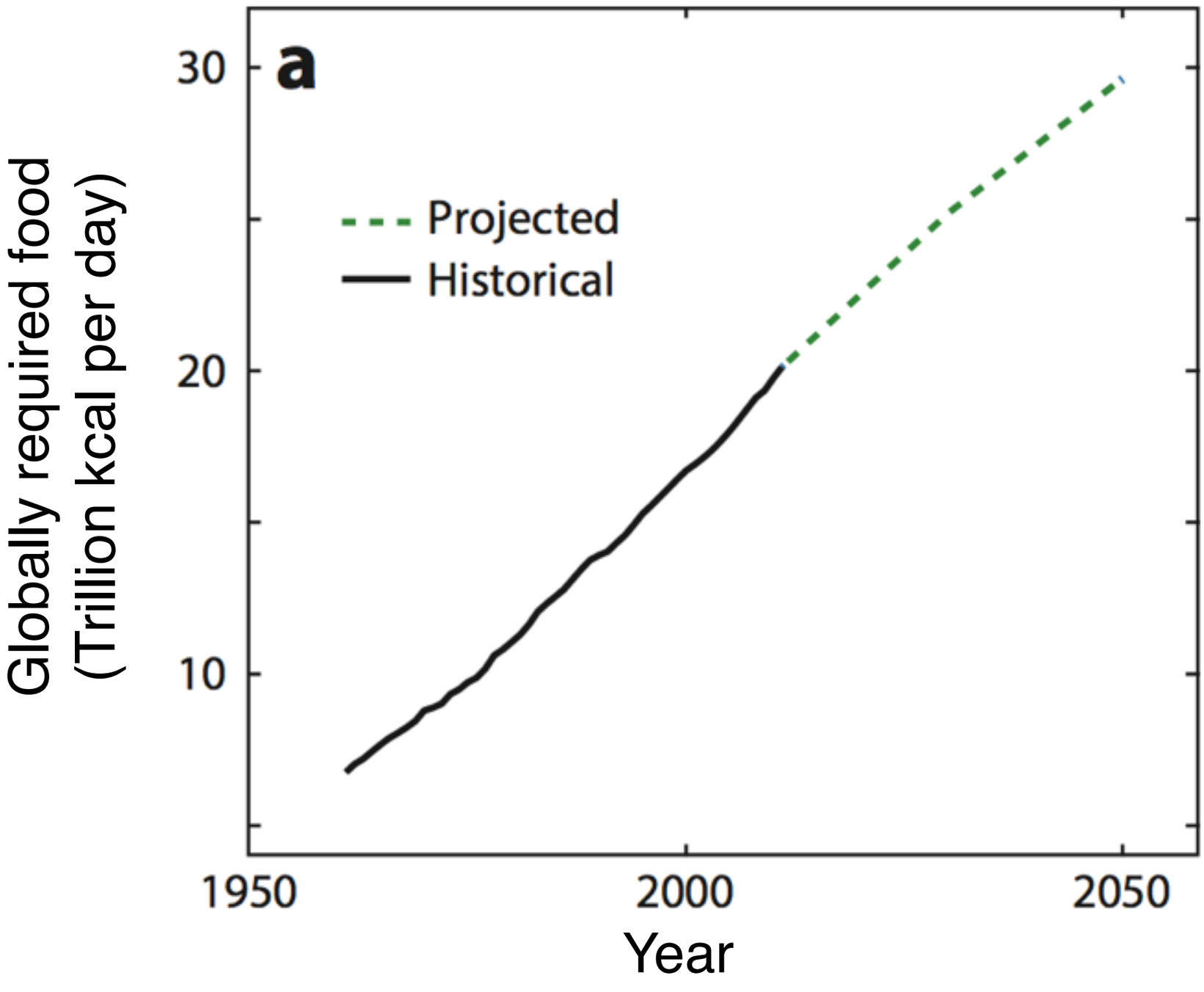

The trend in US corn yield indicates doubling from 1965-2014, though there is substantial volatility.

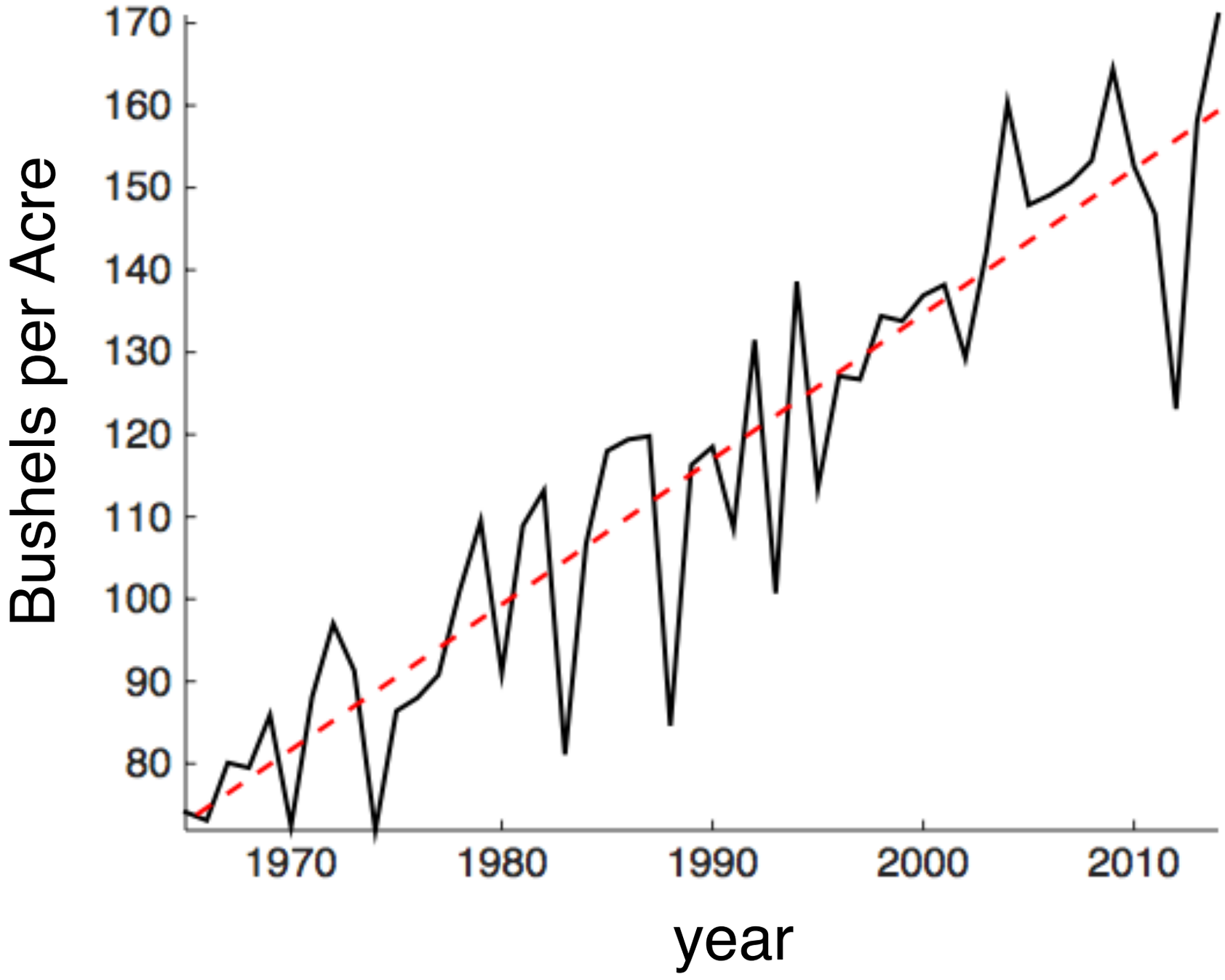

Temperature explains the majority of yield volatility

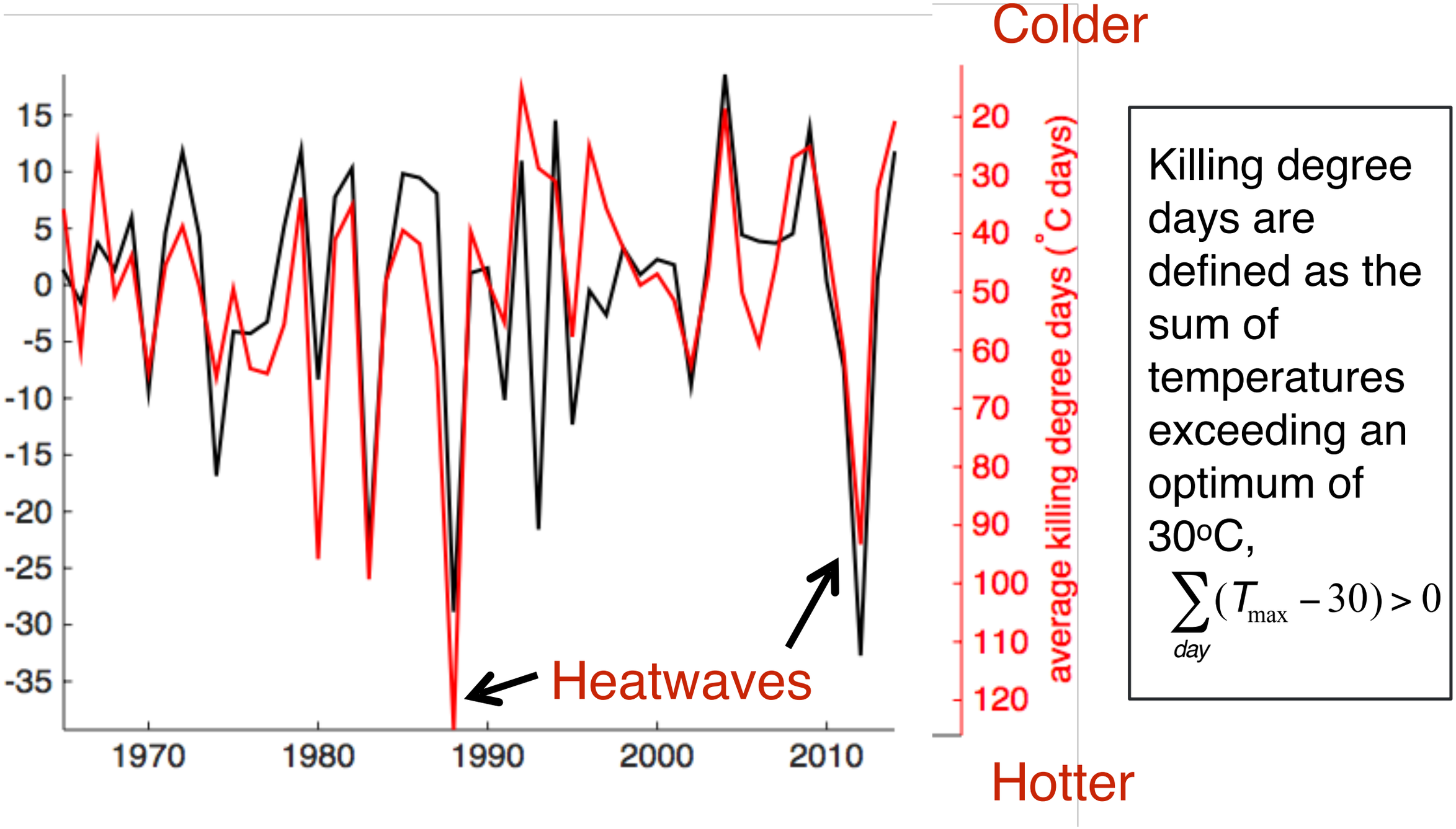

Killing degree days are defined as the sum of temperatures exceeding an optimum of 30°C,

$$\sum_{day}(T_{\max} - 30) > 0$$

Over the last 40 years, mean warming coupled with fewer heatwaves has allowed for longer-maturing crops with less exposure to heat stress.

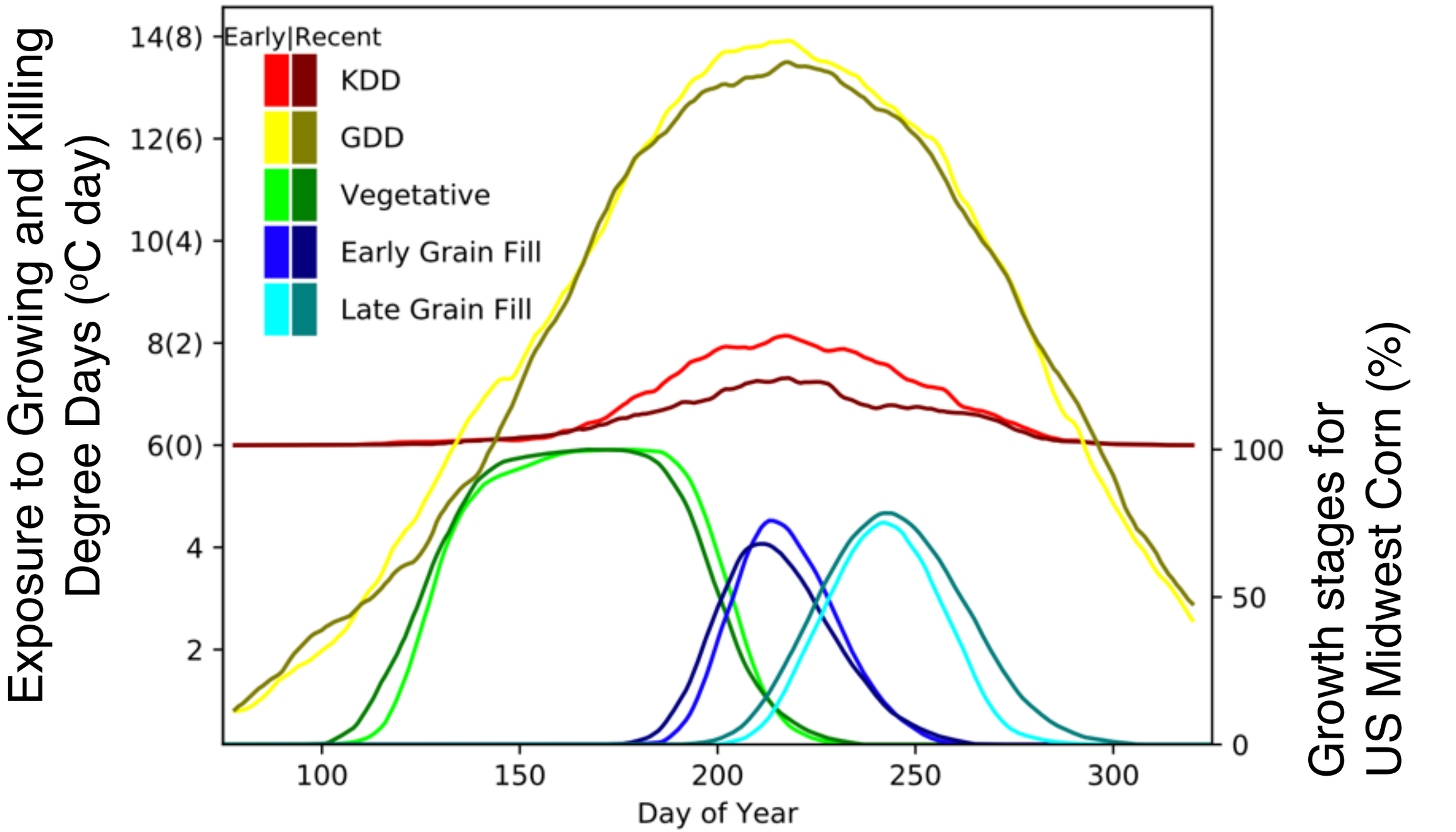

(*Butler* et al., in prep)

28% of yield increases in the U.S. Midwest are attributable to better weather. The case appears similar for China.

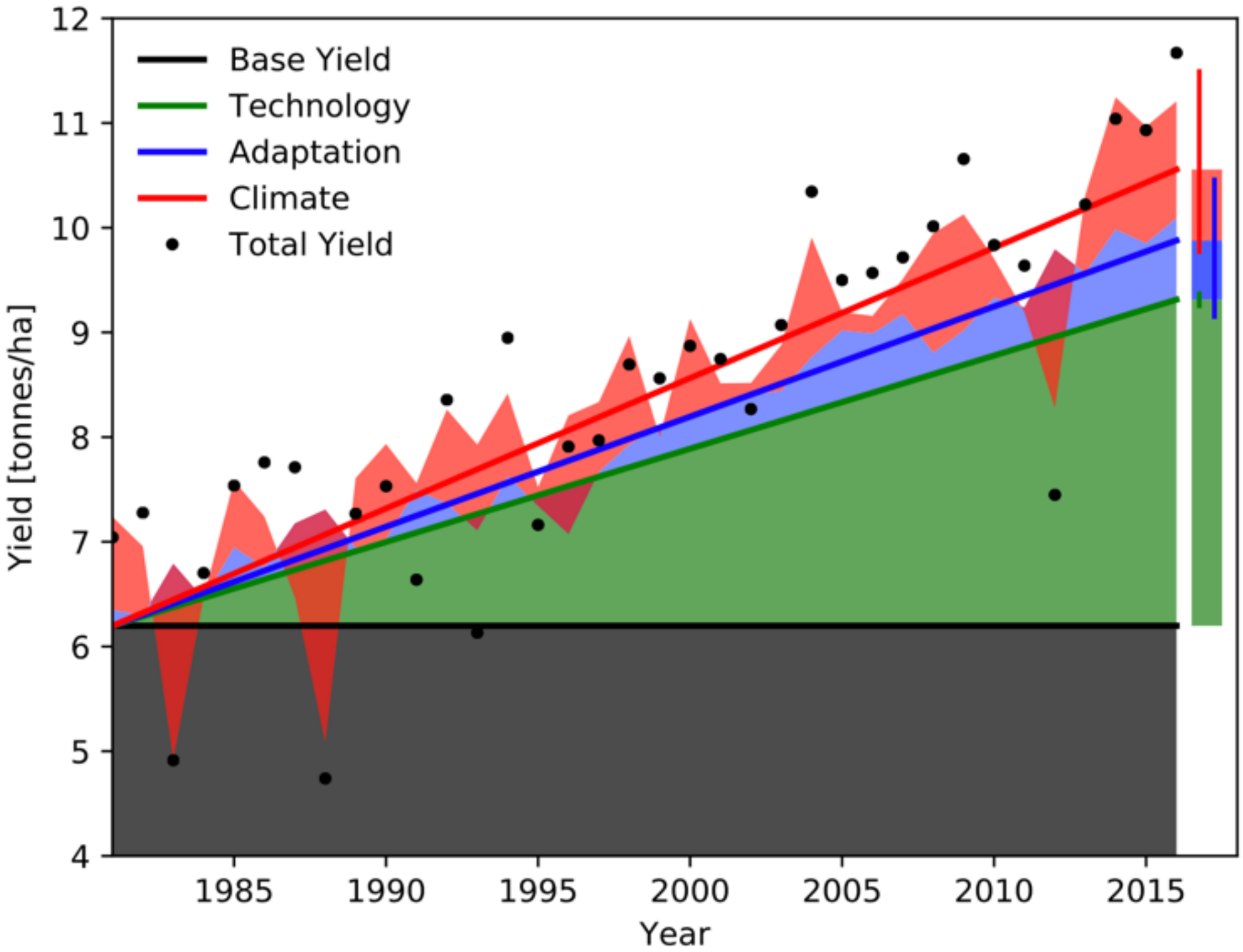

Conclusions

1. The hottest temperature anomalies of the last twenty years are consistent with a simple shift of the historical temperature distribution towards warmer values, when the fact that these events are selected across space and time is also accounted for.
2. There is a pattern, however, regarding cooling of the hottest growing-season temperatures in regions experiencing agricultural intensification.
3. More productive croplands generally have greater capacity for evapotranspiration, leading to increased latent heat flux and reduced sensible heat flux. This effect operates most strongly when vapor pressure deficit is highest, thus suppressing temperatures on the hottest days.
4. Improved weather account for roughly a quarter of improved corn yields in the U.S. Midwest. A reversal in these advantageous trends could jeopardize continued increases in yields in the U.S. and elsewhere.

Increasing pressures on global agriculture

Income-dependence of calorie consumption

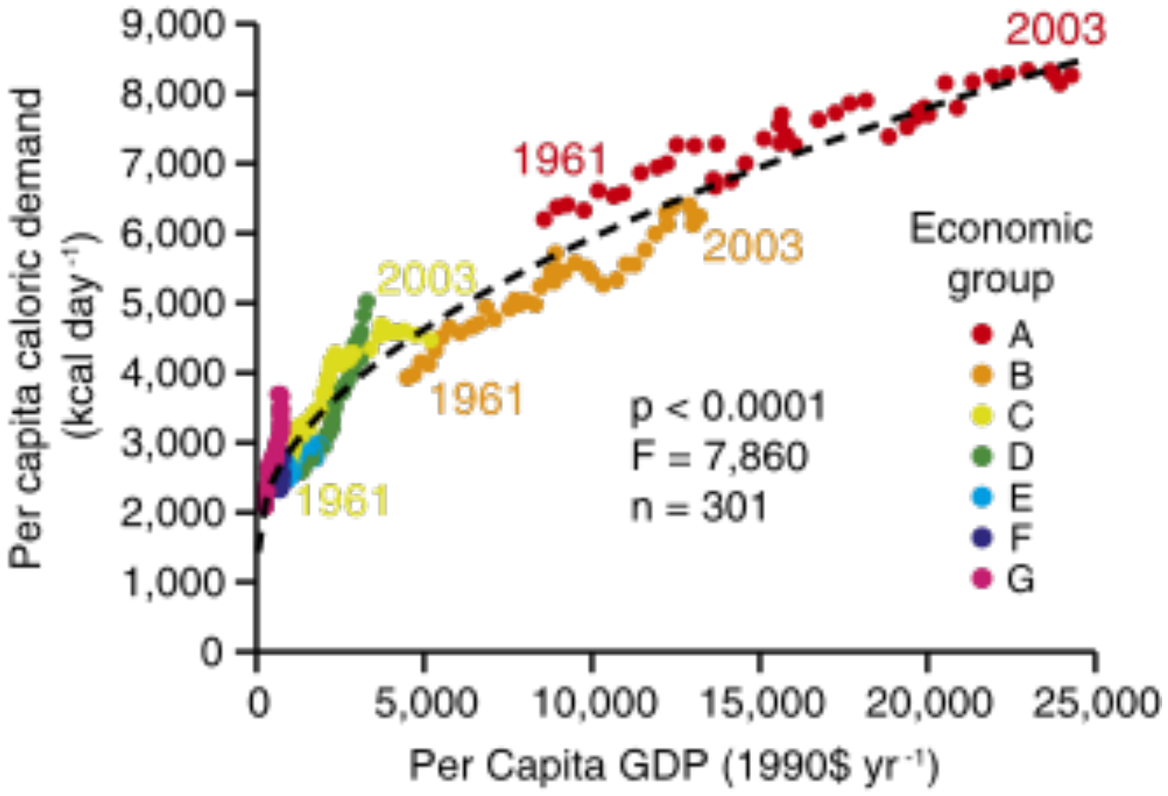

Tilman et al. 2011

Global average temperature change
(relative to 1900–2000 average)

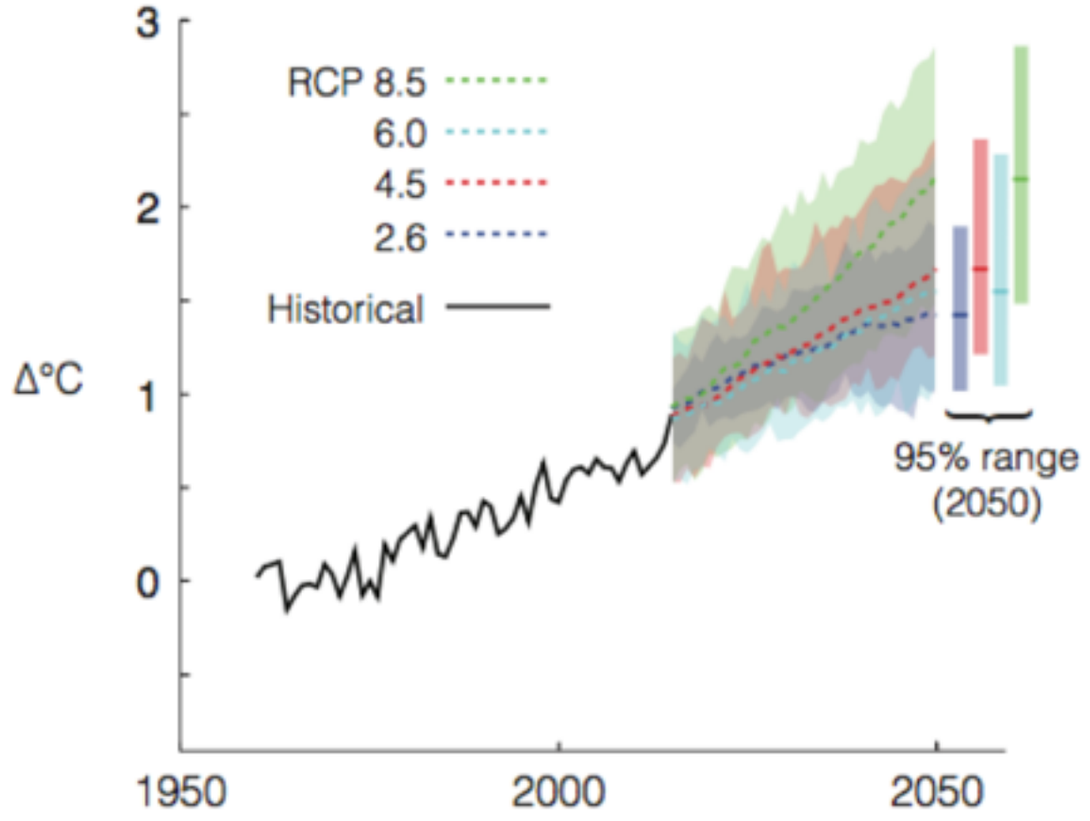

Myers, et al. in press, Ann. Rev.

Calculating changes in cropping intensity

crop NPP is calculated from yield data

$$NPPha_{c,k,y} = \frac{Y_{c,k,y}\, DF_c\, C}{HI_{c,y}\, AF_c}$$

NPPha: NPP per harvested area (g m^{-2} yr^{-1})
Y: yield (t ha^{-1})
DF: dry fraction (%)
C: carbon content (%)
HI: harvest index
AF: aboveground fraction
c is crop, k is county, y is year

sum over 12 summer crops; normalize by county area

$$NPPan_{k,y} = \sum_{c=1}^{12} \frac{NPPha_{c,k,y}\, HA_{c,k,y}}{TA_k}$$

HA: harvested area (hectares)
TA: county area (hectares)

Global trends in summer extreme temps

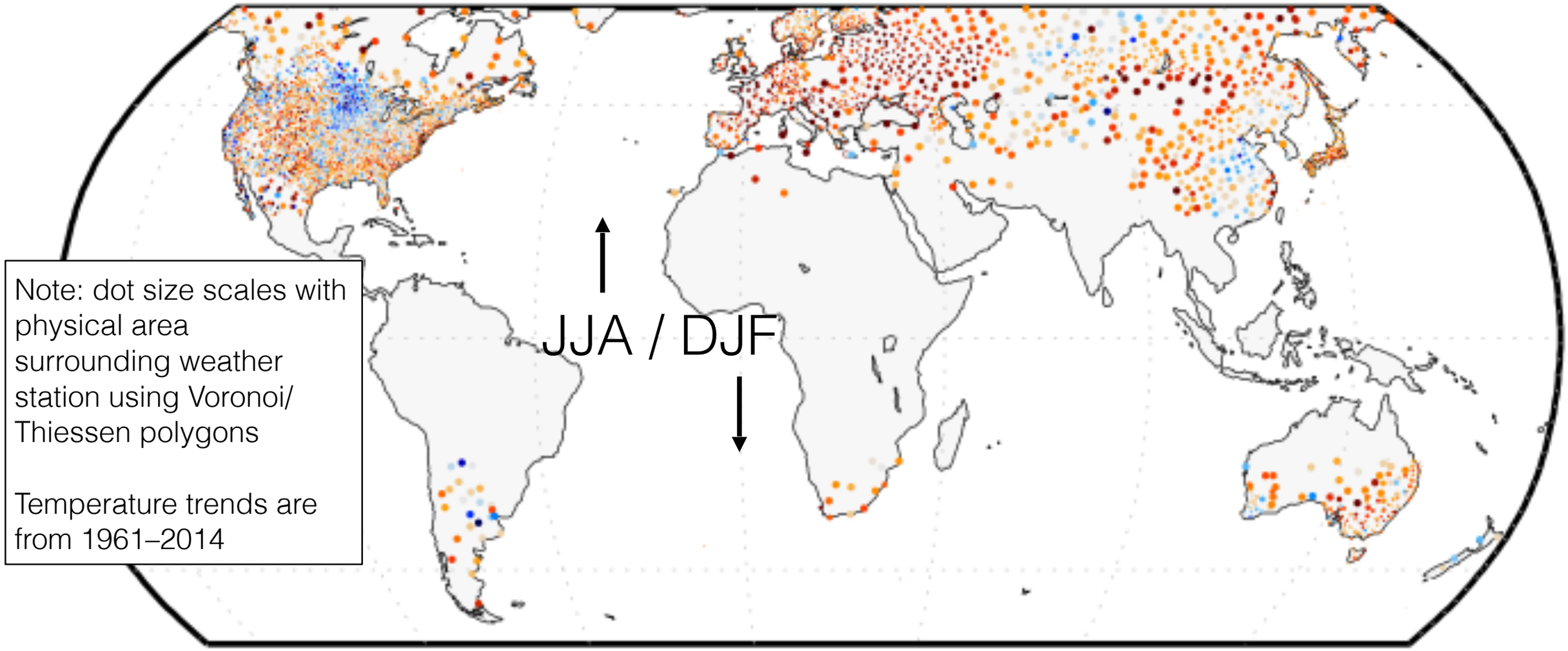

US

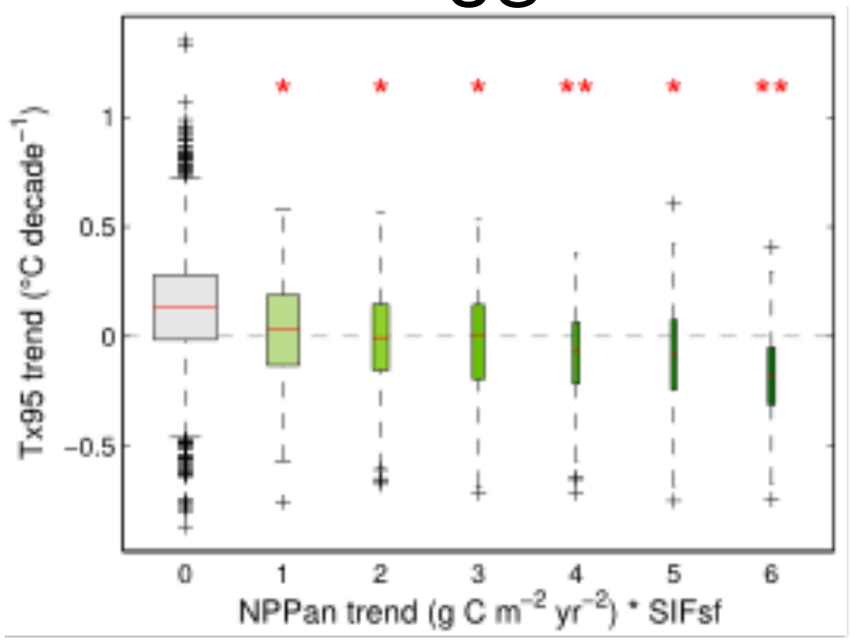

Canada

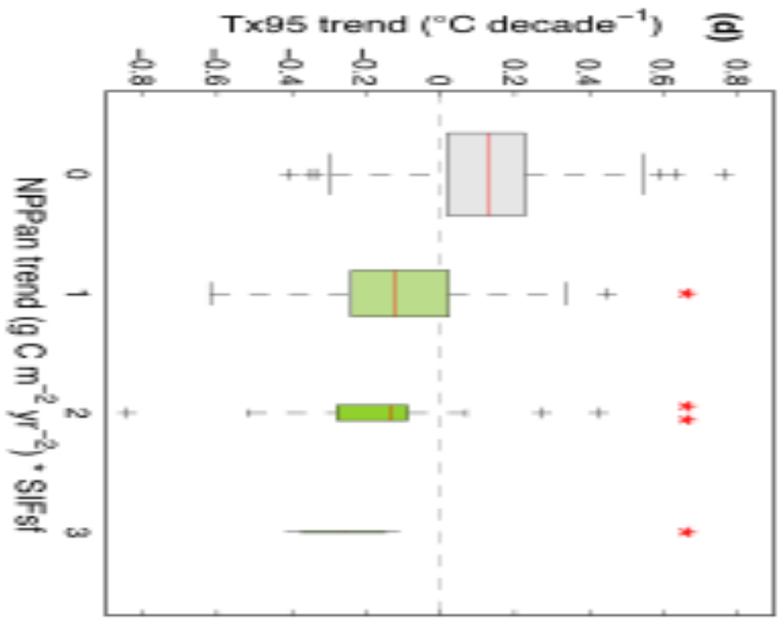

E Asia (north)

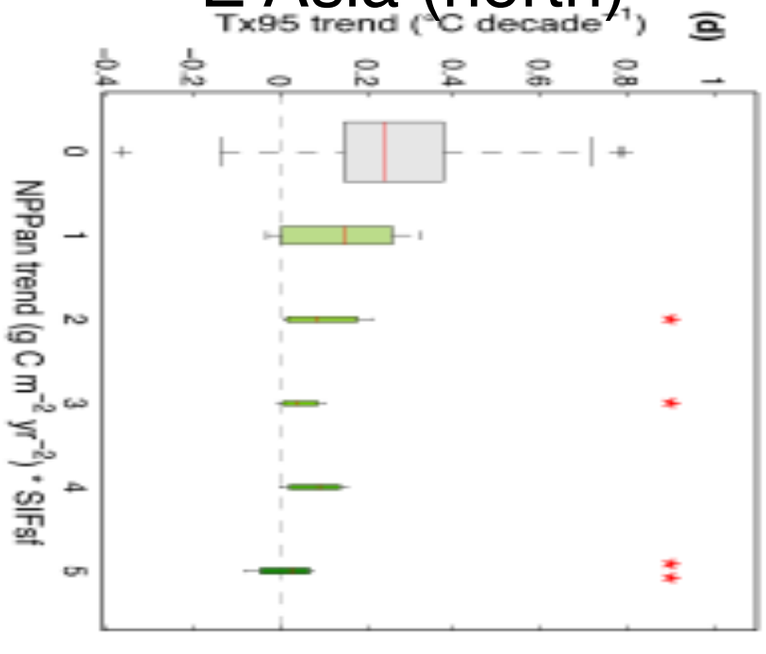

E Asia (south)

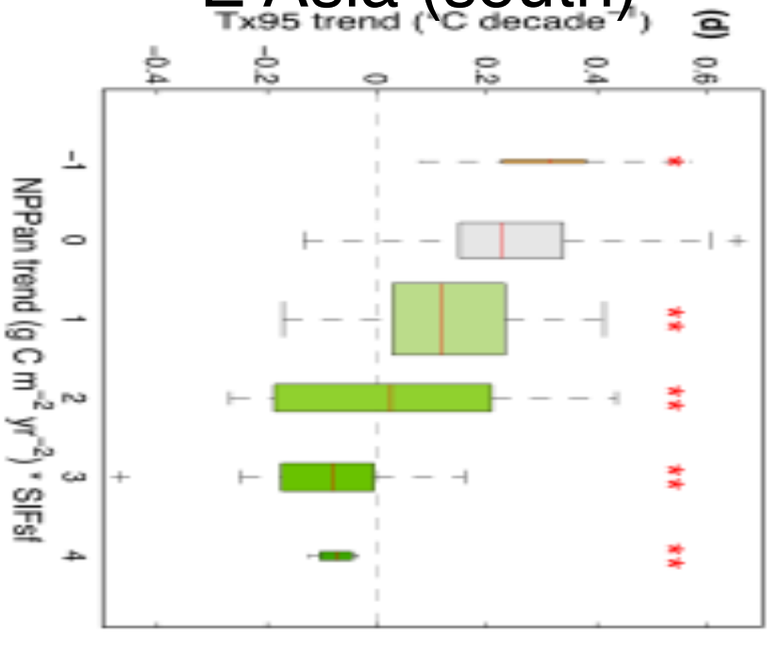

Argentina

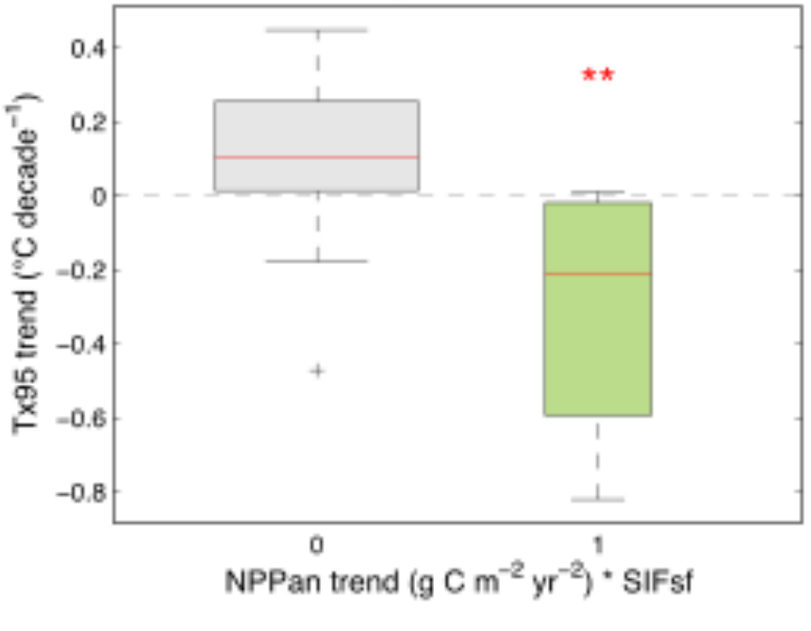

Consistent global NPPan–Tx95 associations since 1961

Central N. America

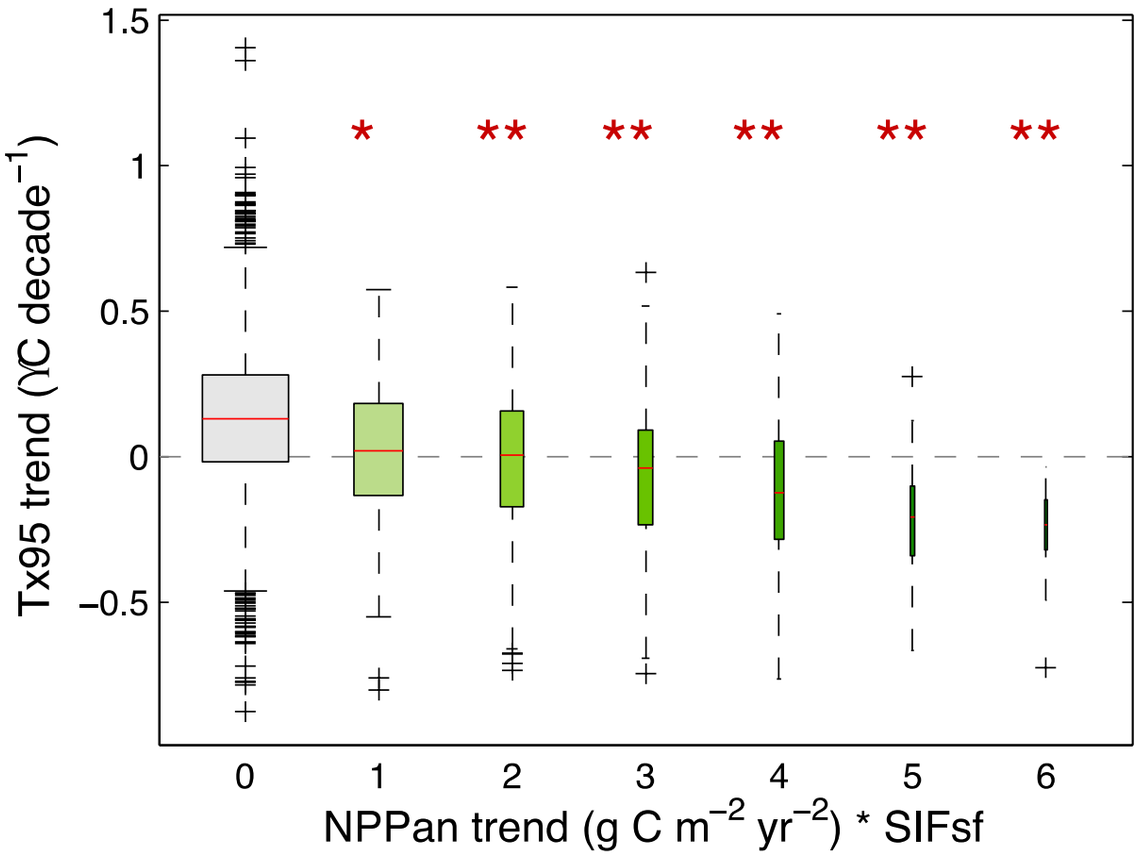

Northern N. America

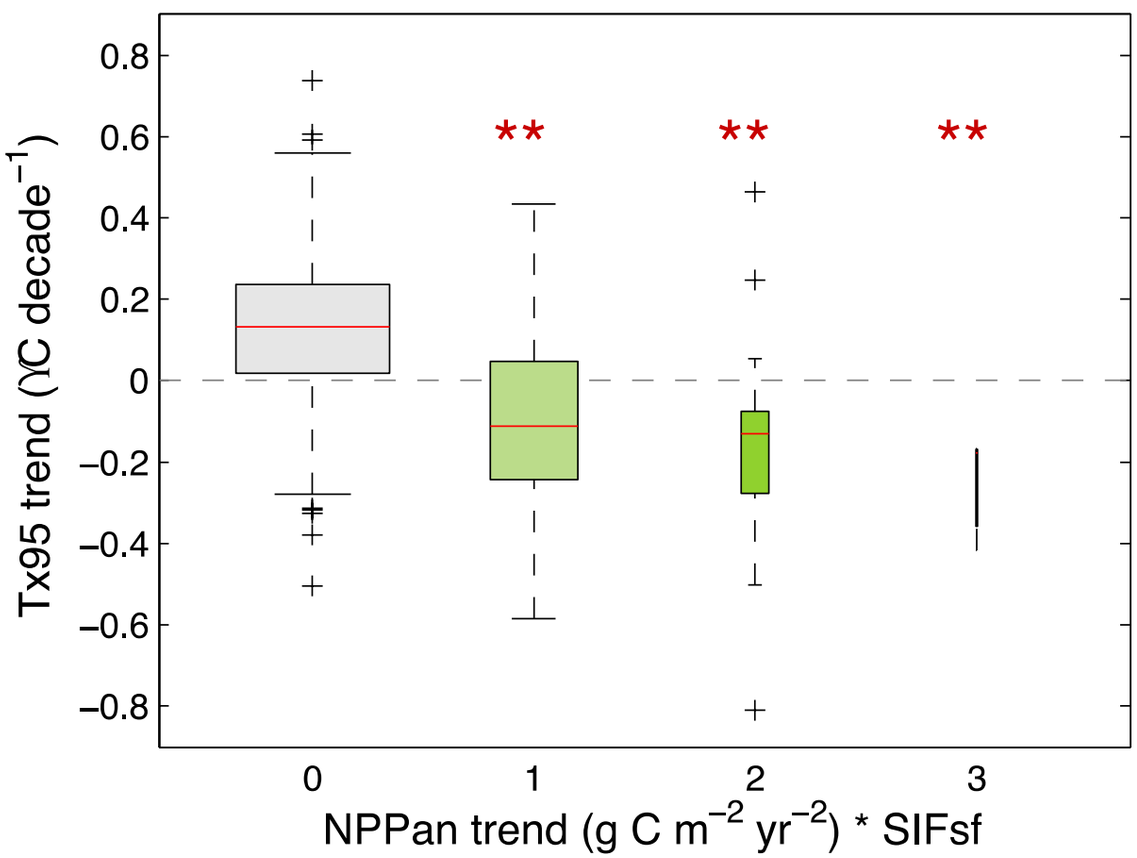

Consistent global NPPan–Tx95 associations since 1961

US Corn Belt

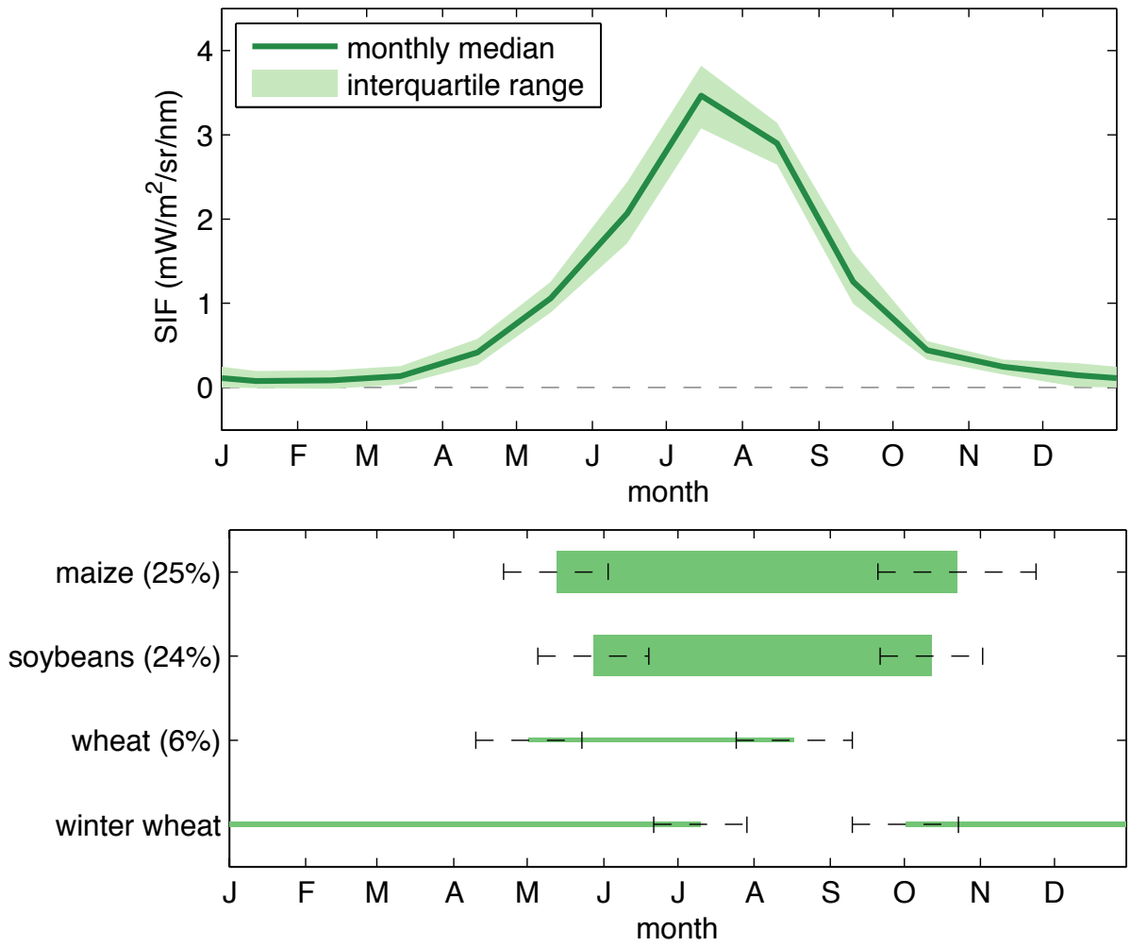

Canadian Prairies

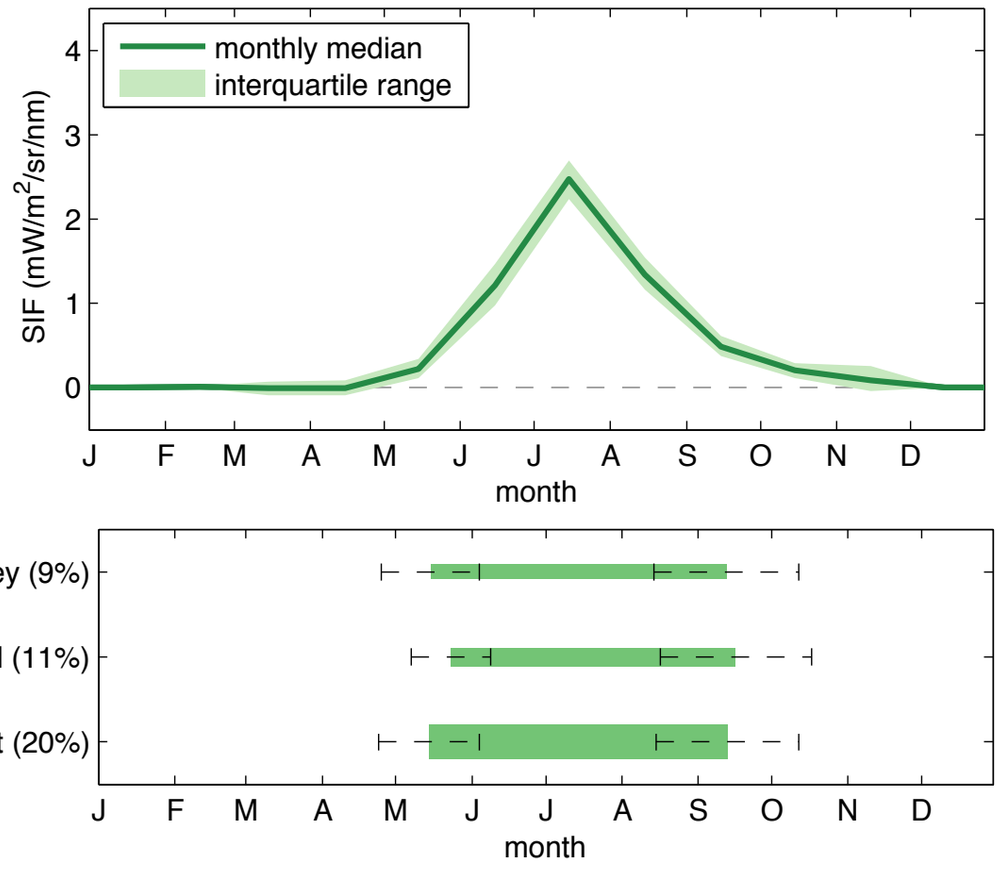

planting/harvest data from Sacks et al. 2010
crop fractions from Monfreda et al. 2008

Consistent global NPPan–Tx95 associations since 1961

East Asia – north of 40°N

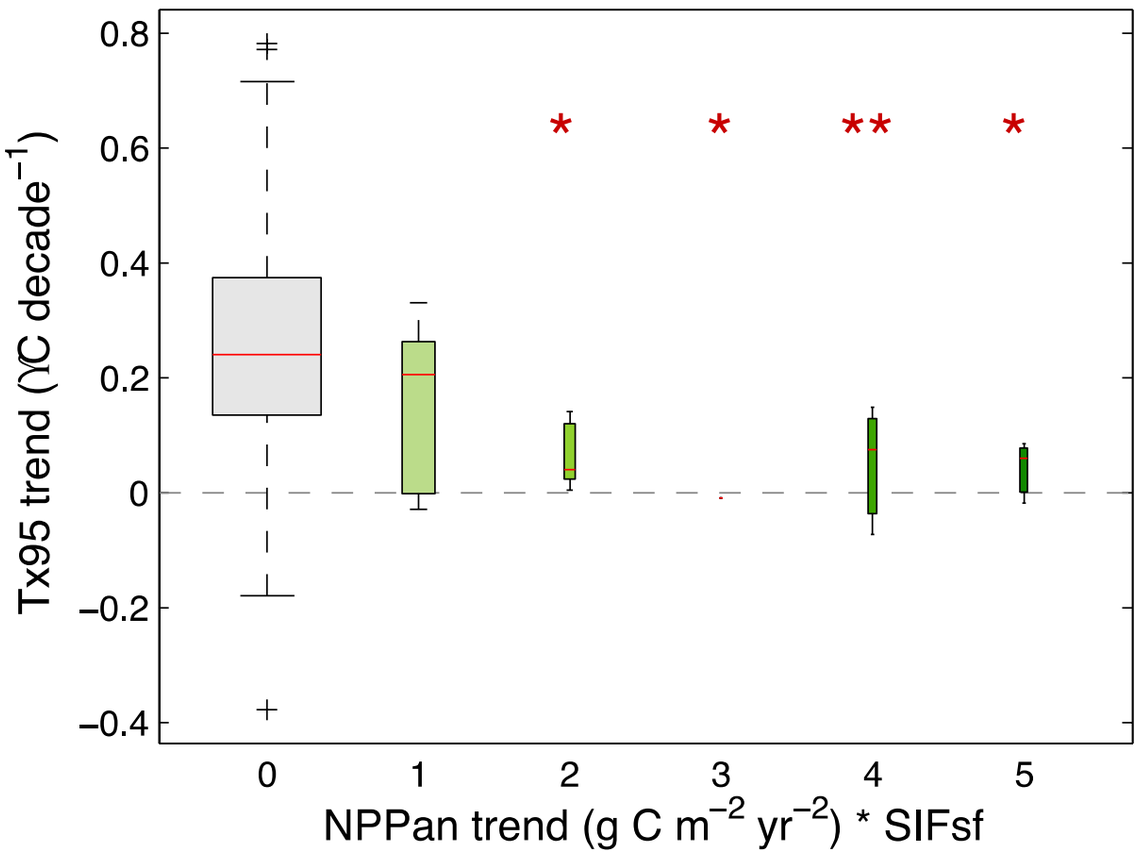

East Asia – south of 40°N

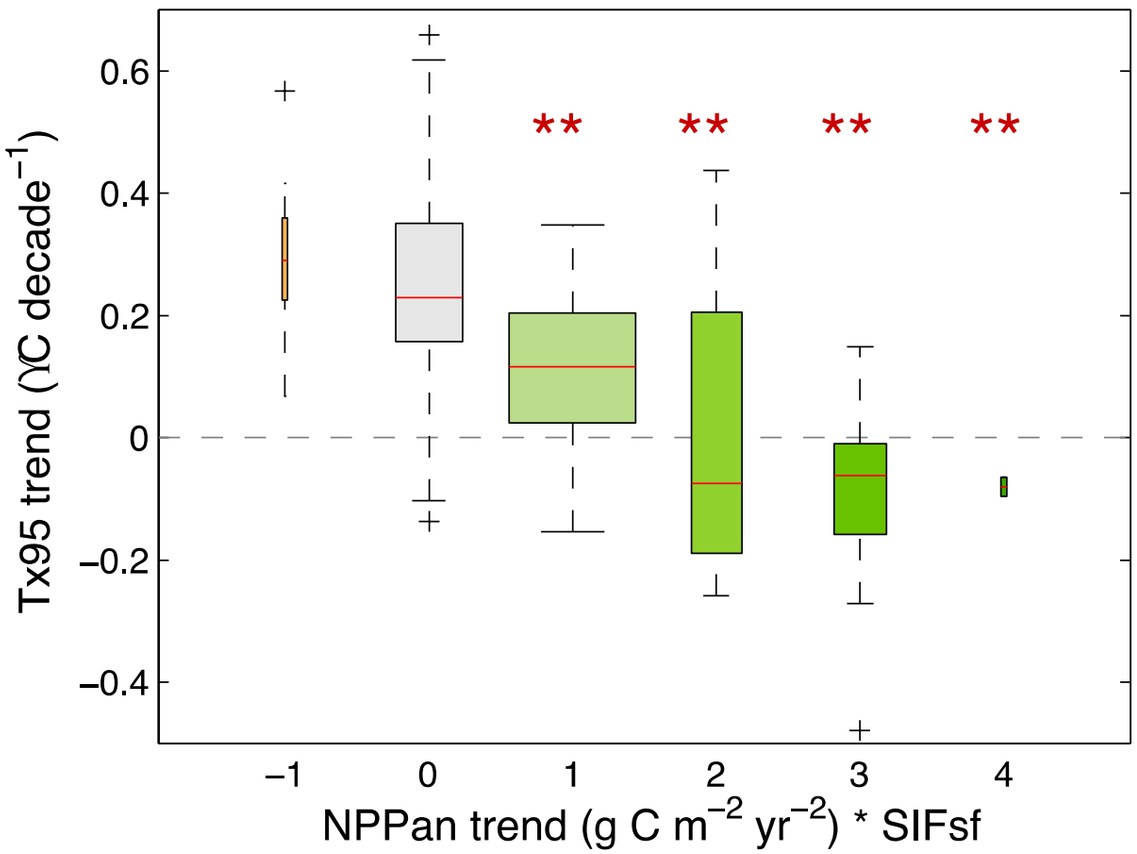

Consistent global NPPan–Tx95 associations since 1961

Northeast China

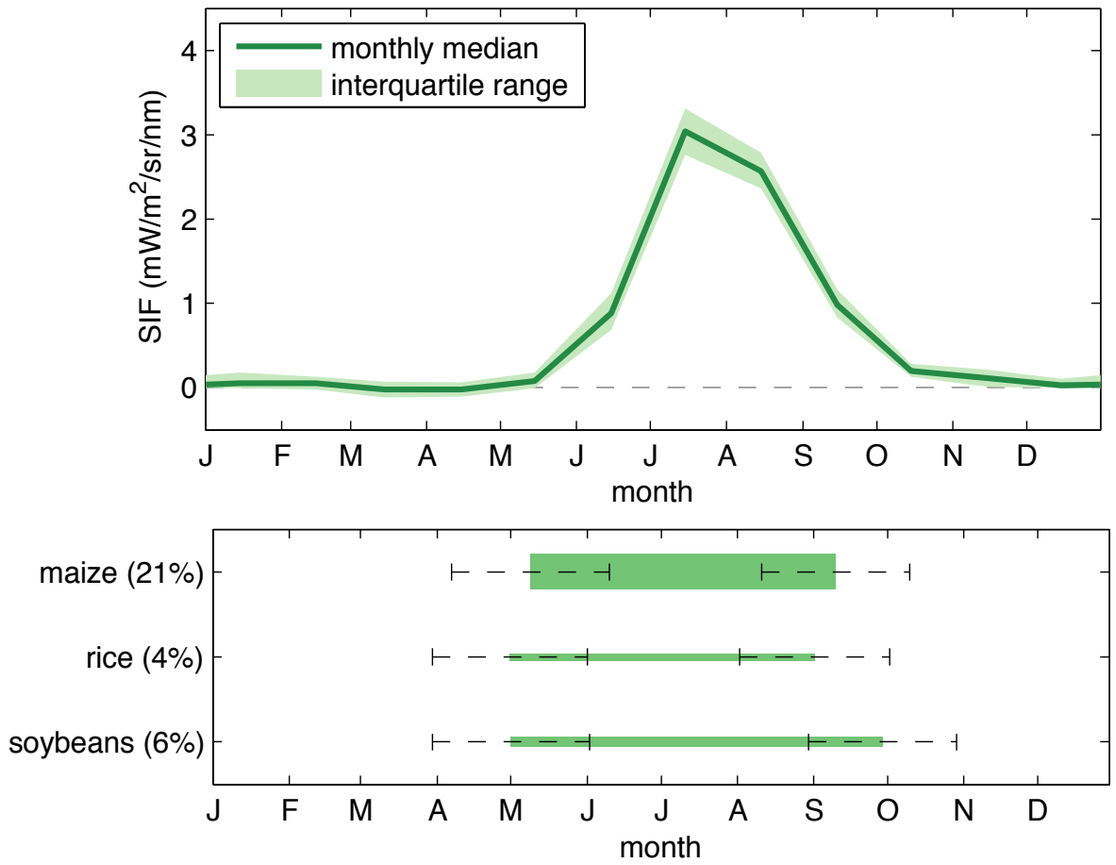

North China Plain

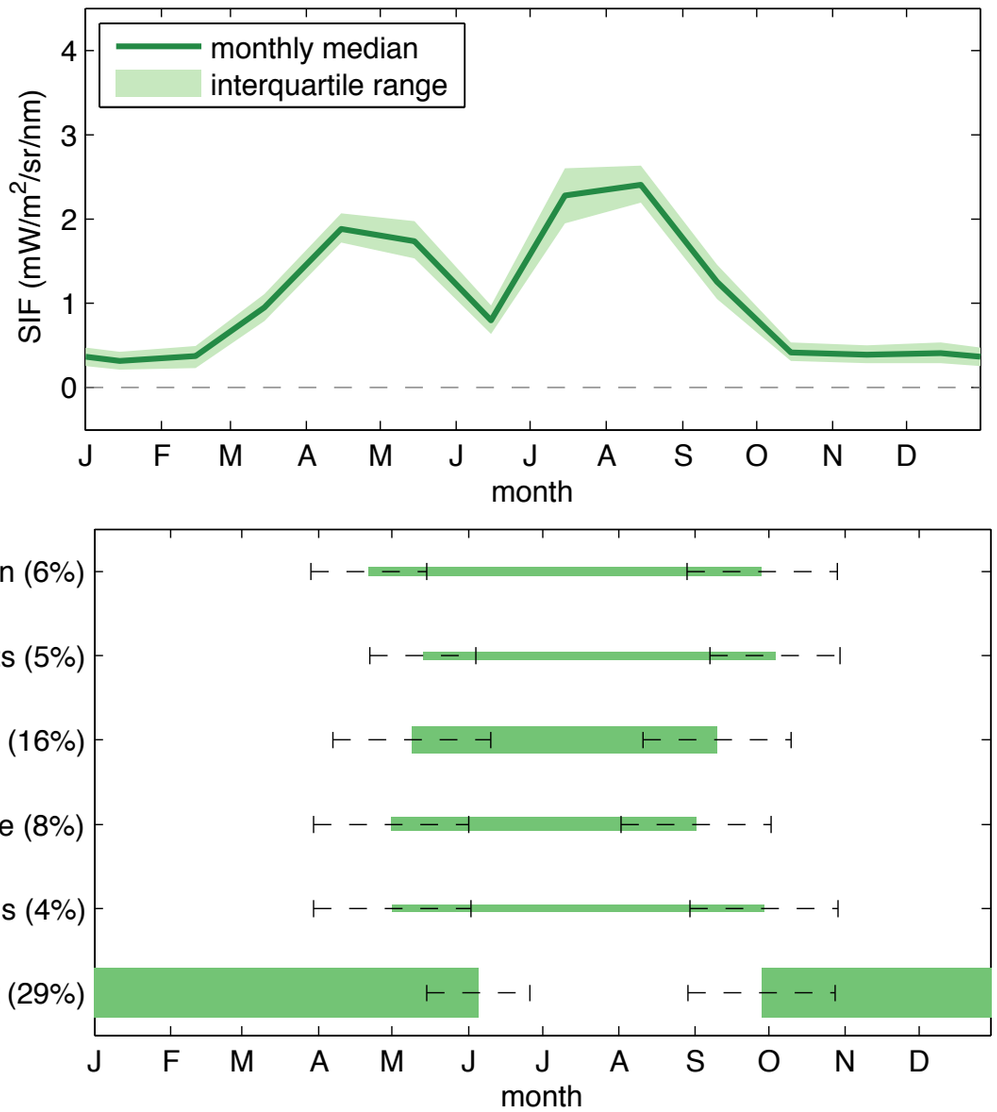

Collaborators

Missy Holbrook

Peter Huybers

Ethan Butler

Andy Rhines

Consistent global NPPan–Tx95 associations since 1961

Western Europe

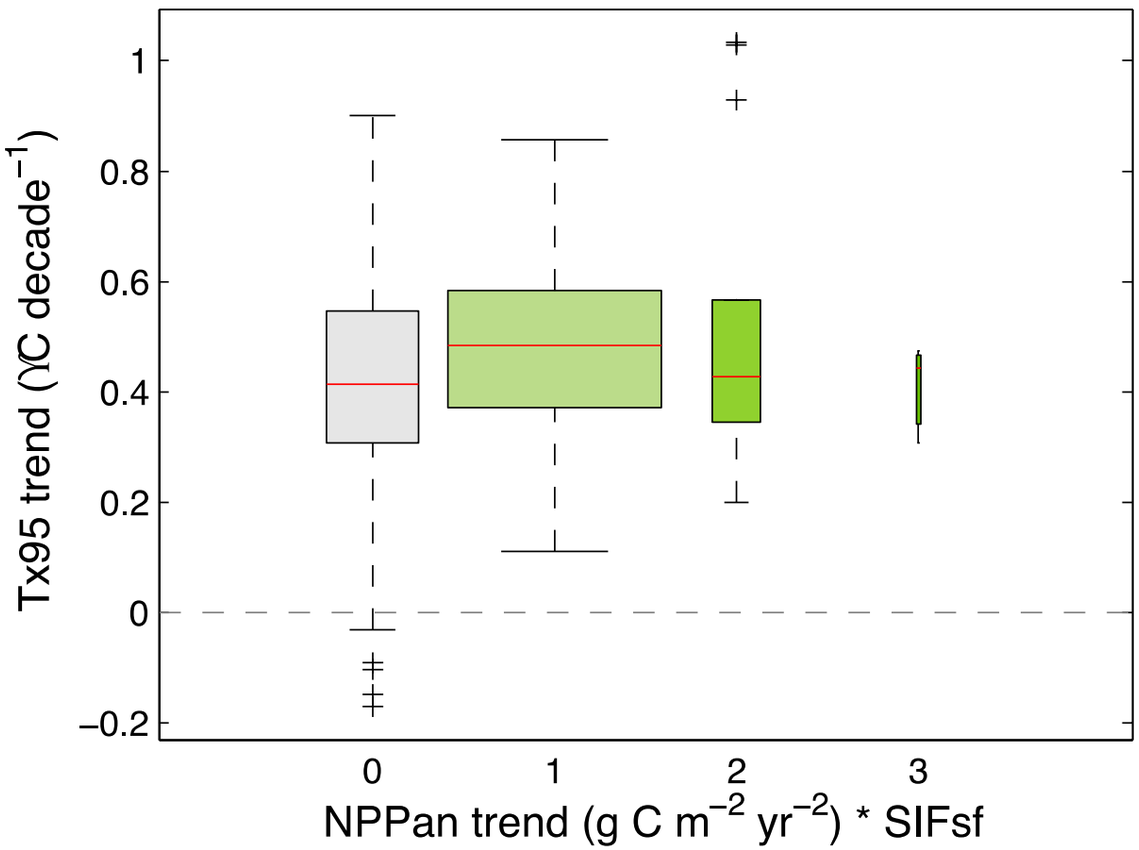

N. France & SE England

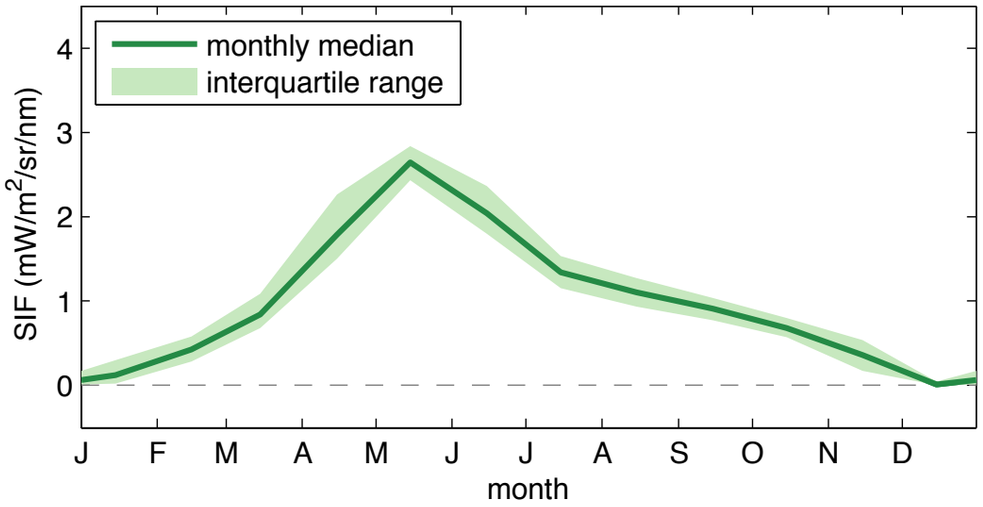

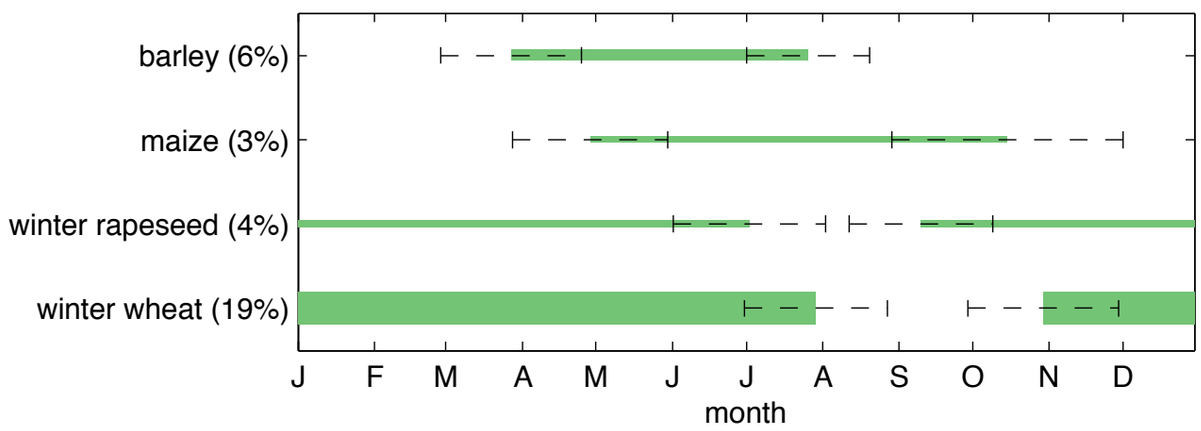

Consistent global NPPan–Tx95 associations since 1961

Argentina

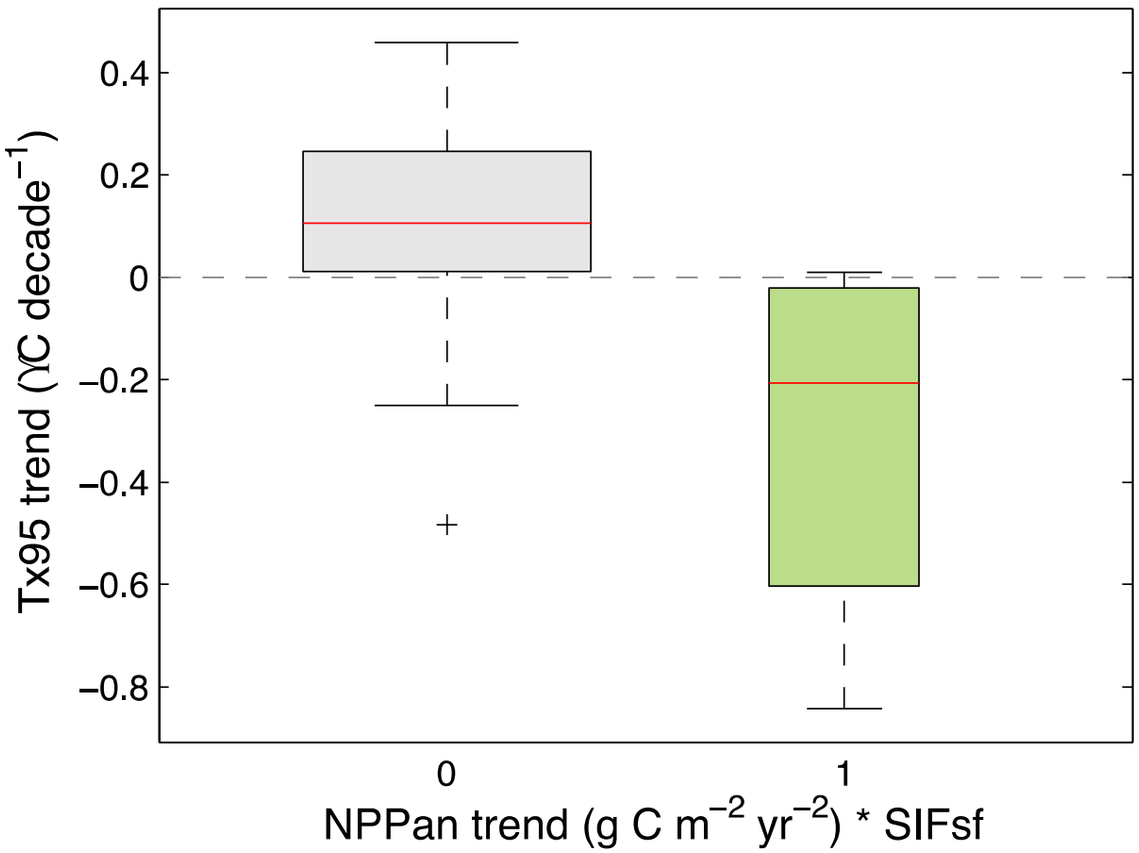

Southern Australia

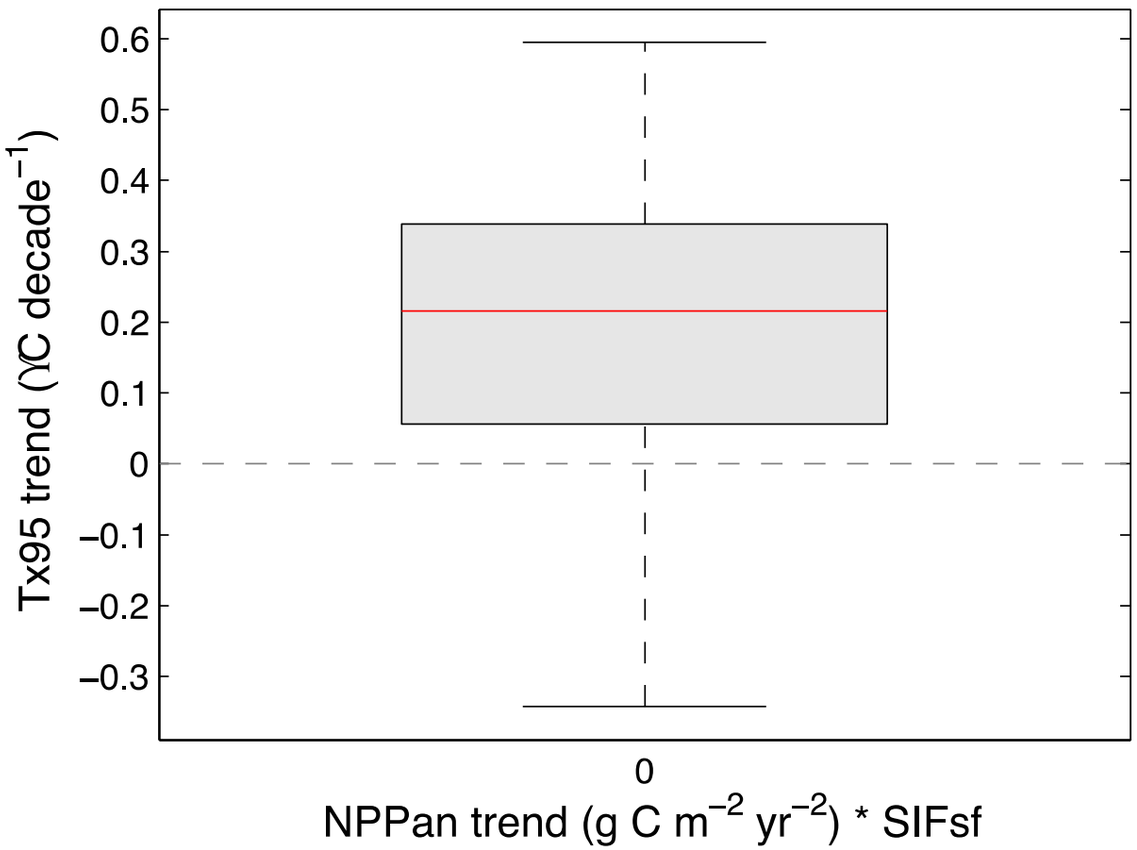

Consistent global NPPan–Tx95 associations since 1961

Argentine Pampas

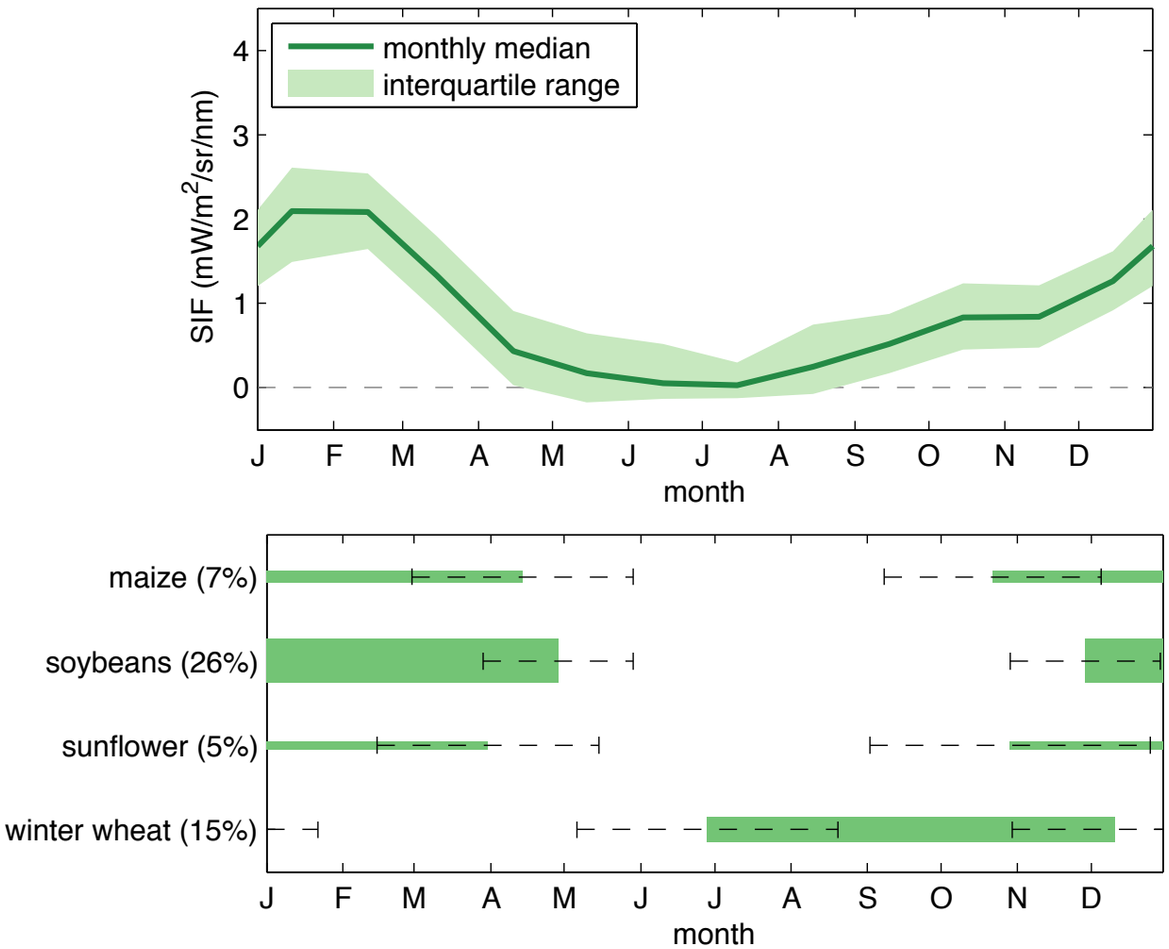

SW Australia

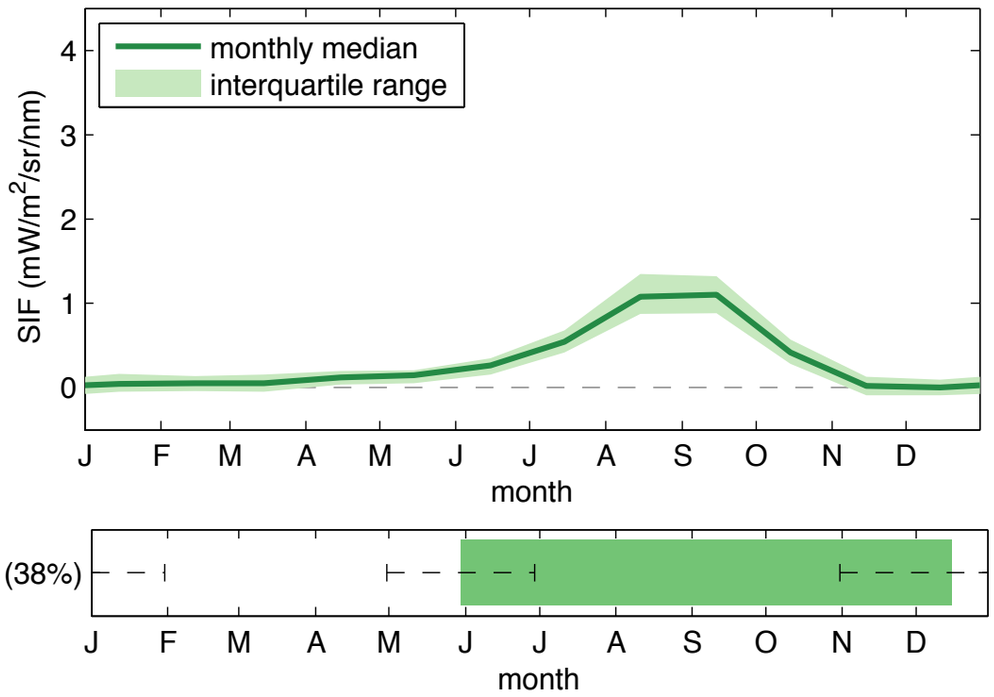

Conclusions

1. The last twenty years featured the warmest years of the last 600 at high latitudes.
2. The hottest temperature anomalies of the last twenty years are consistent with a simple shift of the historical temperature distribution towards warmer values, when the fact that these events are selected across space and time is also accounted for.
3. At more regional levels, changes in daily maximum temperature are variously found to be muted or amplified relative to changes in mean summer temperature.
4. Grassland and shrubland regions show higher summer temperature variability but muted increases in extremes, whereas forest, cropland, and urban regions generally show amplified changes in extremes.
5. Deficits in precipitation are associated with the most extreme temperatures in all regions, but build in over a longer period in regions with amplified extremes. Drying likely causes a loss of evaporative cooling and transition into a temperature regime with higher variance.

But how much does short-run weather tell us about longterm climate impacts? The difference is adaptation.

Killing Degree Day climatology increases from 100 (°C days) in the North to 500 (°C days) in the Southwest. Corn is less sensitive to Killing Degree Days in hotter regions.

Using this spatial adaptation as a proxy for temporal adaptation implies that yields losses from a 2°C warming can be mitigated from 14% to only a 4% decline.

(Butler et al. 2013, 2015)

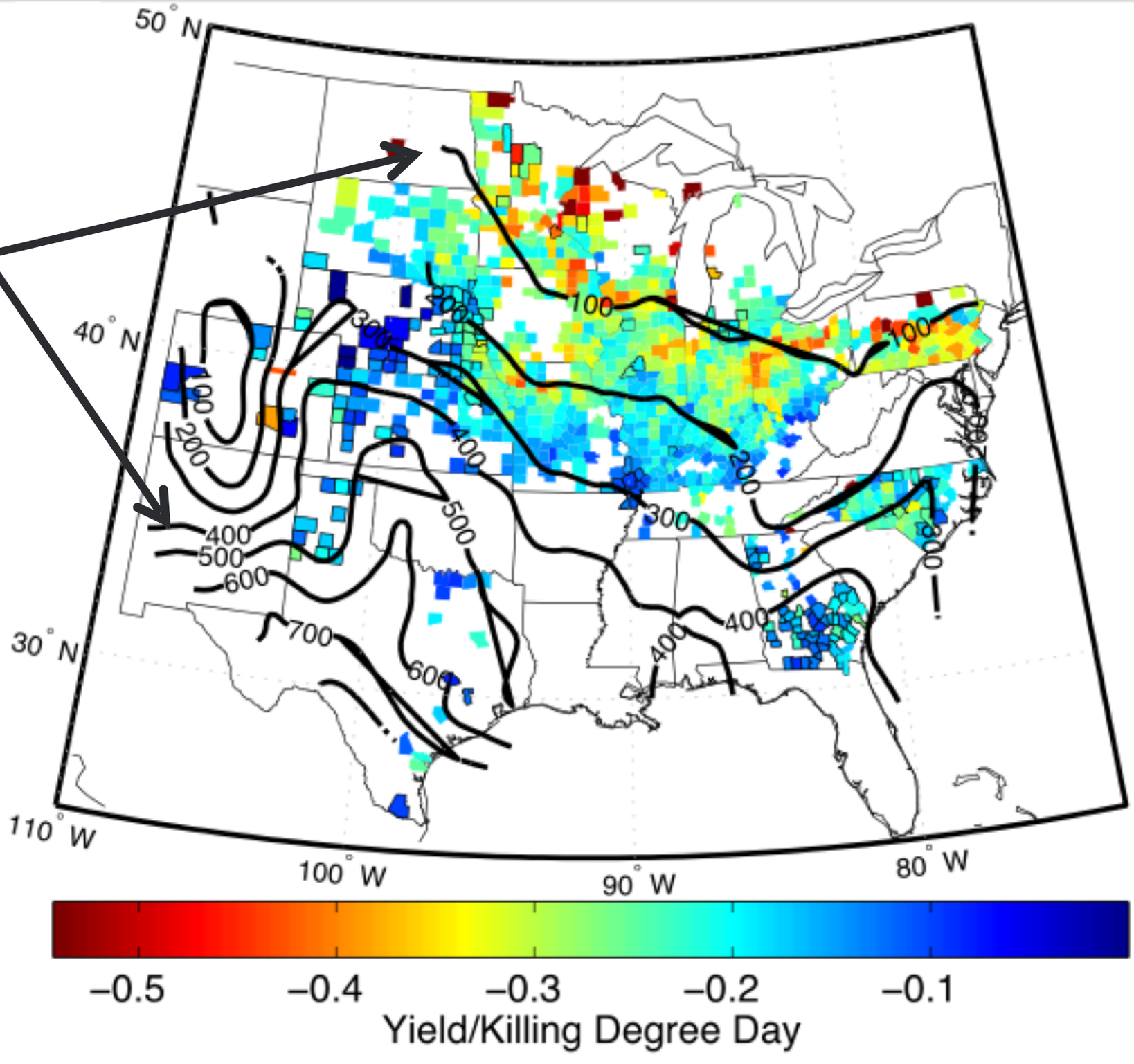

Sensitivity of yield to high temperatures is lower in hotter regions.

Using the observed spatial adaptation as a proxy for temporal adaptation implies that yields losses from warming can be mitigated.

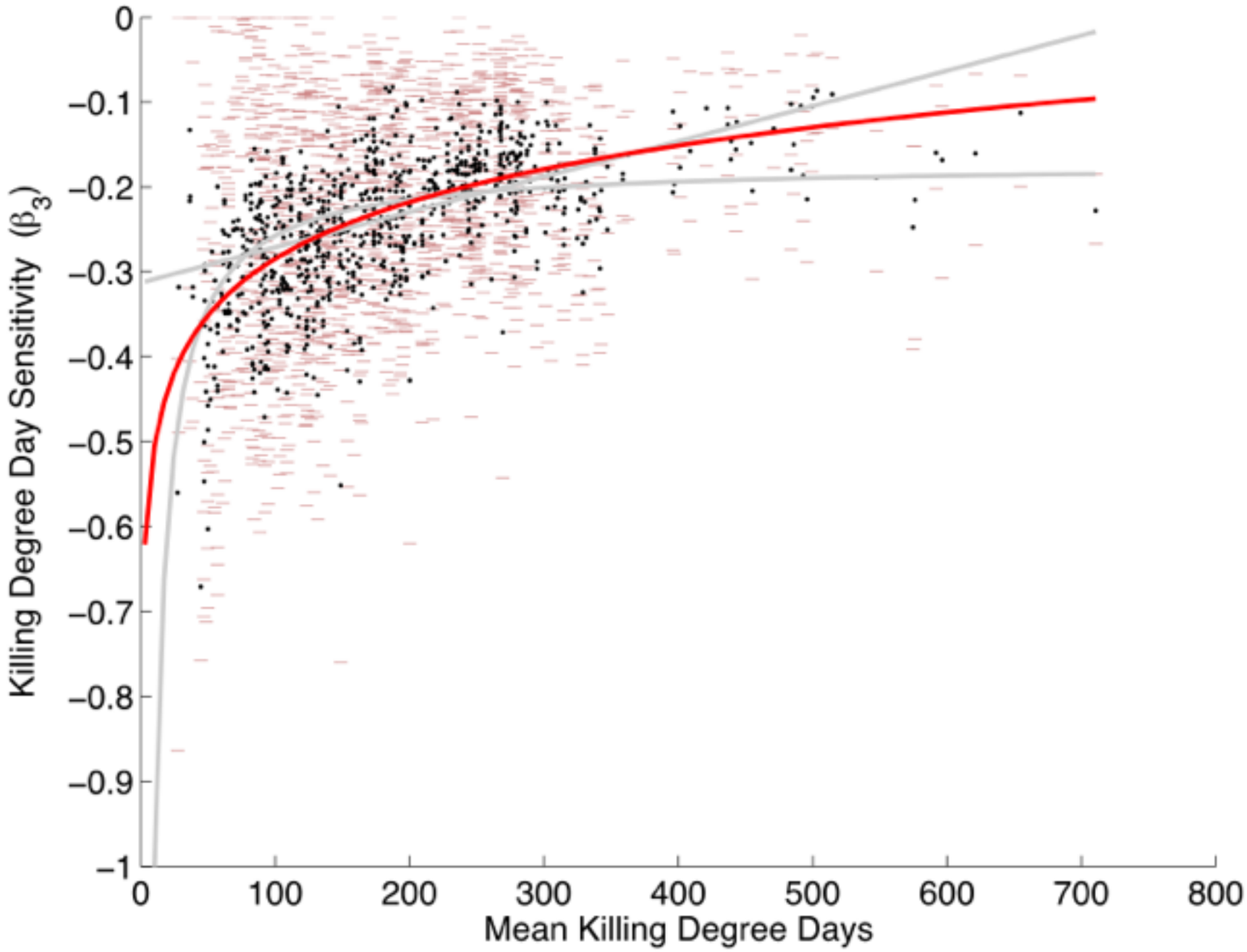

Differences in yield loss without and with adaptation are big; any yield prediction should account for adaptation.

14% loss in production from 2°C warming

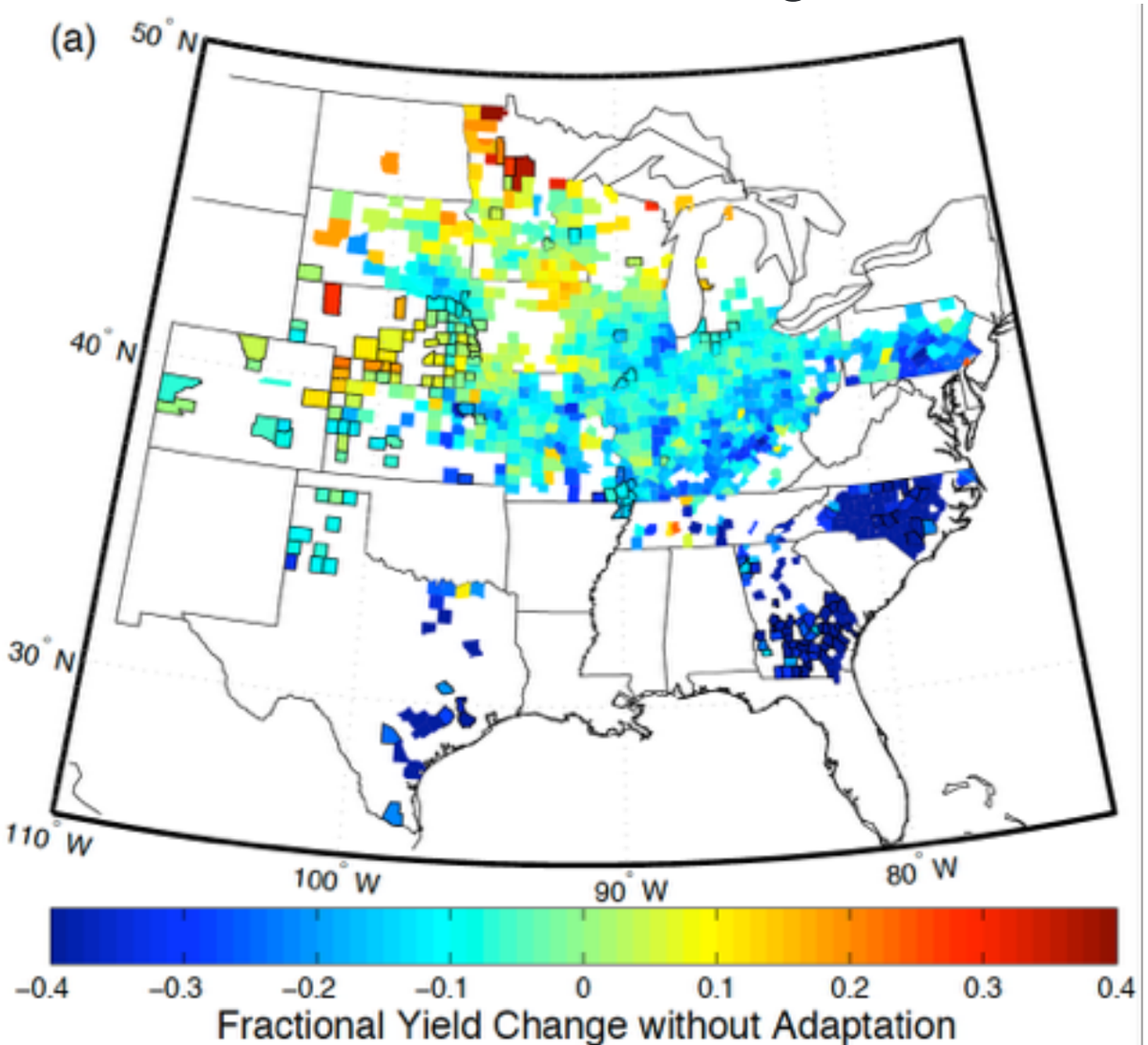

0% loss in production from 2°C warming

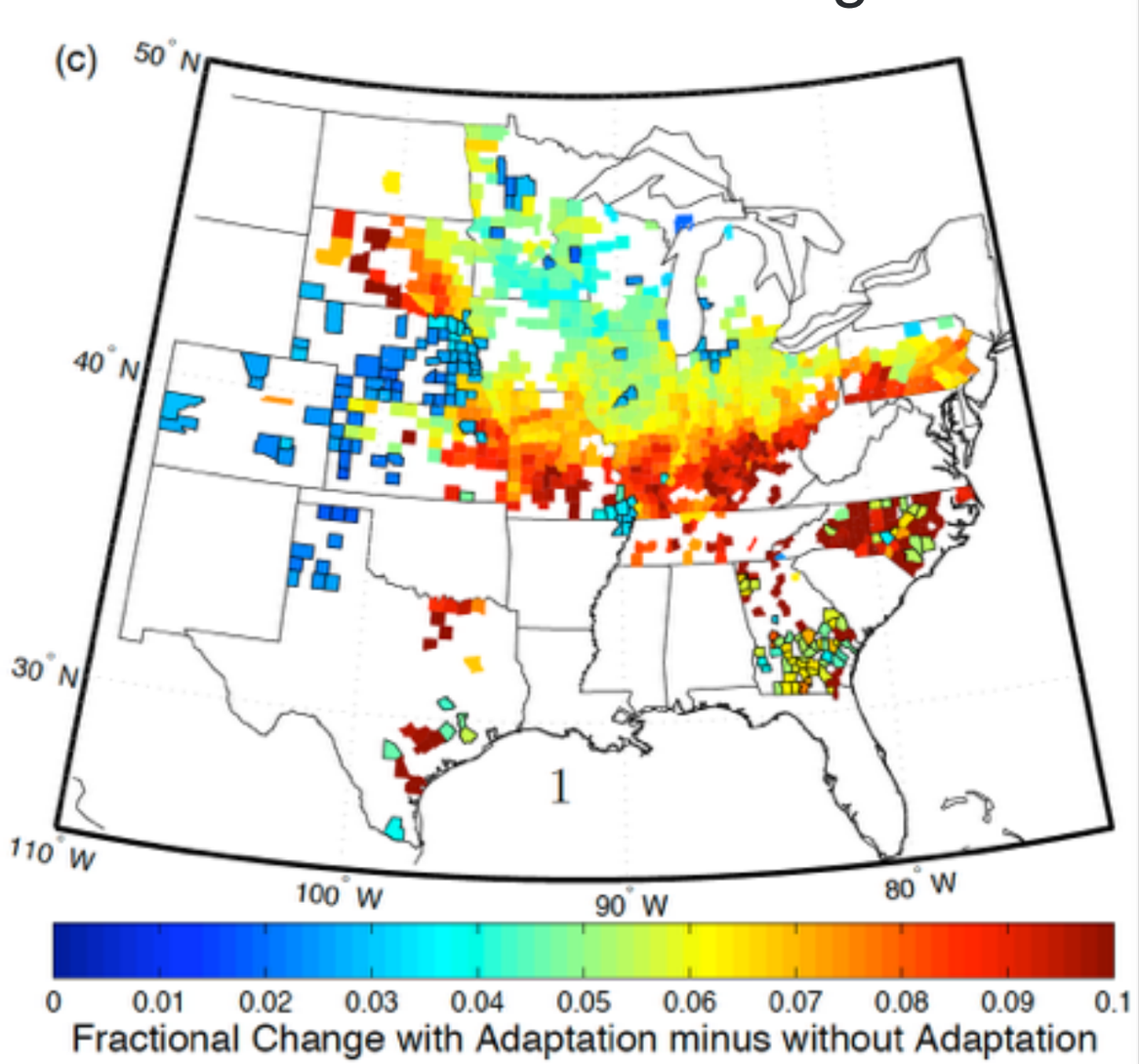

Multi-model projection of changes in rainfall illustratelarge uncertainties

Stippling indicates that the mean change exceeds the 95% interval across models

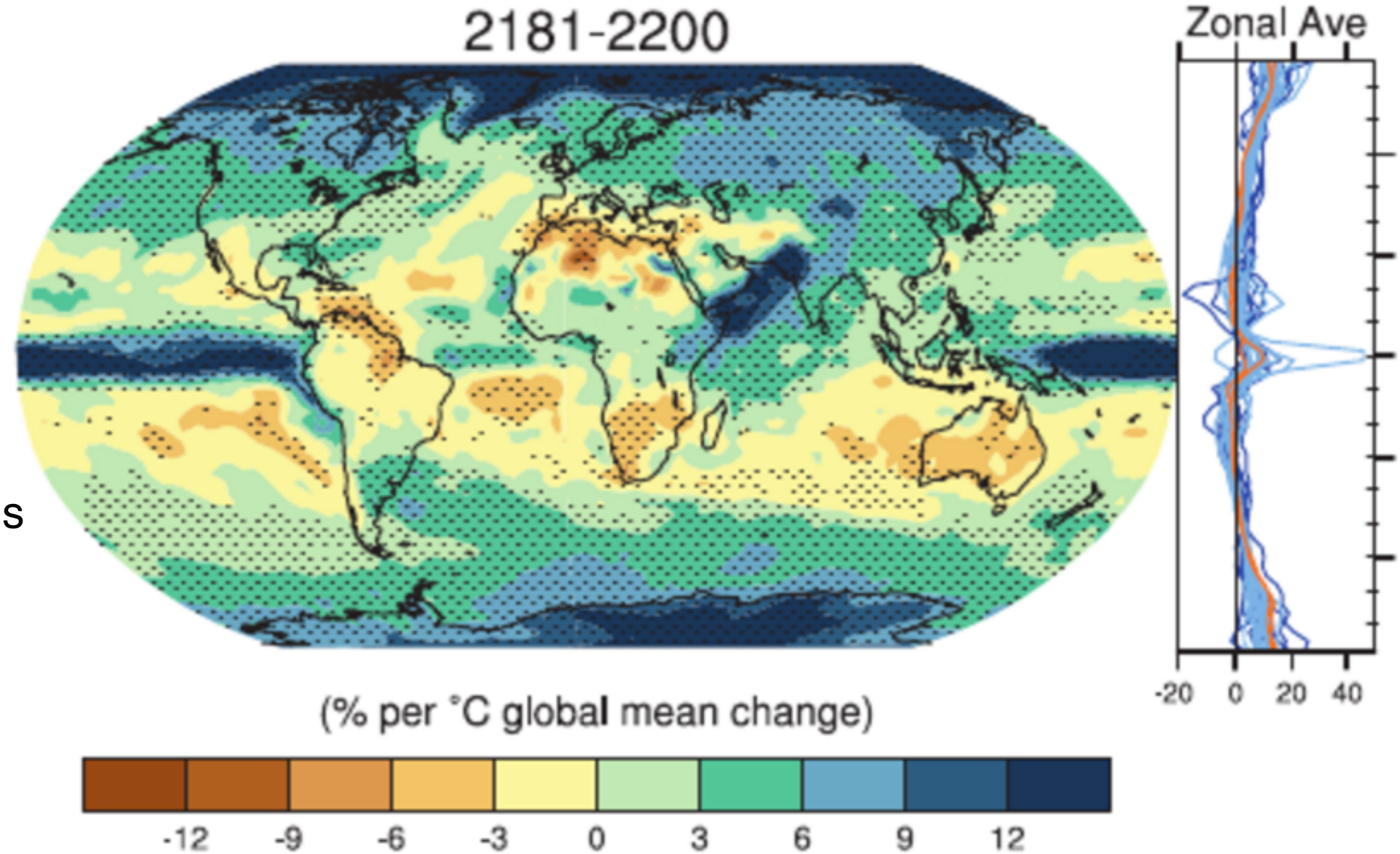

Determining future precipitation patterns is fundamental to understanding the consequences of climate change

(IPCC AR5, WG1)

Can we better predict heatwaves

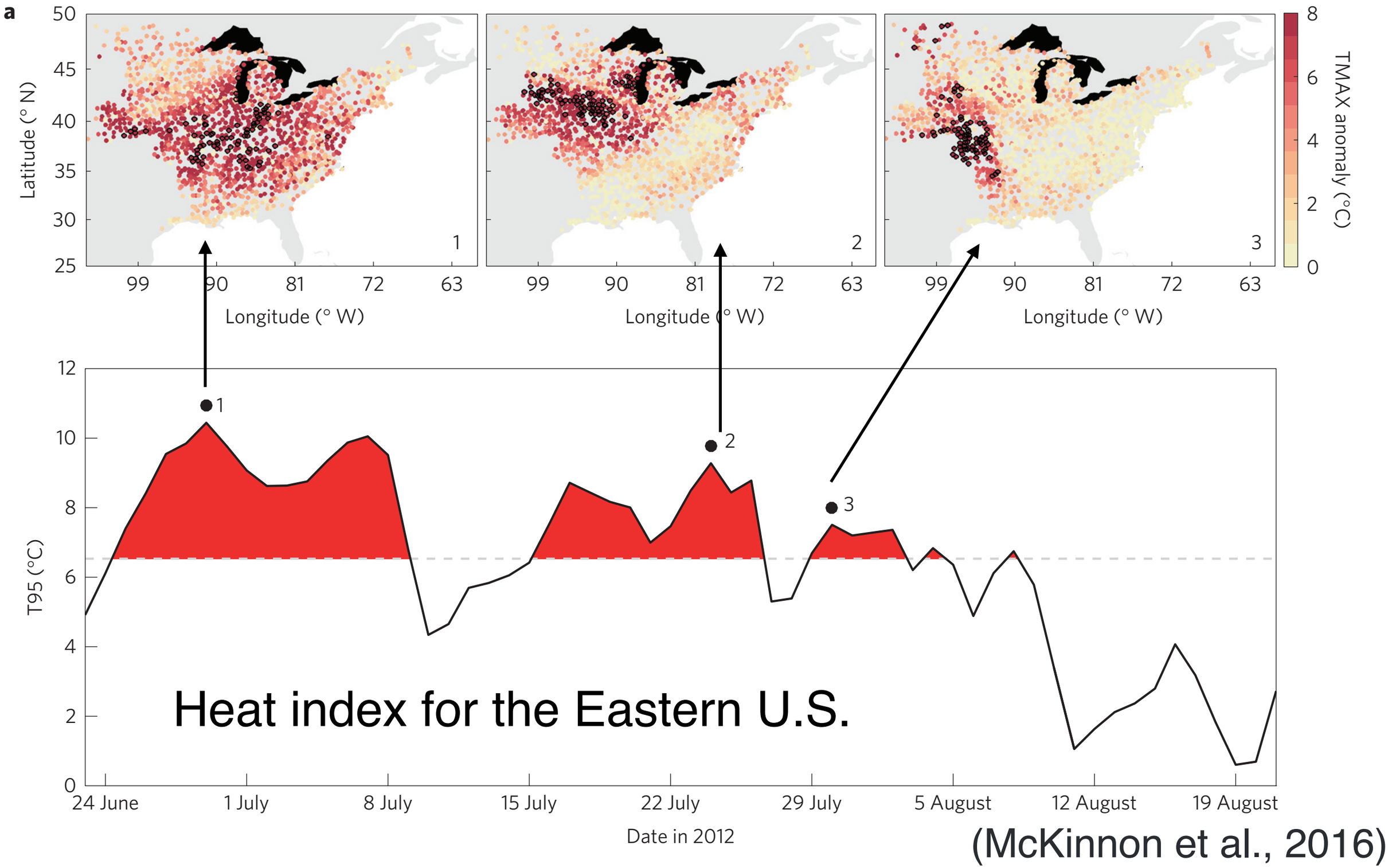

(McKinnon et al., 2016)

Pattern of sea surface temperature associated with summer heat waves in the Eastern US

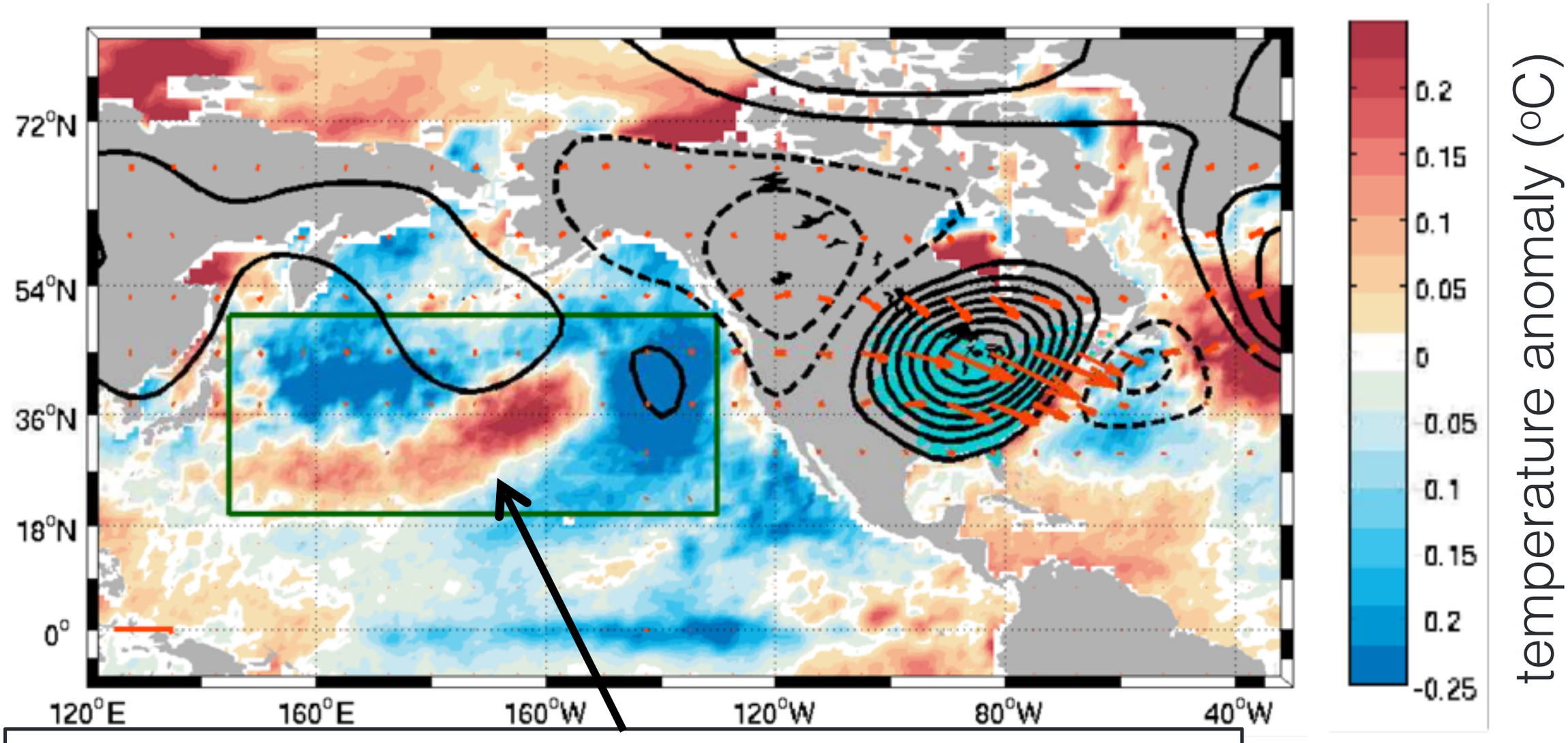

A tri-pole in Pacific mid-latitude sea surface temperature is characteristic during Eastern US heat waves.

(McKinnon et al., 2016)

Pattern five days prior to a heat wave

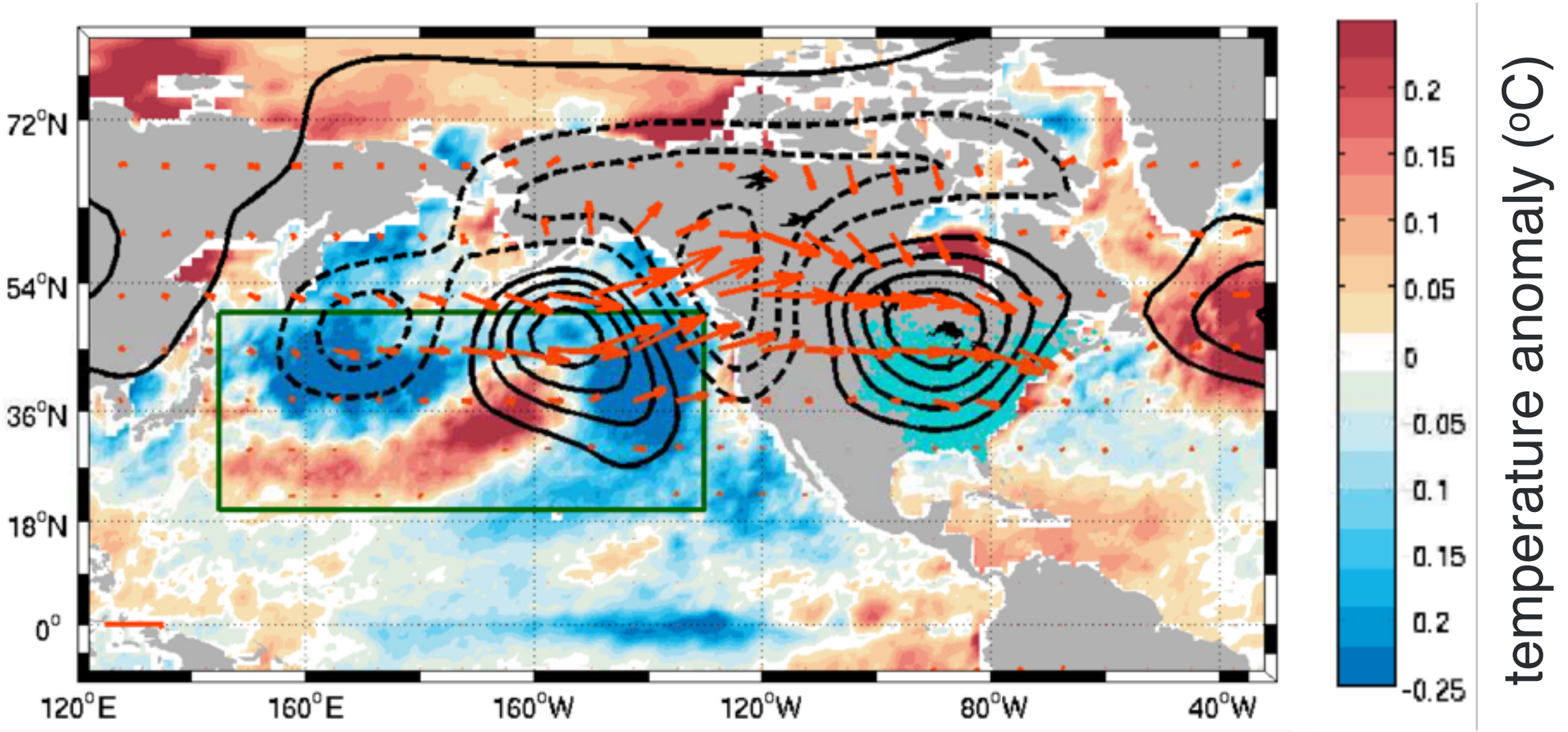

The sea surface temperature tri-pole causes anomalous atmospheric wave activity (red arrows) to converge on the Eastern US.

(McKinnon et al., 2016)

Pattern ten days prior to a heat wave

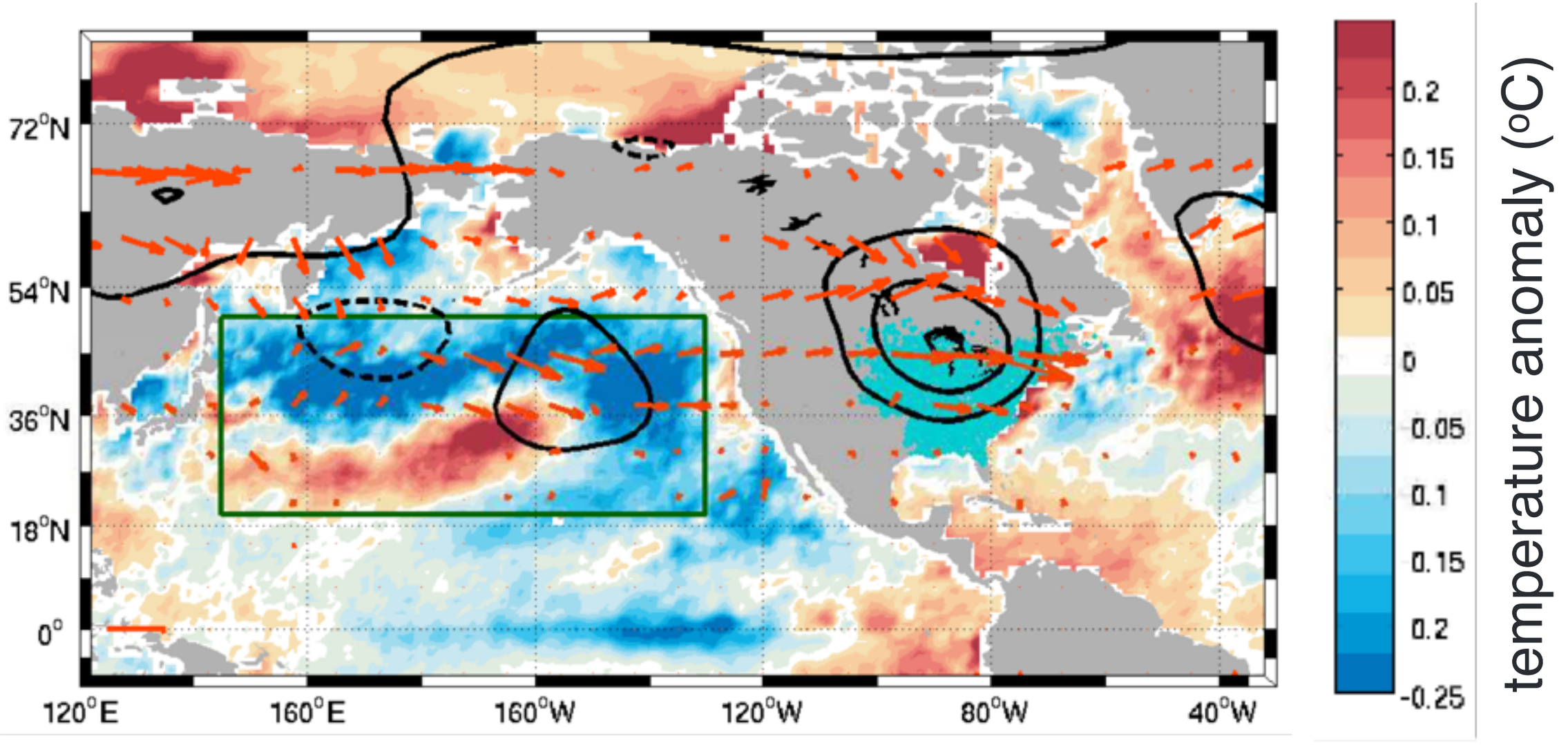

Development of the sea surface temperature tri-pole follows a characteristic pattern that can be reliably tracked more than 40 days prior to a heat wave.

(McKinnon et al., 2016)

Heat wave odds up to 40 days out change by >2X for one-sigma anomalies in the prediction pattern

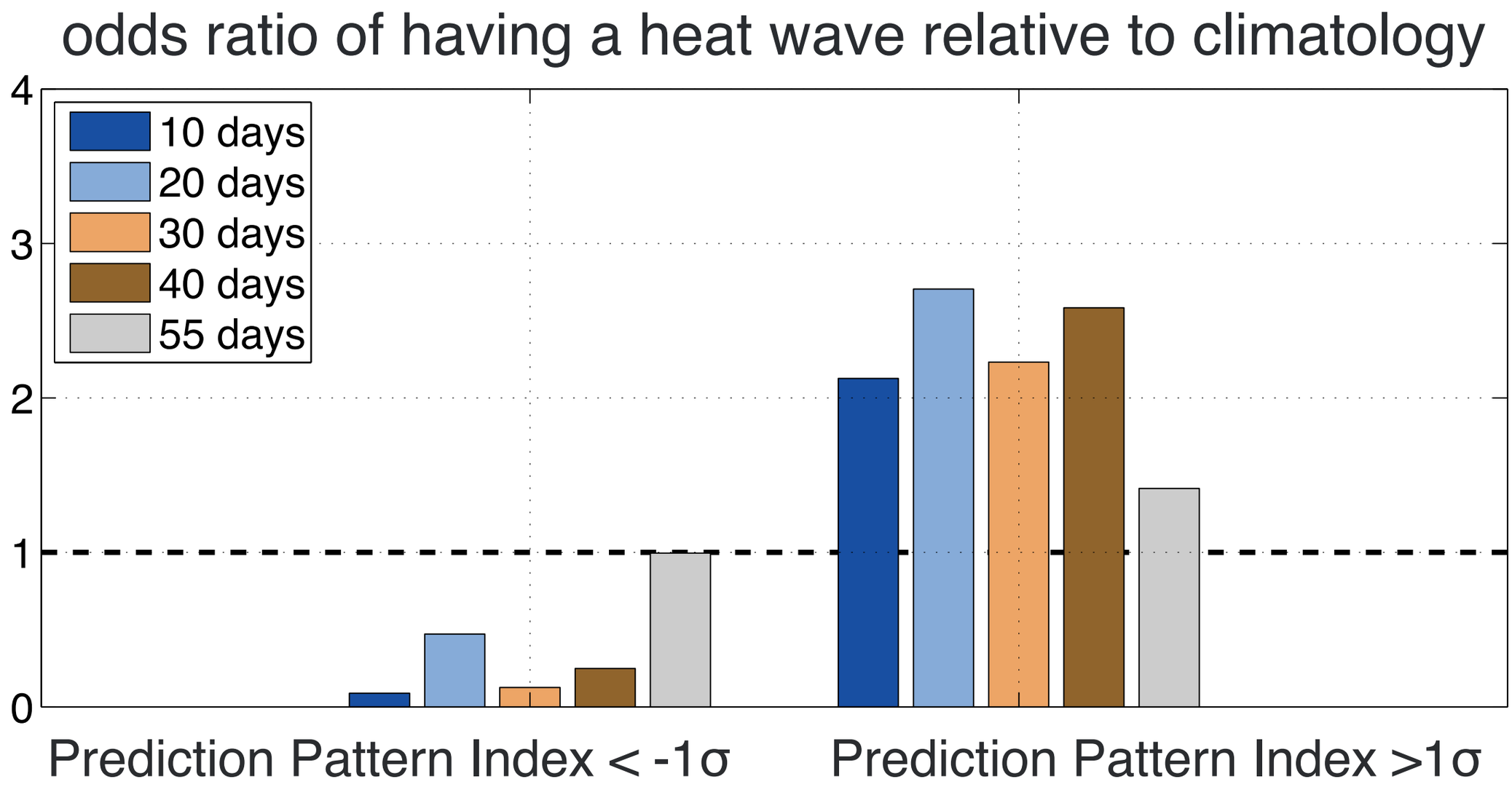

(significance is confirmed through cross-validation on withheld data)

(McKinnon et al., 2016)

Animation: co-evolution of SST, z300, WAF across the NH

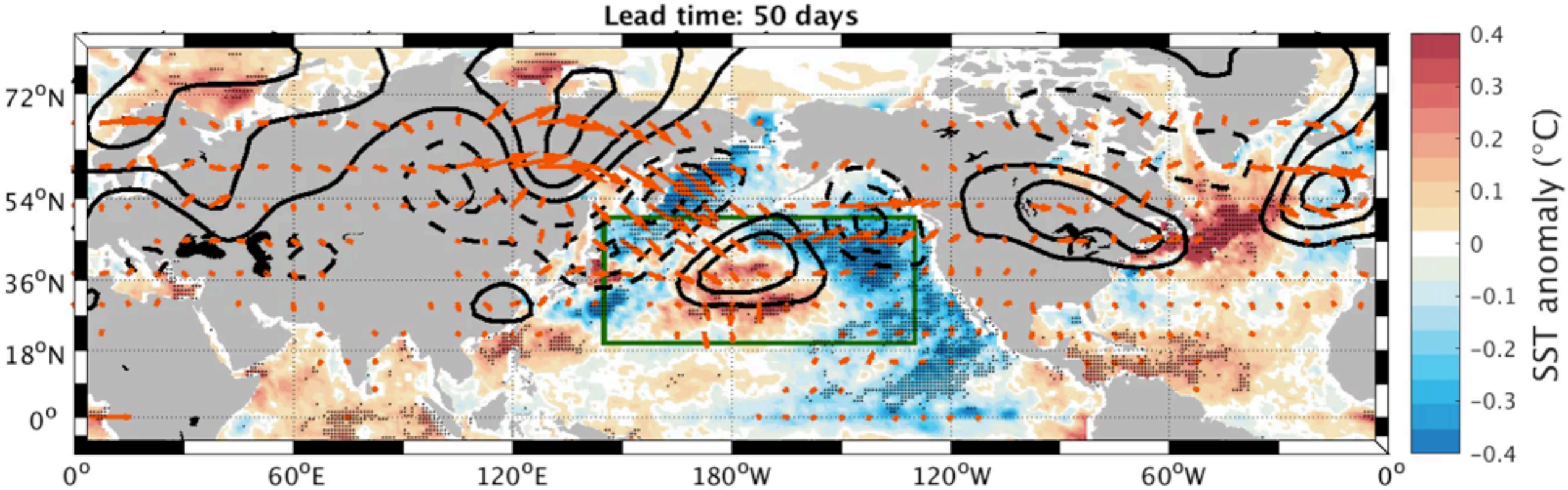

Quantifying regional heat: T95 = spatial 95th percentile of TMAX′

heat event

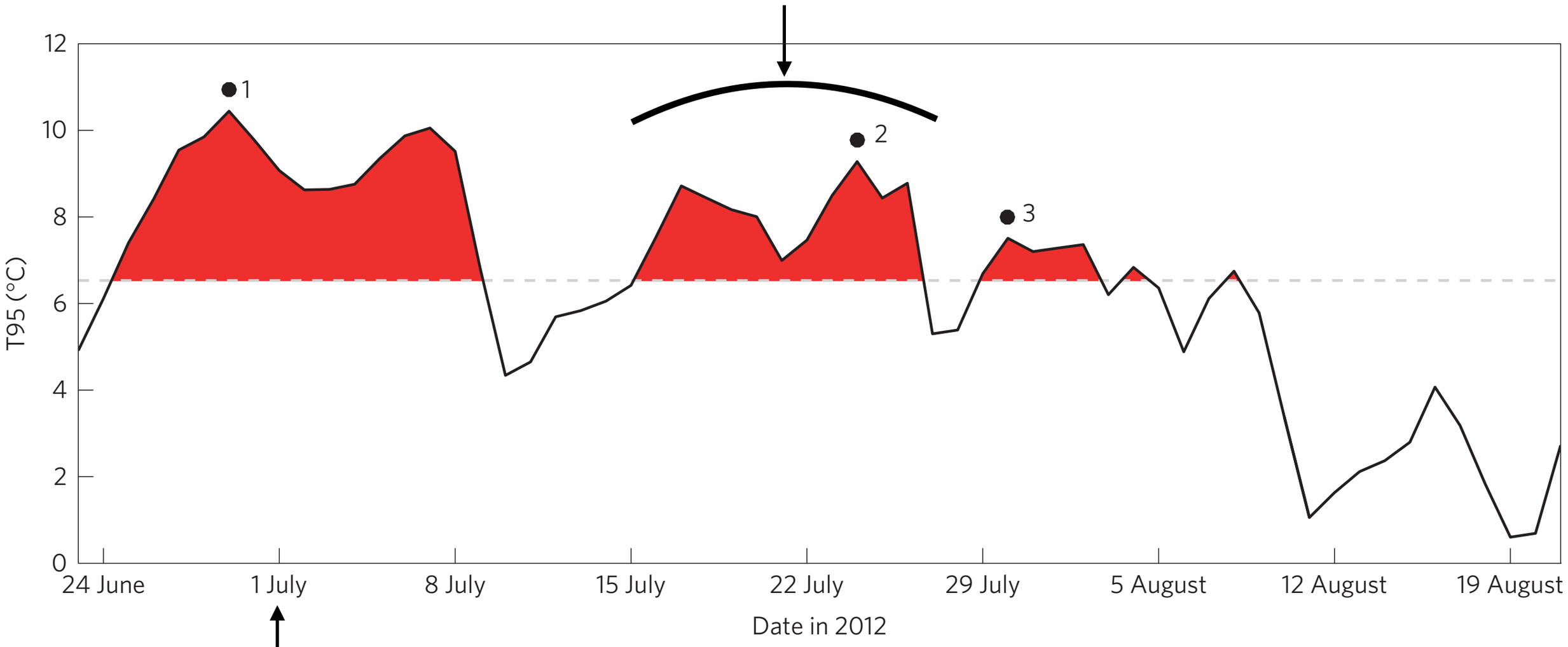

hot day

SST anomalies on hot days exhibit structure in the midlatitude Pacific

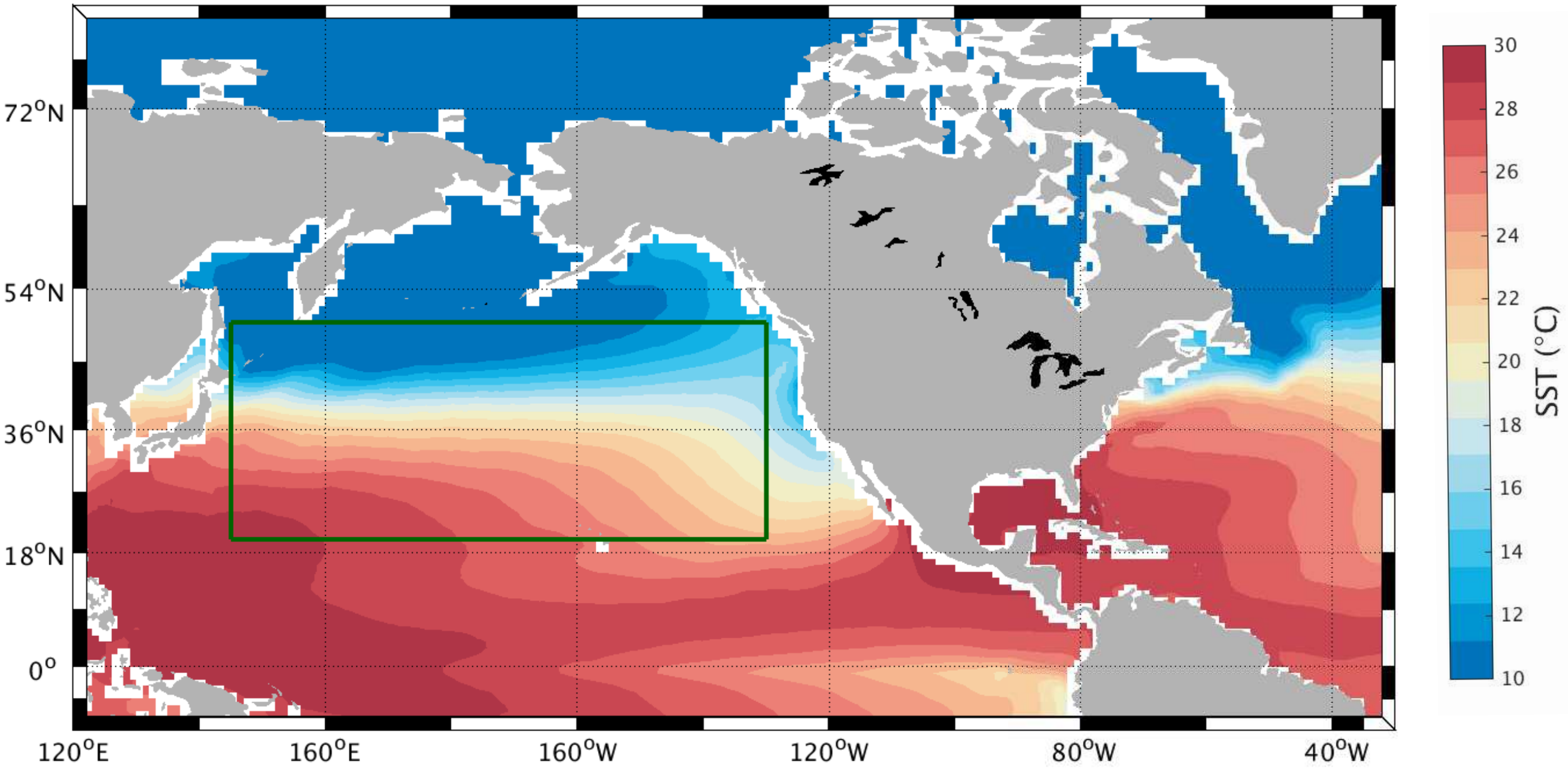

SST anomalies on hot days exhibit structure in the midlatitude Pacific

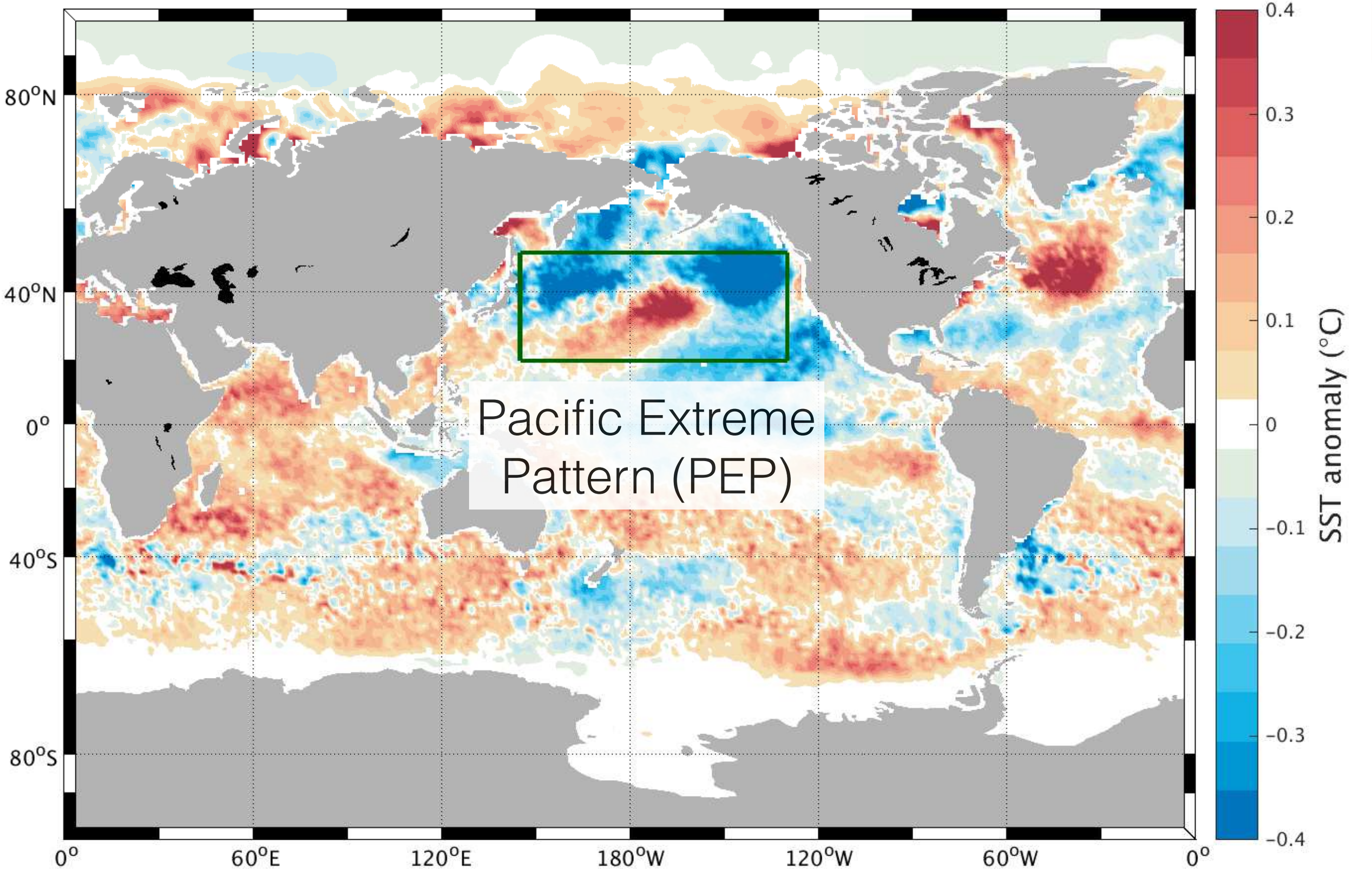

Pacific SSTs skillfully predict hot days at lead times up to 50 days

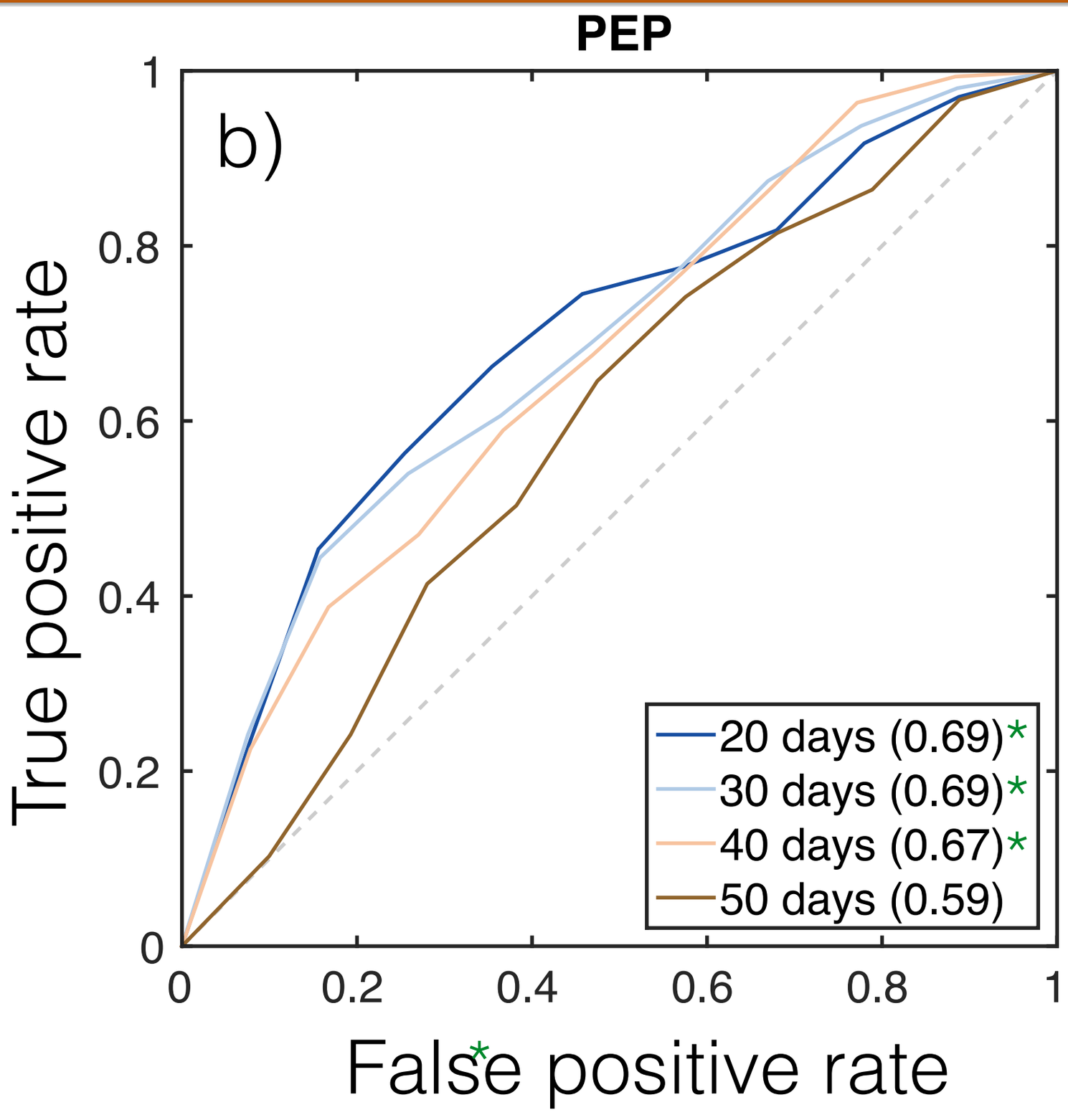

ROC scores ≥ 0.6 significant at the 0.05 level

A mechanistic interpretation of intensification-driven cooling

- More productive croplands have greater capacity for evapotranspiration, leading to increased latent heat flux and reduced sensible heat flux. Greatest temperature impact occurs on hot days.

- Additionally, this would tend to increase atmospheric moisture and precipitation, consistent with precipitation and humidity trends (e.g. Brown and DeGaetano 2013).

- Cooling by enhanced evapotranspiration can be tested by examining the relationship between cooling and drought.